

SANDIA REPORT

SAND86-8056 • UC-62c
Unlimited Release
Printed September 1987

RS-8232-2/ 662/2

C2

The Developmental Status of Solar Thermochemical Hydrogen Production



8232-2/066212



00000002 -

C. W. Pretzel and J. E. Funk

Prepared by
Sandia National Laboratories
Albuquerque, New Mexico 87185 and Livermore, California 94550
for the United States Department of Energy
under Contract DE-ACO4-76DP00789

Issued by Sandia National Laboratories, operated for the United States Department of Energy by Sandia Corporation.

NOTICE: This report was prepared as an account of work sponsored by an agency of the United States Government. Neither the United States Government nor any agency thereof, nor any of their employees, nor any of the contractors, subcontractors, or their employees, makes any warranty, express or implied, or assumes any legal liability or responsibility for the accuracy, completeness, or usefulness of any information, apparatus, product, or process disclosed, or represents that its use would not infringe privately owned rights. Reference herein to any specific commercial product, process, or service by trade name, trademark, manufacturer, or otherwise, does not necessarily constitute or imply its endorsement, recommendation, or favoring by the United States Government, any agency thereof or any of their contractors or subcontractors. The views and opinions expressed herein do not necessarily state or reflect those of the United States Government, any agency thereof or any of their contractors or subcontractors.

Printed in the United States of America
Available from

National Technical Information Service
5285 Port Royal Road
Springfield, VA 22161

NTIS price codes
Printed copy: A06
Microfiche copy: A01

SAND86-8056
Unlimited Release
Printed September 1987

THE DEVELOPMENTAL STATUS OF SOLAR THERMOCHEMICAL HYDROGEN PRODUCTION

Carl W. Pretzel
Solar Central Receiver Systems Division
Sandia National Laboratories, Livermore

James E. Funk
University of Kentucky
Lexington, Kentucky

ABSTRACT

This report discusses the status of development on solar thermochemical hydrogen production. It discusses the results of recent experiments of components for the solar interface. Various process designs that have been proposed are examined and areas of technical concern are discussed.

The process has the potential for having the highest efficiency for producing hydrogen from water. Development has consisted of process flowsheet designs for using nuclear heat sources, several solar interface conceptual designs, and experiments for solar central receiver components. Conceptually, the flowsheets show how the chemical process plant is to actually be built. Each stream is identified and temperature, pressure, and composition are specified. The function of each piece of process equipment -- reactors, heat exchangers -- is defined. Design requirements such as conversion, heat transfer, etc., and materials of construction are established.

While many uncertainties still exist, we have identified no major technical problems that will prevent the production of solar thermochemical hydrogen if additional analysis and experimentation are completed. An economic assessment was performed by determining hydrogen product costs using realistic solar availability conditions. The conclusions list the major areas that need continuing work.

SOLAR THERMAL TECHNOLOGY

FOREWORD

The research described in this report was conducted within the U. S. Department of Energy Solar Thermal Technology Program. This program directs efforts to incorporate technically proven and economically competitive solar options into our nation's energy supply. These efforts are carried out through a network of national laboratories that work with industry.

In a solar thermal system, mirrors or lenses focus sunlight onto a receiver where a working fluid absorbs the solar energy as heat. The system then converts the energy into electricity or uses it as process heat. There are two kinds of solar thermal systems: central receiver systems and distributed receiver systems. A central receiver system uses a field of heliostats (two-axis tracking mirrors) to focus the sun's radiant energy onto a receiver mounted on a tower. A distributed receiver system uses three types of optical arrangements -- parabolic troughs, parabolic dishes, and hemispherical bowls -- to focus sunlight onto either a line or point receiver. Distributed receivers may either stand alone or be grouped.

This report summarizes the status of solar thermochemical hydrogen production. It discusses the results of recent experiments of components for the solar interface. Various process designs that have been proposed are examined and areas of technical concern are discussed. The economics of the process are estimated based on realistic conditions for solar energy availability. The conclusions list the major areas needing continuing work.

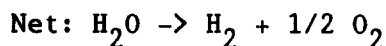
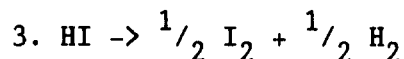
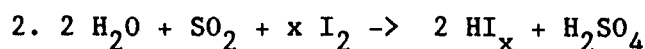
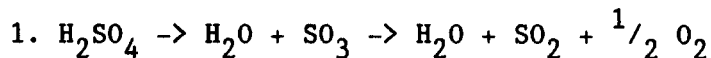


EXECUTIVE SUMMARY

Solar thermochemical hydrogen production could supply a clean fuel from totally renewable resources. Compared to other methods of hydrogen production, such as electrolysis, thermochemical reactions have potentially higher process efficiencies. The best developed hydrogen thermochemical cycle is the GA Technologies' sulfur iodine process. Development for the process began as an application to produce fuel using heat from nuclear reactors. Lately, chemical process development has included concepts for energy storage to interface with solar thermal central receiver systems. Component experiments have also been recently conducted. These experiments involved a ceramic heat exchanger to vaporize sulfuric acid and a catalytic reactor that decomposes sulfuric acid. Both of these are high temperature components that would operate inside the receiver. The purpose of this report is to review the status of both the chemical process itself and the process as a fuels and chemicals application for solar thermal central receivers. Estimates of the economics of the process were determined using updated cost information for solar heat and realistic conditions for solar energy availability.

Chemical Processes:

The process may be summarized in three chemical reactions:



Reaction 1 decomposes sulfuric acid into sulfur dioxide, oxygen and water. It is the high temperature, endothermic reaction step that would be accomplished in the solar central receiver. The nominal outlet temperature of the process stream is 870^o C. Reaction 2 uses the sulfur dioxide, SO₂, to combine with water and an excess amount of iodine to form a non-stoichiometric form of hydrogen iodide, HI_x. The purpose of the excess iodine, along with excess water that does not appear in the reaction equation, is to allow for formation of two liquid phases that make the separation of hydrogen iodide, HI, feasible. The reaction occurs at 117^o C and is slightly exothermic. Reaction 3 decomposes the hydrogen iodide at 27^o C to form the hydrogen product.

For chemical plant design, GA Technologies has organized the process into five sections:

Section I HI and H₂SO₄ Synthesis.

This accomplishes Reaction 2: because it is unique to the GA Process, it is called the main solution reaction.

Section II SO₂ Synthesis.
Accomplishes Reaction 1

Section III HI Separation.
This prepares the exiting process stream from Reaction 2 for Reaction 3. It is where the HI is separated from the water and the iodine.

Section IV HI Decomposition.
The final chemical step: Reaction 3.

Section V Energy Transport
This section includes the heat and power transfer systems between the four chemical process sections.

In Section III phosphoric acid is added to the solution of HI and water. This forms and separates the HI from the excess iodine and water. However, dilute phosphoric acid is also produced by this step. It must be reconcentrated in one of the most energy consuming and capital intensive operations of the process.

The total process contains three major recirculation streams, phosphoric acid, water and iodine. In addition, the sulfur dioxide exits the central receiver at 870°C and must be cooled to 95°C before it is sent to Reaction 2. This makes heat recovery very important to maintain a high thermal efficiency for the process.

GA Technologies estimates that the overall thermal efficiency using a continuous heat source is 47%, and 40% with a solar interface. If heat recovery systems were not used, the efficiency would drop to 13%.

Significant improvements in the process are still possible. Recent progress in flowsheet development has identified an operation where HI is decomposed at 300°C and 2.0 MPa. This would eliminate Section III and raise the thermal efficiency by approximately 3 percentage points. Also, the decomposition fraction of sulfuric acid increases with temperature. Because nuclear reactors and metallic heat exchangers are not capable of obtaining temperatures much higher than 900°C, little consideration has been given to higher temperature designs. One estimate, however, is that a ceramic reactor operating at process stream exit temperatures of 1086°C would result in an efficiency of 53% for continuous operation. Such temperatures could be achieved in solar central receivers.

Solar Interfaces:

A main feature of the solar interface is the generation of sufficient SO₂ reagent so that the Reaction Steps 2 and 3 can be operated continuously.

Three solar interface designs have been examined. The first uses two receivers; one to heat nitrate salt to supply some of the heat

required at lower temperatures and for energy storage. A second receiver operates at the higher temperature required to decompose sulfuric acid. To operate the hydrogen production plant continuously, enough SO_2 reagent must be produced and stored during the daytime hours to supply the plant through the nighttime and periods of low insolation. The SO_2 is stored in an aqueous solution at low pressures, 0.2 MPa.

The second design uses one receiver that decomposes sulfuric acid but splits the SO_2 into two streams. One SO_2 stream is stored in an aqueous solution as in the first design. This is used for reagent purposes. The second stream contains the oxygen produced in the decomposition reaction and is stored as a gas. During the night this $\text{SO}_2 - \text{O}_2$ mixture supplies heat to the chemical plant by forming sulfuric acid in the reverse of the reaction performed in the receiver during the day.

The third design produces elemental sulfur to use as a storage medium. During the day a disproportionation reactor converts some of the SO_2 to sulfur. At night, the sulfur is combusted in air to create energy for the chemical plant in addition to supplying the SO_2 reagent needed at night. The design of the chemical plant is modified to accommodate the increased process stream flow that occurs at night when the SO_2 is diluted with nitrogen from the combusted air. Additional modifications may also be needed to account for the difference in heat and power obtained from the sulfur combustion as compared to the energy needs of the chemical plant. Flowsheets do not exist for this interface, but it appears that the vapor recompression operation for phosphoric acid reconcentration in Section III requires more power but less heat than is supplied by sulfur combustion. Another reconcentration method, such as direct contact heat exchangers, may be required.

Capital cost estimates were made for the first two designs. High gaseous storage costs appear to make the second design undesirable. Elemental sulfur may be a very inexpensive storage medium, but the reaction to produce the sulfur is not well known, and more research is required before components can be defined for estimating the costs of the sulfur production equipment.

Component Experiments:

Two sulfuric acid decomposer component experiments have been performed. The first operated at atmospheric pressure in a series of tests in the solar receiver at the Advanced Components Test Facility. The second used a decomposer designed for the higher pressures expected in a commercial design. This second experiment was performed in an electrically heated cavity, where simulated solar environments could be controlled to conduct transient tests. These experiments provided data on the performance of reactors designed for indirect, reradiated flux; on the use of Incoloy 800H alloy for construction, the behavior of two different catalysts: platinum and iron oxide; and the corrosion resistance of aluminide coated Incoloy 800H as well as coupons of other candidate alloys.

The catalytic reactor performs well. Performance predictions based on the assumption that the chemical reaction was always at equilibrium were not far from the observed behavior during the experiments. Kinetic effects will not be a problem. With a platinum catalyst the reaction is very near to equilibrium through the entire length of the reactor tube. With iron oxide, the reaction is slow at first, where the process stream temperature is relatively cool. However, in the upper, hotter portions of the reactor the iron oxide catalyst becomes very active, and the reaction achieves conversion very near equilibrium conditions. The first experiment revealed an unsuspected incompatibility between aluminide coated Incoloy 800H and the iron oxide catalyst. Corrosion rates for bare Incoloy 800H and iron oxide were lower and may be acceptable. Extended periods of reactor operation are needed to determine if the corrosion rate is acceptable for commercial reactor construction. The transient performance of the reactor is well behaved. The time constant for power transients is much longer than for flow transients. The power transient is dominated by the insulation in the cavity wall and can therefore be controlled by receiver design. This will make feasible control schemes possible.

A third experiment tested the performance of a ceramic heat exchanger for vaporizing concentrated sulfuric acid. A silicon carbide tube material and ceramic-to-metal seal designs were tested. Tests were conducted on the hot end seal to determine if a seal could be maintained if tubes and manifold become misaligned. It was demonstrated that an angular movement of 0.5° between the metal seal and the ceramic tube could be tolerated. This effort also included 6 month long laboratory corrosion tests of silicon carbide in boiling and vaporized sulfuric acid. Corrosion effects were negligible.

The third experiment was performed in a resistance heated cavity to provide uniform temperature control and allow transient testing. This experiment was more narrow in scope than the reactor experiments. A single tube was used in the experiment. Both the ceramic tube and seals performed successfully during continuous and transient testing. Because of the high conductivity of silicon carbide, actual vaporizers could be heated by direct solar flux and would not require the solar flux to be reradiated from cavity walls, a potential cost saving benefit.

These experiments are a successful first step in developing components for the sulfuric acid decomposition of Section II. Receiver design is still an open issue. Interface studies suggest that integrated receiver/reactors are superior. Having the chemical reactor in the receiver requires the use of indirect flux heating. While this appears to require unacceptably large receivers, it avoids the use of an additional heat exchanger/reactor in the chemical plant. Alternates to the catalyst packed tube reactor design have been proposed based on two dimensional models that predicted radial temperature gradient effects would adversely affect catalytic reactor performance. These radial gradient effects were not observed in the experiments, and one dimensional models were

found adequate for predicting reactor performance. Alternate reactor designs may be more desirable, but this would be due to lowered construction costs, not chemical performance. Additional analysis of these reactors is needed before a commercial design can be selected. The receiver/reactor concept would also include the vaporizer, recuperators and condenser. Currently, the vaporizer lags behind the reactor in experimental and design development.

The high corrosion rates of metals in boiling or condensing sulfuric acid make the use of ceramics desirable for these applications. Metallic construction may be feasible for the recuperators and, possibly the condenser, if control procedures can be developed to minimize liquid acid exposures and maintain high conversion rates for the decomposition reaction in the exit stream. As ceramic technology progresses, the operating temperature of the receiver can be increased to the point of eliminating the use of a catalyst and optimizing the chemical performance of the decomposition reaction.

Economic Analysis:

The economics for solar thermochemical hydrogen production were evaluated by determining hydrogen product costs. The cost of solar heat was determined using performance and cost data recently developed for a 320 MWt Solar Central Receiver System. A correction factor was included to account for the higher receiver operating temperature (900°C) used here. Prior economic analysis of thermochemical hydrogen double-counted parts of the receiver. They were included in both the chemical plant and solar plant equipment. Here, the vaporizer and decomposer were considered part of the chemical plant. Capital costs for most of the chemical plant were derived from previous studies based on individual component cost estimates of a continuously operating plant. The cost is derived using accepted chemical engineering methods for flowsheets where detailed designs are not yet available and is considered to be accurate within 30%. Two different evaluations were conducted.

The first used simplified assumptions for the operation of the chemical plant. Solar costs were treated as industrial process heat. The cost of solar heat was calculated based on annual hours of operation for a receiver at 900°C given an average cloudiness factor. The chemical plant was assumed to operate continuously. The size of the Section II/solar interface was tripled. Eight hours of daily solar operation were considered adequate to provide energy and reagent needs of the chemical plant for 16 hours of night operation. The chemical plant used the elemental sulfur storage with capital cost increases to account for nitrogen dilution of the process stream. The capital costs for the sulfur storage interface were derived from an estimate by judging its relative complexity to a nuclear reactor interface that uses helium as an intermediate heat transfer medium. Solar thermochemical hydrogen shows a price range of from 38.0\$/GJ for low cost heliostats ($\$40/\text{m}^2$) to $\$45.5/\text{GJ}$ for current costs of glass metal heliostats ($\$120/\text{m}^2$).

The second economic evaluation used the SOLERGY program with weather

data taken at Solar One to determine the effects of actual weather conditions on the operation of the chemical plant. For a chemical plant, continuous operation is desired to maintain steady state conditions for the chemical reactions. Different system configurations were examined, with solar multiple and storage capacity being the major variables. A third variable, set point, which has no effect on the capital investment of the plant, was also used. It is the energy level in storage at which chemical plant operation begins after a weather forced shut down. More complex dispatch strategies are not useful because income for chemical production is not a function of the time of day as it can be for electricity production. These three parameters were varied to minimize the annual number of plant starts. The results show a storage capacity which is the equivalent to 100 hours of solar plant operation will limit plant starts to only a few per year. There is little advantage to storage capacities greater than this. This is one half the seasonal storage capacity configured by GA Technologies with the elemental sulfur storage system. With glass/metal heliostats, and a system configuration for 8 annual plant starts (4.0 solar multiple, 27 hours storage), the cost of hydrogen is \$55.4/GJ. This is a modest increase compared to the first simplified analysis.

A variation of the analysis assumed that much less storage would be needed if a larger number of plant starts could be tolerated. This would be accomplished by using warm stand-by equipment to prevent thermal cycling of the chemical plant, compressing the SO_2 for reagent storage as a liquid, and using nitrate salt storage. This system design would use 6.25 hours of storage, have 80 annual plant starts, and achieve a hydrogen product cost of \$48.3/GJ with glass/metal heliostats and \$41.5/GJ at \$40/m² for heliostats.

Compared to present bulk hydrogen costs from the steam reforming of methane (16\$/GJ), the price disparity is similar to that for current capabilities for solar electricity and the long term electricity cost goals. For the use of hydrogen as a primary energy carrier, the program goal is \$9/GJ.

Technology Assessment:

Thermochemical hydrogen production is not a mature process compared to other solar thermal applications. Development is still required to determine the optimal design and the benefit of identified potential process improvements. Heat recovery is important to the efficiency of this process. Process/trade-off studies are required to determine the balance of capital investment to the value of thermal efficiency improvements. The studies must also optimize the size of components constructed of expensive materials needed to withstand the corrosive process streams. Process flowsheets should be designed to match the chemical process to the solar interface. The elemental sulfur storage concept needs considerable work before its performance can be assessed. Other solar interface concepts that use storage methods and heat transfer media that are suitable for both the solar plant and the chemical plant should also be

considered. In particular, the power cycles in Section V must be simplified. The process has potential for improved performance at the higher temperatures obtainable with solar thermal central receivers; especially as ceramics technology improves. Additional flowsheet development is needed to determine the process performance at higher operating temperatures. At present, interface studies indicate an integrated receiver design is best. A comparative analysis of the various sulfuric acid decomposer concepts is needed to establish the optimal reactor design. Development for the sulfuric acid vaporizer is in a very early stage and development for recuperators and condensers must be initiated. Experiments that operate for extended periods are required to determine catalyst performance and corrosion resistance of materials of construction in order to qualify components for commercial plant operation.

CONTENTS

	<u>Page</u>
EXECUTIVE SUMMARY	7
1. INTRODUCTION	19
2. STATUS OF THE GA PROCESS	22
A. Process Description	22
B. Research History	25
C. Chemistry of the Process	26
D. Flowsheet Development	35
E. Component Design and Materials Issues	38
F. Internal Heat Recovery	39
G. Recirculation of Process Streams	43
H. Process Thermal Efficiency	44
3. STATUS OF THE SOLAR INTERFACE	46
A. Temperature and Heat Requirements	46
B. Interface Descriptions	48
i. Nitrate Salt - SO ₂	48
ii. SO ₂ - O ₂	52
iii. Elemental Sulfur	53
iv. Decomposer Interfaces	55
C. Component Designs	57
i. Decomposer Experiments	57
ii. Decomposer Design	63
iii. Vaporizer	66
iv. Condenser and Recuperators	71
D. Receiver Designs	72
4. ECONOMIC CONSIDERATIONS	74
A. Capital Costs, Efficiency, and Production Costs	74
B. Irreversibilities, Efficiency and Production Cost	80
C. Effect of Solar Availability	82
D. Liquid SO ₂ Storage	94
5. OTHER CYCLES	98
6. CONCLUSIONS	103
REFERENCES	108

ILLUSTRATIONS

<u>No.</u>		<u>Page</u>
1-1	History of Thermochemical Hydrogen Process Development	20
2-1	Equilibrium Curves for SO_3 Decomposition	24
2-2	Mass Balance of the GA Process	27
2-3	Section II - SO_2 Synthesis	28
2-4	Section I - HI Synthesis	29
2-5	Section III - HI Separation, Using Phosphoric Acid Separation Technique	30
2-6	Section IV - Hydrogen Production from HI Decomposition	31
2-7	Energy Flows and Enthalpy Changes for Continuous Operation	32
2-8	University of Aachen Flowsheet Replacement for Sections III and IV	37
3-1	Daytime Energy Flows and Enthalpy Changes for Molten Salt Heat Storage - SO_2 Solution Storage	49
3-2	Nighttime Energy Flows and Enthalpy Changes for Molten Salt Heat Storage - SO_2 Solution Storage	50
3-3	Atmospheric Pressure Sulfuric Acid Decomposer Solar Experiment	58
3-4	High Pressure Sulfuric Acid Decomposer Experiment	59
3-5	Insulation Design Detail for Inlet Manifold	61
3-6	Catalyst Performance	62
3-7	Single Tube Ceramic Acid Vaporizer Experiment	67
3-8	Hot End Seal Design	68
3-9	Cold End Seal Design	69

<u>No.</u>		<u>Page</u>
4-1	Flowsheet Design Considerations	81
4-2	Process Related Costs for Solar Thermochemical Hydrogen	84
4-3	Chemical Plant Starts, Solar Multiple = 2.8	90
4-4	Chemical Plant Starts, Solar Multiple = 4.0	91
4-5	Production Fraction for Different System Configurations	92
4-6	Annual Capacity Factor for Different System Configurations	93
4-7	Hydrogen Costs for Elemental Sulfur Storage Using Solar Availability Data	95
4-8	Hydrogen Costs for Nitrate Salt and Liquid SO ₂ Storage with Warm Standby	97
5-1	Sulfuric Acid Based Thermochemical Hydrogen Cycles	99
5-2	Thermochemical Hydrogen Cycles Under Development in Japan	100
6-1	Evolutionary Path for Solar Thermochemical Hydrogen Receiver	105

Tables

<u>No.</u>		<u>Page</u>
2-1	Energy Balance for the Process Sections	41
2-2	Internal Heat Recovery in Section II	41
2-3	Internal Heat Recovery in Section III	42
2-4	Internal Heat Recovery in Section IV	42
3-1	Heat Demand of the Chemical Process	47
3-2	Transient Behavior of the Decomposer Reactor	64
4-1	Capital Costs of the Chemical Plant	76
4-2	Solar Heat Costs	78
4-3	Cost of Solar Thermochemical Hydrogen	79
4-4	Exergy Loss, Thermal Efficiency and Product Cost Component for the Process Sections	83
4-5	Annual Production Results - Solar Multiple of 2.7	87
4-6	Annual Production Results - Solar Multiple of 3.2	87
4-7	Annual Production Results - Solar Multiple of 4.0	88
4-8	Capital Costs for Plant Design with Liquid SO ₂ and Nitrate Salt Storage	96
5-1	Current Japanese Research Activities in Thermochemical Hydrogen	99

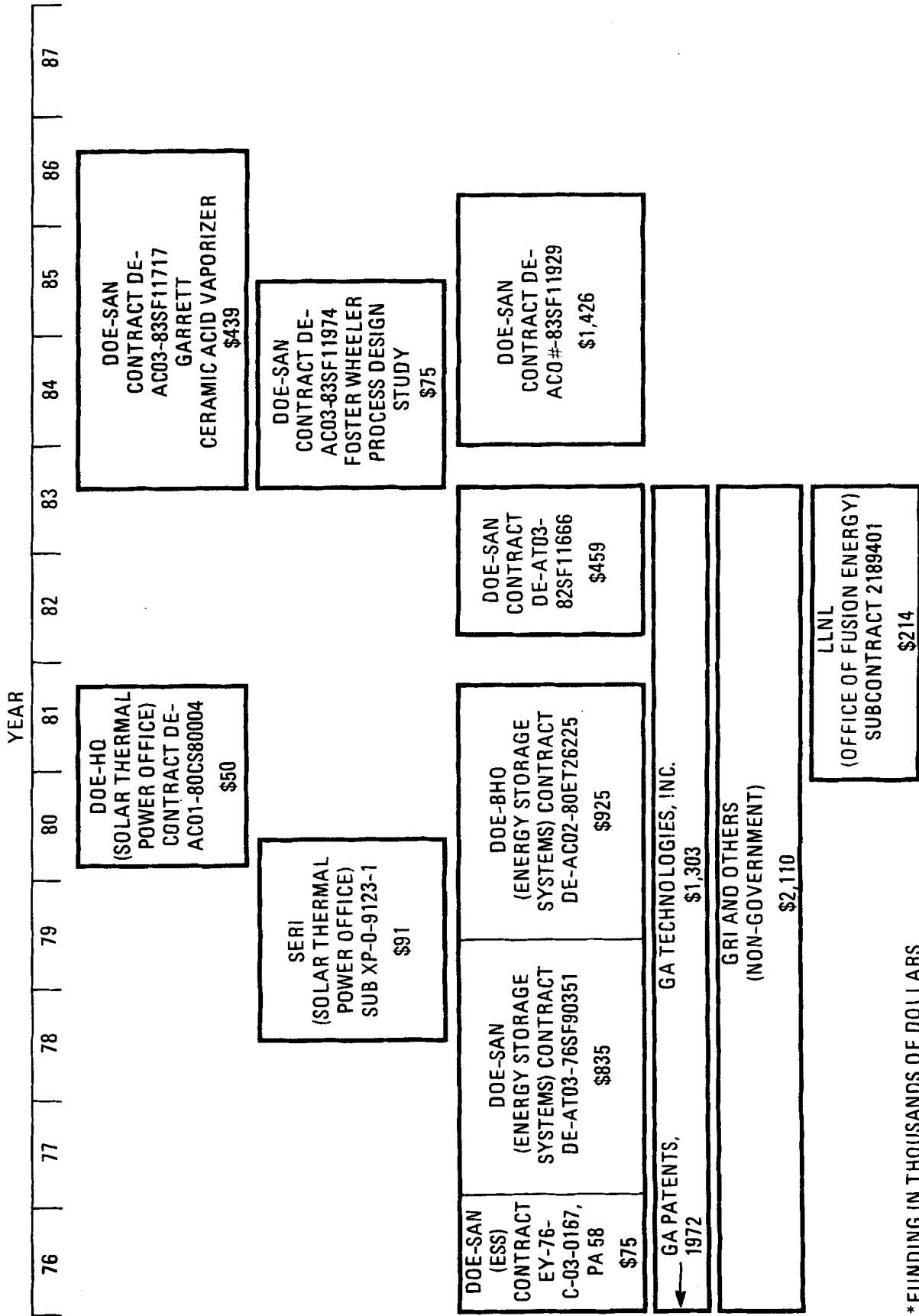
1. INTRODUCTION

The solar thermal central receiver program has developed electrical power generation systems with steam Rankine cycles using thermal transfer media at temperatures up to 593°C. Electricity, however, represents only a portion of the nation's energy needs. For the year 2000, it has been estimated that electrical needs will represent 35 quads of the nation's total energy consumption of 92 quads. Natural gas for residential, commercial, and industrial needs totals 38 quads, and transportation needs are estimated at 17 quads (Ref. 1). Hydrogen has the potential for being a fuel transported through pipelines on a scale similar to natural gas utilities as well as being used as a fuel for aerospace and, possibly, ground transportation. To this end, there are numerous research and development efforts to produce hydrogen, develop hydrogen powered vehicles and equipment, and adapt existing equipment to be fueled with hydrogen. As an energy source, hydrogen has several important advantages. It is environmentally sound; it does not introduce oxides of carbon into the atmosphere or require large scale mining operations. Hydrogen can be produced from water; so it is a renewable resource from a readily available feedstock.

There are several ways to produce hydrogen from water: thermal decomposition, photolysis, thermochemical reactions and electrolysis. Of these only thermochemical and electrolytic methods have been identified that can achieve hydrogen production on a practical scale. While electrolysis is at present better developed, thermochemical reactions have potentially higher process efficiencies.

Many possible thermochemical hydrogen cycles have been discovered (Ref. 2). Of these, the GA Technologies cycle is the best developed. Originally proposed as a heat application for high temperature gas reactors (HTGR's) using nuclear fission energy, this cycle has recently been examined for use with solar thermal central receiver systems. The process requires temperatures of at least 800°C, with substantial chemical improvements occurring up to 980°C. With solar, temperatures of up to 870°C -- the recommended operating temperature of the current process design -- have already been demonstrated. It is believed that the higher temperatures may be possible. To an extent, the increased operating temperature capabilities of solar make it a more attractive energy source than nuclear.

Figure 1-1 shows the program history of the GA process in terms of contracted experiments, studies and funding. Approximately 8 million dollars have been spent to develop the process since GA patents identified the key elements in 1972. The Department of Energy has funded numerous projects during this development. During 1976 through 1981, a bench scale system was designed and constructed that demonstrated the operation of the cycle and tested components of the chemical process on that scale. The design and construction of a solar catalytic reactor started in 1979 and ended in 1983 with the successful completion of a solar receiver test at the Advanced



* FUNDING IN THOUSANDS OF DOLLARS

Figure 1-1 History of GA Thermochemical Hydrogen Process Development

Components Test Facility at the Georgia Technical Research Institute. That test was recently followed by a high pressure reactor experiment performed in a simulated solar environment. Engineering studies have been performed to examine methods to interface the chemical plant to the central receiver system, to devise appropriate chemical energy storage concepts and to define the total plant efficiency and capital costs. A conceptual design was performed by Foster Wheeler for the purpose of defining solar experiments at the Central Receiver Test Facility and at Solar One which would include the entire chemical plant. A contract was placed with Garrett Airesearch to develop a ceramic acid vaporizer. In addition, in conceptual studies, commercial scale thermochemical hydrogen plants have been configured to interface with three designs for nuclear fusion reactors (Refs. 3,4,5)

In Section 2, a description of the thermochemical hydrogen process is given, reviewing the chemical process components unique to the process and the present status of flowsheets for the process. The activities and process steps where possible future improvements can be made are described.

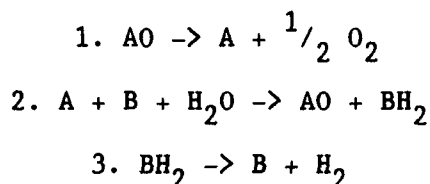
In Section 3, the development of the solar energy interface is described, and a summation of recent solar component experiments is given. Areas where the component designs need further development are presented. At the present time, the solar interface subsystem design exists only as a preliminary concept as part of the chemical process flowsheet.

In Section 4, a description of the economics of the process is included. This section is not the result of a conceptual design but rather an effort to show the economic sensitivities of the process. This section indicates which portions of the process have the greatest influence on the cost of the hydrogen produced, where further work is possible to reduce costs, and where efforts will result in the greatest economic improvements in the final production cost of thermochemical hydrogen. Other suggested thermochemical cycles are briefly described in Section 5. Principal conclusions are presented in Section 6.

2. STATUS OF THE GA PROCESS

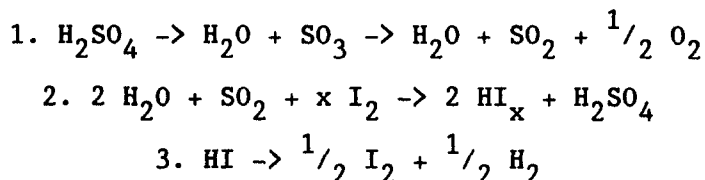
A. Process Description

Thermochemical cycles consist of several reactions to dissociate water into hydrogen and oxygen. These cycles perform that function through the formation of hydrogen and oxygen occurring in two different physical locations; making separation possible and avoiding the problem of a reverse reaction back to water. Practical two step thermochemical cycles have not been identified; here the process will be envisioned in three steps with two reactants in addition to water being required. A reducing agent "A" in Reaction 1 is used to liberate the oxygen, while an oxidizing agent "B" is used to extract the hydrogen as shown in Reaction 3. In order for the cycle to be successful, there must be a "closure" reaction that will combine the oxidizing and reducing agents with water, Reaction 2.



For Reaction 1 to be suitable, it must have a large increase in entropy so that the temperature increase required for the reaction to occur (i.e. to cause the free energy change of the reaction to be negative) will be attainable in practice. Typically this means that the reaction will result in the formation of more product molecules than reactants and that they will be gaseous. Reaction 2 is where water is introduced into the cycle and requires that the products, AO and BH₂, must be separated and sent to two different locations for the production of the oxygen and hydrogen. The work required for separation can be significant, and because the cycles often include miscible fluids, the identification of practical separation methods is important. Reaction 3 is where hydrogen is produced by the thermal decomposition of a reactant; it is important that the reactant identified for use here is less stable than water and that its products are easy to separate.

The GA Thermochemical Cycle is based on sulfur and iodine where the reducible reactant is sulfuric acid, H₂SO₄, and I₂ is the oxidizing agent. The chemical reactions are:



For gas handling systems, elevated pressures are used to reduce equipment sizes and capital costs. Reaction 1 would be performed in the range of 0.5 to 1.0 MPa. Figure 2-1 shows the conversion to SO_2 at equilibrium as a function of temperature and pressure. As can be seen, the equilibrium shifts toward the production of less SO_2 at higher pressures. Operating at higher pressures is not an optimum for the chemical reaction, but it is believed that the capital cost reductions will lower the overall production cost. At the present time, it is believed the minimum lies between 0.5 and 1.0 MPa. As part of Reaction 1, concentrated sulfuric acid would be vaporized at 325-425°C and 56 kJ/mole. The sulfuric acid vapor thermally decomposes (without the need of a catalyst) into water vapor and sulfur trioxide gas. This is a highly endothermic reaction of 103 kJ/mole that occurs between 425 - 625°C. At higher temperatures the sulfur trioxide decomposes to sulfur dioxide and oxygen in another endothermic reaction (92 kJ/mole). The current process design defines the upper temperature for this reaction at 870°C. This temperature is defined by the practical structural limits for metallic component construction. In addition, at these temperatures, the reaction requires a catalyst. As Figure 2-1 shows, the equilibrium conversion continues to increase with higher temperatures. At 980°C, the reaction would achieve greater than 90% conversion and, at such temperatures, would not require a catalyst (Ref. 5). After Reaction 1 the product gases would be cooled. At room temperature the SO_2 would exist as a gas; however, it could be stored in an aqueous solution with water or compressed and stored as a liquid at elevated pressures.

Reaction 2, which is sometimes called the Bunsen Reaction, is performed at 117°C and is mildly exothermic, 42 kJ/mole. Because this reaction is performed in aqueous solutions, it is sometimes called the main solution reaction. It is important that all the sulfuric acid be removed before proceeding to Reaction 3. The amount of iodine added to the reaction, x , is in excess of the reaction requirement. This number varies with different GA flowsheets, but is typically between 4 (Ref. 5) and 12.2 (Ref. 6). At stoichiometric ratios, the reaction stream contains H_2O , HI and H_2SO_4 in one single phase. GA found that additional iodine causes the solution to separate into two liquid phases, a lighter phase of sulfuric acid and water, and a heavier phase of HI, iodine and water. For the heavier phase, the partial molar free energies of water and HI are 26.04 and 2.5 kJ/mole, respectively. At least this much energy must be supplied as work to separate the two components.

In Reaction 3 the HI is decomposed in the presence of a catalyst. At 27°C, this reaction is slightly endothermic, 10.0 kJ/mole, and has a free energy change of 16.0 kJ/mole. By comparing this free energy change to that of other halogens that could have been used in Reaction 2, one can see why iodine has been selected. Bromine is the next most suitable halogen but HBr has a free energy change of 110.4 kJ/mole, much higher than that for HI. All hydrogen halides are much more stable than HI and would be correspondingly difficult to decompose to produce hydrogen. Reaction 3 is carried

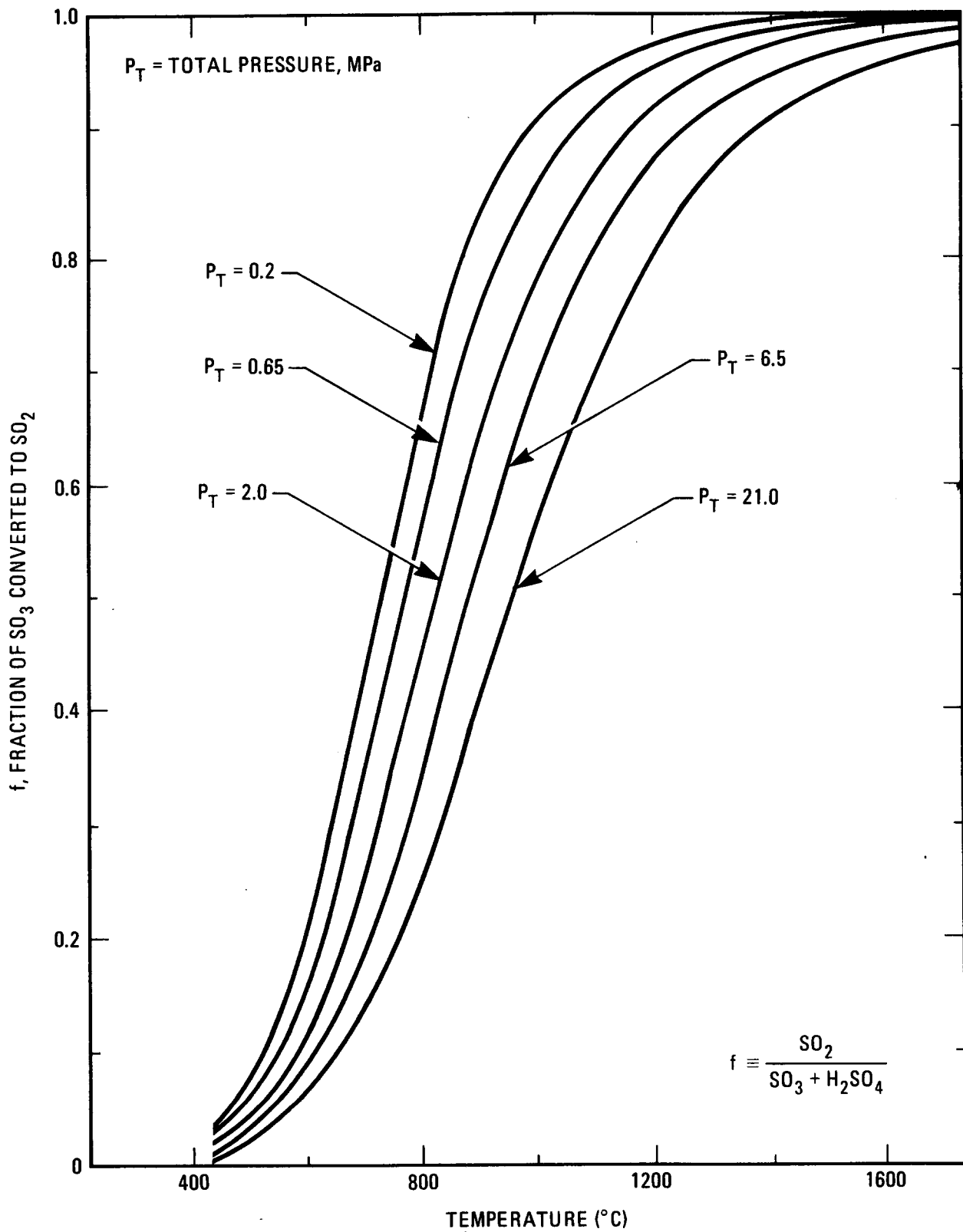


Figure 2-1 Equilibrium Curves for SO_3 Decomposition

out at 120°C and 5.0-8.4 MPa or 300°C and 2.0 MPa, depending on the process design.

Reactions 1,2 and 3 sum to equal the decomposition reaction for water. Compared to other chemical processes, the chemical components are simple and "clean" with no problems of undesirable side reactions and back reactions. In practice, however, several process streams carry significant quantities of both products and reactants. Additional steps are required to reconcentrate and separate the chemical components. There has been a considerable amount of work to determine the phase equilibria of HI - H₂O - I₂ and the other systems to help in these designs (Refs. 2,5,6,7). Some of the process streams are very corrosive; careful design for these process stream components is required. In addition, only a portion of the energy input to Reaction 1 becomes chemical energy in the form of SO₂. The energy contained in the form of sensible heat of the 870°C process stream must be recovered as the process stream is cooled to 120°C for use in the next reaction. This energy can be used to supply heat and work for the reconcentration and separation steps.

B. Research History

During the 1960's serious consideration was given to methods to produce hydrogen from water and make it a primary energy carrier. A number of water splitting cycles using various combinations of chemical reagents were identified. Some of these would also be termed hybrid cycles because electrolysis was added to some of the processing steps. An examination of thermodynamic data identified the sulfur - iodine cycle as one of several promising candidate cycles (Ref. 8). The Reactions 1 and 3 were well known previously, but the cycle had not been developed because the HI and the sulfuric acid could not be separated from the balanced form of Reaction 3; typically SO₃ would form before HI would separate from the sulfuric acid (Ref. 7). During the studies of 1972 - 1973, it was discovered that the excess iodine would separate the two products that started the development of the GA Technologies thermochemical hydrogen cycle. Efforts in the development of the cycle included the formulation of two detailed flowsheets, one in 1979 and another in 1981. The "1981" process is the latest design that is documented in detail. Additional improvements in separation of the HI from Reaction 2 and decomposition of HI have been made. Further work on the phase equilibria of the product streams has been performed but has not been incorporated into a new detailed flowsheet. Work related to Reaction 1 has just been completed to determine chemical behavior in components beyond the bench-scale size and for a solar environment.

C. Chemistry of the Process

For the purposes of defining process flows and performing the required energy and material balances, the cycle is divided into five sections.

Section I HI and H₂SO₄ Synthesis.

This accomplishes Reaction 2: because of its uniqueness to the GA process, it is called the main solution reaction.

Section II SO₂ Synthesis.

Accomplishes Reaction 1: this is the point at which thermal energy is added to the process. If no other energy sources are used, it represents the solar energy interface and supplies the total energy required for the decomposition of water.

Section III HI Separation.

This prepares the exiting process stream from Reaction 2 for Reaction 3. It is where the HI is separated from the water and the iodine. In terms of the product stream, it connects Section I to Section IV, not Section II.

Section IV HI Decomposition, or H₂ Production

The final chemical step: Reaction 3.

Section V Energy Transport

This section is not part of the chemical process. It includes the heat and power transfer systems between sections. For a solar central receiver it would include the storage system and part of the solar interface. It has been defined on the component level for nuclear plants but not for solar plants.

Figure 2-2 shows the mass transfer between the different sections that is required to form 1 molecule of H₂. There is a large recirculation of water between Sections I and II and an even greater recirculation of water and iodine between Sections I and III. Figures 2-3 through 2-6 show the major components and function of each section. The energy listed for each unit is what is needed to generate 1 mole of hydrogen. Figure 2-7 shows the energy flows for a continuously operating plant. Section II, shown in Figure 2-3, not only performs the decomposition of sulfuric acid, but also includes the concentration of the dilute acid as it comes out of Section I. A concentrator uses 50 kJ to increase the acid concentration from 57 to 98%. The acid increases in temperature from 120°C to 360°C; and a pump is used to increase the pressure to 0.86 MPa. The acid is vaporized using 145 kJ to raise its temperature to 527°C. At this point 86% of the sulfuric acid has been converted to SO₃ and the pressure has dropped to 0.8 MPa. This gas then enters the catalytic reactor where a total of 254 kJ is used to achieve 74% conversion to SO₂. The gas is now at 870°C and 0.53 MPa. The gas is cooled to 306°C and 0.3 MPa where it begins to condense. The unreacted SO₃ and the available water recombine to form sulfuric acid. At the outlet of the condenser, a

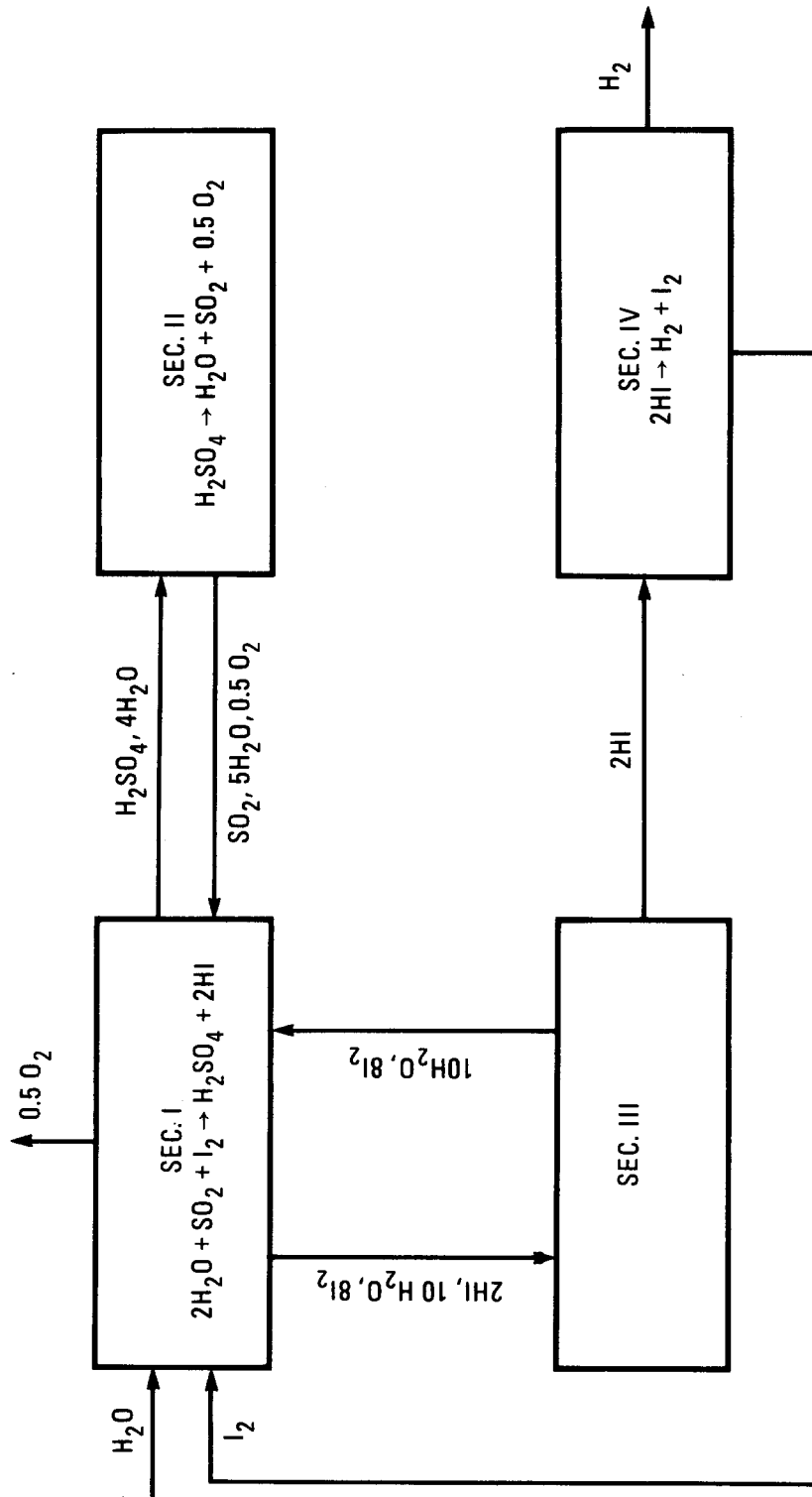


Figure 2-2 Mass Balance of the GA Process

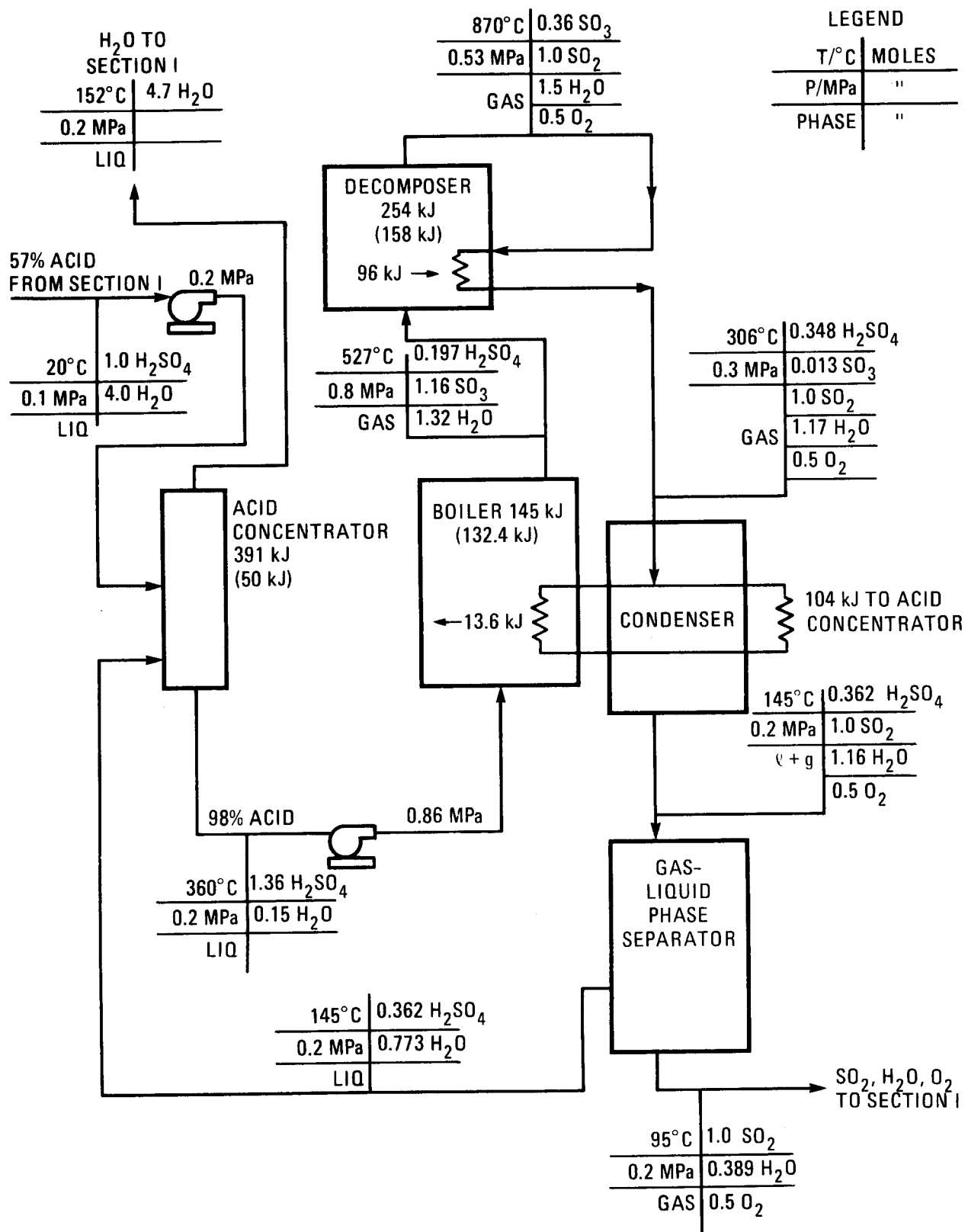


Figure 2-3 Section II - SO₂ Synthesis. Molar quantities are for one mole of hydrogen product. Gross heat loads are given with net values in parenthesis.

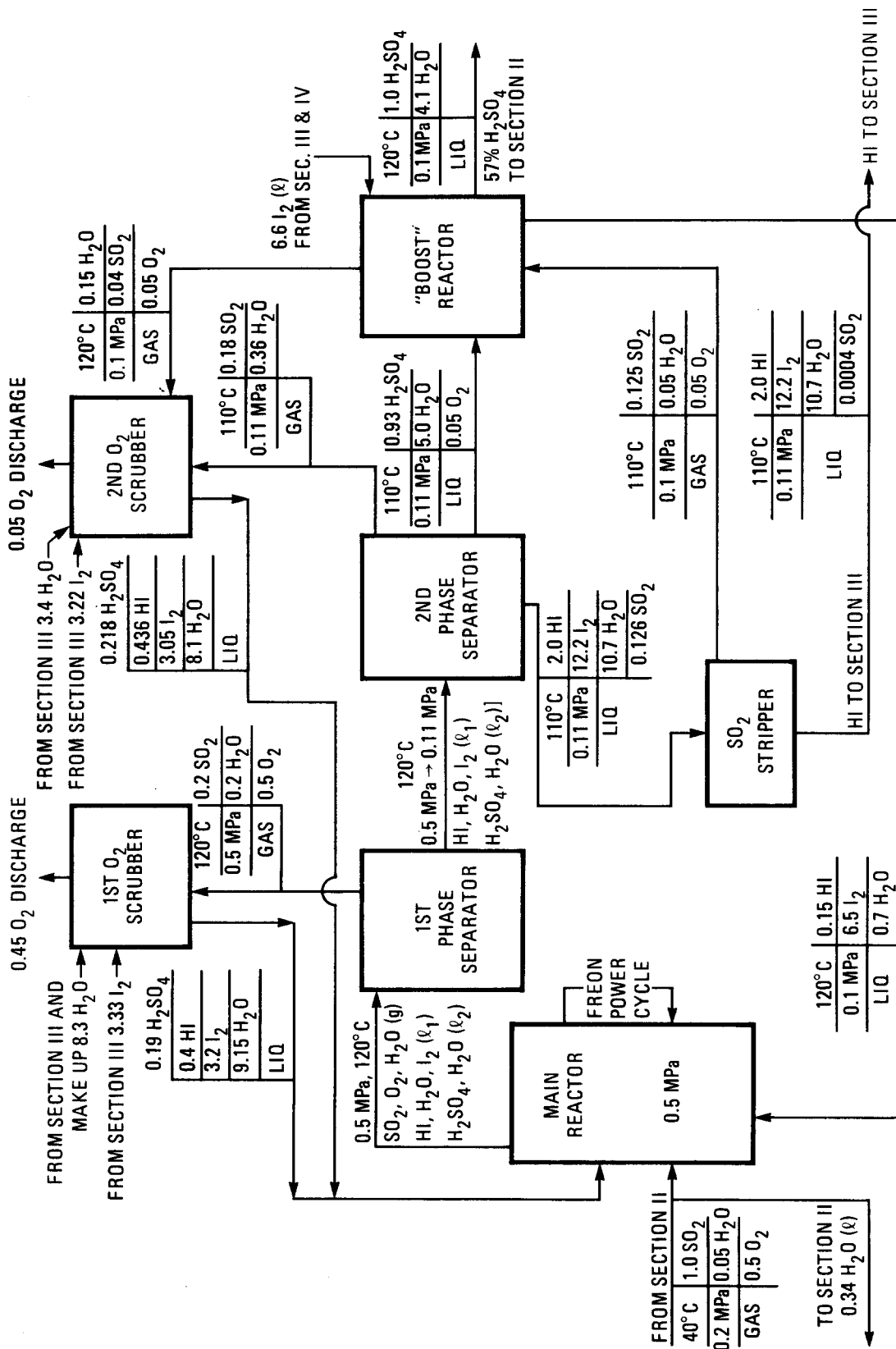


Figure 2-4 Section I - HI Synthesis. Molar quantities are for one mole of hydrogen product.

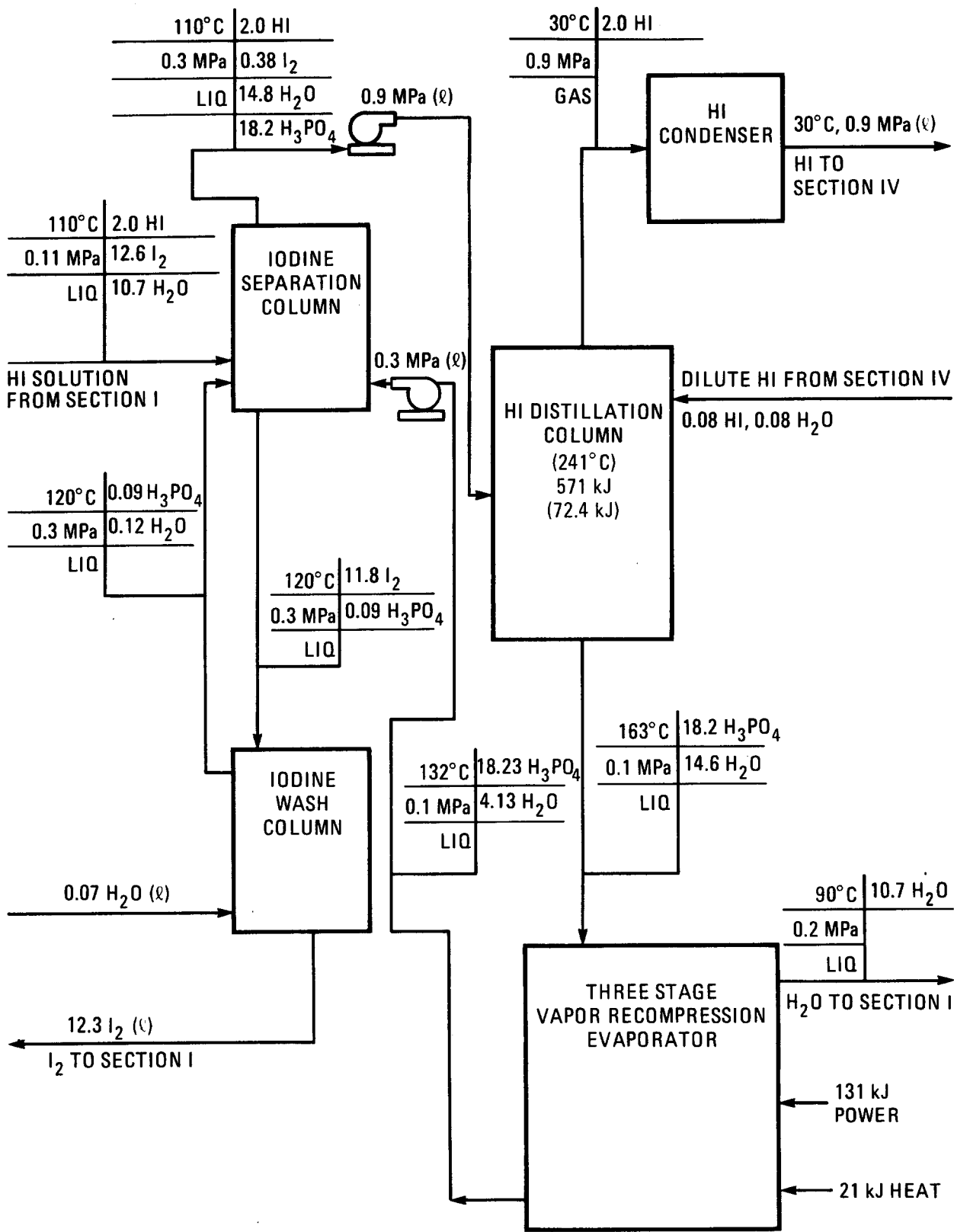


Figure 2-5 Section III - HI Separation, Using Phosphoric Acid Separation Technique. Molar quantities are for one mole of hydrogen product. Gross heat loads are given with net values in parenthesis.

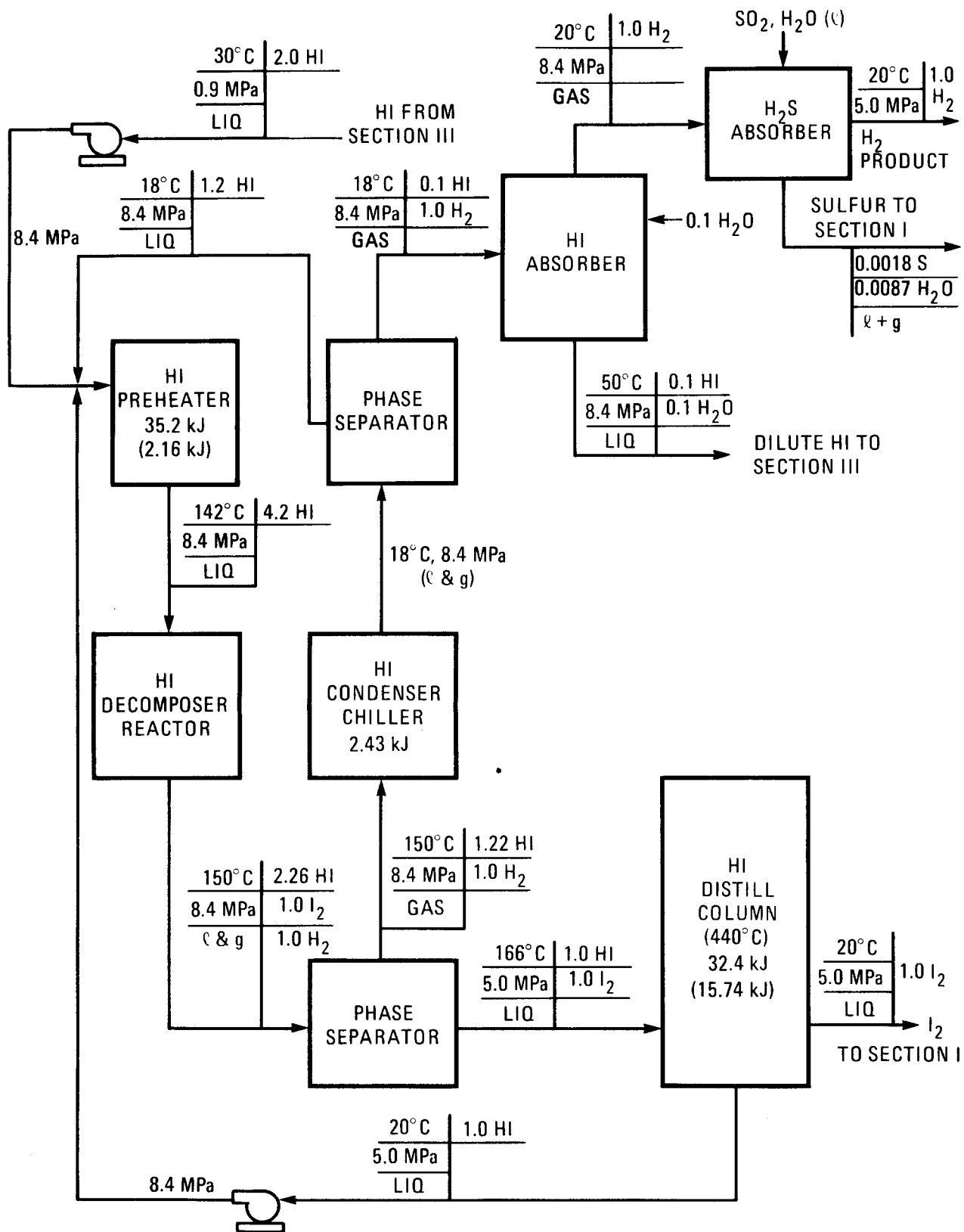


Figure 2-6 Section IV - Hydrogen Production from HI Decomposition. Molar quantities are for one mole of hydrogen product. Gross heat loads are given with net values in parenthesis.

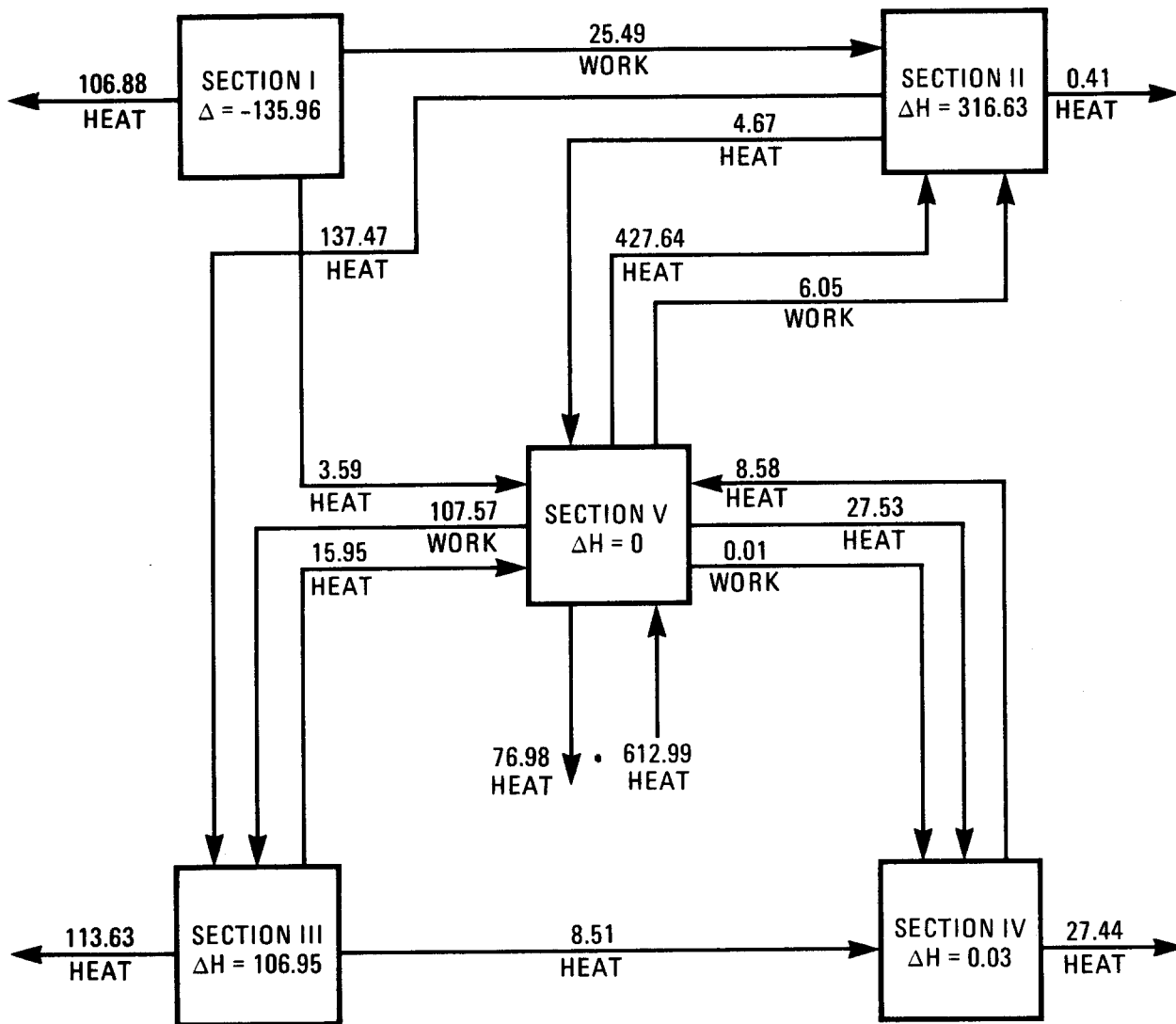


Figure 2-7 Energy Flows and Enthalpy Changes for Continuous Operation
 Quantities are kilojoules for one mole of hydrogen product.
 Reject heat is represented by unconnected arrows.

145°C liquid plus gas stream is separated with two thirds of the water and sulfuric acid as liquid and a gas stream of SO₂, O₂, and H₂O returned to Section I. In this design, the decomposer outlet gases recoup 96 kJ to the decomposer and the condenser transfers 13.6 kJ to the boiler. This would reduce the decomposer heat demand from 254 to 158 kJ and the boiler from 145 to 132.4 kJ; however, in a solar design it is doubtful the recuperation could be done in such an efficient manner. The gross heat demand of the concentrator is high, 391 kJ, but 236 kJ are internally recouped. The decomposer outlet contributes 104 kJ to the concentrator, primarily from the condenser. A 154 kJ heat demand would result without this heat recovery. The two pumps use a total of .007 kJ of work.

In Section I, the reaction actually occurs in four locations. The main reactor performs 52% of the total reaction forming the two liquid phases and a gas phase with oxygen and SO₂. This gas phase is separated and goes through a scrubber where fresh iodine is added to the gas to eliminate SO₂ from the oxygen that will be discharged. This performs 19% of the reaction.

The pressure of the two liquid phases is reduced and a gas phase of SO₂ and water is produced. The gas is sent to a second scrubber where a small amount of O₂ is produced and 22% of the reaction is accomplished.

The two liquid phases are also separated. Before sending the HI, water and I₂ liquid to decomposition (Sections III and IV), the SO₂ that is dissolved in the liquid must be removed to prevent side reactions that would form elemental sulfur and H₂S in Section IV. A small amount of oxygen from the scrubbing reactors is used in a stripping reaction to remove the SO₂ from the liquid stream as a gas.

Finally a "boost" reactor is used to perform the last 7% of the reaction. It has two functions: to recover the SO₂ from the stripper reactor effluent and to concentrate the sulfuric acid stream as much as possible before returning it to Section II. This way, the acid is concentrated from 50 to 57% in a useful fashion, using the main reaction, instead of using evaporation which is a parasitic load on the process. While it does not show on any of the flowsheets, the dilute sulfuric acid returned to Section II contains a trace of iodine. Because of its cost, it is important that the iodine is recovered and returned to Section I. This takes place in the first stages of the acid concentration in Section II.

The reactants for Section I are added at different points. The purpose of this is to have a fresh undiluted reactant added to each of the reactors to help drive the overall reaction to completion. The water from Section III and makeup water is added to Section I in the two scrubber reactors. Iodine from sections III and IV is added to the two scrubbers and the boost reactor. The effluent of these three reactors, containing H₂SO₄, HI, and large amounts of H₂O and I₂, is sent to the main reactor where the SO₂ stream from Section II enters Section I.

Section I does not have a large energy transfer. The main reactor operates at 0.5 MPa so the SO_2 stream must be compressed. The compressor and various pumps consume 5.58 kJ of electricity. However, a freon power cycle is run off the main reactor and 27 kJ of electricity is produced by the section.

Section III does not perform any of the three reaction steps. Instead, it separates the HI from solution in order to send pure HI to Section IV. To do this 18.2 moles of phosphoric acid, H_3PO_4 , must be added. This causes two liquid phases to separate, one rich in iodine, the other a solution of HI, water and phosphoric acid. Before the iodine is returned to Section II, a small stream of water is used to remove the minor fraction of phosphoric acid dissolved in the iodine. The HI liquid then is compressed from 0.3 to 0.9 MPa and distilled to separate it from the phosphoric acid and water.

The diluted phosphoric acid must now be concentrated to 83% for reuse in iodine separation and the water returned to Section I. The three stage vapor recompression evaporator that does this is a large capital cost item where the large amounts of shaft power (131 kJ) are needed to drive the compressors. In addition, it consumes 21 kJ of heat.

The HI distillation column operates with a heat demand of 571 kJ; however, most of this, 375 kJ, is internally recovered and another 146 kJ comes from the heat recovered within the section. Only 72.41 kJ of heat for HI distillation comes from outside Section III. In this section large amounts of heat and power are needed, so the need for recuperation is very important. The section has many internal heat transfer circuits.

In Section IV, it is important to take the decomposition reaction to the farthest possible extent. Large amounts of recycling and chemical processing were required in the previous sections to obtain the pure HI stream. The size and, therefore, the capital costs of those sections must be greatly increased if Section IV can convert only a small fraction of the HI into hydrogen and iodine. However, only 42% conversion can be achieved, so two recycle streams are used within the section. The pressure of the HI is increased to 8.4 MPa and it is preheated to 142°C . The decomposition of HI results in a two phase stream which is separated into a liquid with HI and iodine and a gas of HI and hydrogen.

The liquid is distilled into pure iodine, which is returned to Section I, and HI, which is returned to the feedstream for the decomposer reactor. While most components for Section IV are relatively low temperature, portions of this distillation column operate at 440°C .

The gas is cooled with an absorption chiller and condensed into another two-phase stream. After phase separation the hydrogen gas

is washed of HI and H₂S and reduced to a delivery pressure of 5.0 MPa. The liquid phase is virtually pure HI and is recycled to the decomposer. Very little HI leaves Section IV: only 0.1 of the 2 moles are not reacted. However, within the section, there is a significant recycling stream, 1.2 moles of HI, in order for the 2 moles of HI to produce the 1 mole of hydrogen gas.

Because the decomposition reaction is exothermic, the heat demands of the components in this section are small. The HI preheater has a heat demand of 35.2 kJ but after recuperation needs only 2.16 kJ from outside the section. Similarly the HI distillation column operates at 32.4 kJ, but because of its higher operating temperature requires 15.74 kJ heat input. The absorption chiller used 2.43 kJ of heat. Because the pressure of the decomposer is 8.4 MPa and the iodine distillation column and hydrogen delivery pressure are at 5.0 MPa, turbines provide 1.15 kJ to other sections.

D. Flowsheet Development

The chemical engineering flowsheet shows how a chemical process is actually to be built. Each stream is identified and temperature, pressure, and composition are specified. The function of each piece of process equipment -- reactors, heat exchangers, etc., is defined by the flowsheet. Design requirements such as conversion, heat transfer, etc., and materials of construction are established by the flowsheet. Chemical and physical properties for the chemical components of the process must be available or estimated, and it is often necessary to conduct laboratory investigations along with flowsheet development.

The flowsheet provides the information necessary to estimate the overall efficiency of a process and to design the process equipment. Cost estimates may be made after the equipment is designed. The quality of the cost estimate depends on the confidence placed in the flowsheet and the amount of detail in the equipment design.

Flowsheet development and laboratory studies for the GA process were started in 1973 and have continued since then. A major achievement of the GA process development program was the discovery of conditions under which the products of the main solution reaction separate into two phases. The chemical operations required to handle the upper H₂SO₄ phase are straightforward. The lower HI-bearing phase is more difficult. It forms an azeotrope, where both the HI and water vaporize together during distillation, and prevents the separation of HI. GA extracts the water with H₃PO₄ and thereby frees the HI for decomposition into H₂ and I₂. The H₃PO₄, diluted with water, however, must now be concentrated, a costly and energy intensive operation. The GA flowsheets that utilize phosphoric acid to liberate the HI were designed to achieve a high overall process thermal efficiency. This requires a great deal of internal heat recovery, particularly in the phosphoric acid concentration operations. It employs vapor recompression and much power for the required compressors.

There are promising alternatives to the H_3PO_4 approach. In research and engineering work performed at the Technical University of Aachen, FRG, (Refs. 10, 11, 12) HI is decomposed directly from the liquid phase in a distillation column. Preliminary indications are that the efficiency can be increased by 2-3 percentage points at costs slightly lower than the H_3PO_4 approach.

In Figure 2-8 the lower phase of the main solution reaction is pumped up to a pressure of 2.0 MPa and then flows through a regenerative heat exchanger (WAT-7 in Figure 2-8) where it is heated to 250°C. It then flows into a distillation column which is operating at 300°C and 2.0 MPa. Some of the HI decomposes directly into H_2 and I_2 and a mixture of HI, H_2O and H_2 is taken off the top of the column. The hydrogen is separated and some of the HI is sent to a decomposition process while the balance is returned to the column along with the water as reflux. A water-rich stream and an iodine-rich stream are taken off at the bottom of the column and sent through the regenerative heat exchanger, WAT-7, after which they are returned to Section I. This heat exchanger is large since it must handle the full flow of the lower phase from Section I.

The materials problems associated with I_2 and HI in solution at high concentrations and temperatures are severe and will require expensive equipment. The heat exchanger, which exchanges heat between the streams flowing to and from the reactor/distillation columns is large and expensive. More work is required and planned on the HI decomposition step. During the next two years, the Aachen workers plan to prepare a completely new flowsheet and cost estimate for the GA process.

Detailed flowsheets for the 1979 and 1981 GA processes exist for a continuously operated plant with a 3000 MWt 900°C helium heat source from an HTGR reactor (Ref. 6). Flowsheets also exist for a solar plant to annually supply 1,168 GWh_t to a scaled down 1979 plant. This solar plant uses a maximum process stream temperature of 870°C and operates Sections I, III, and IV continuously but Section II shuts down at night. It produces sufficient SO_2 during the day to supply Section I for continuous operation. Two energy storage methods were examined. Only the flowsheets for the solar portion are given (Ref. 9). A third energy storage technique using elemental sulfur has also been presented. A flowsheet was prepared for the sulfur preparation portion of a solar interface (Ref. 13) where but the balance of the interface and the rest of the chemical plant are not shown. GA has estimated that the addition of the solar interface to their process will lower the overall efficiency to about 40%. The work done to date may be characterized as a partial adaptation of previous work done for the HTGR. More flowsheet development, both to improve the GA process and to adapt it completely to a solar heat source, is required.

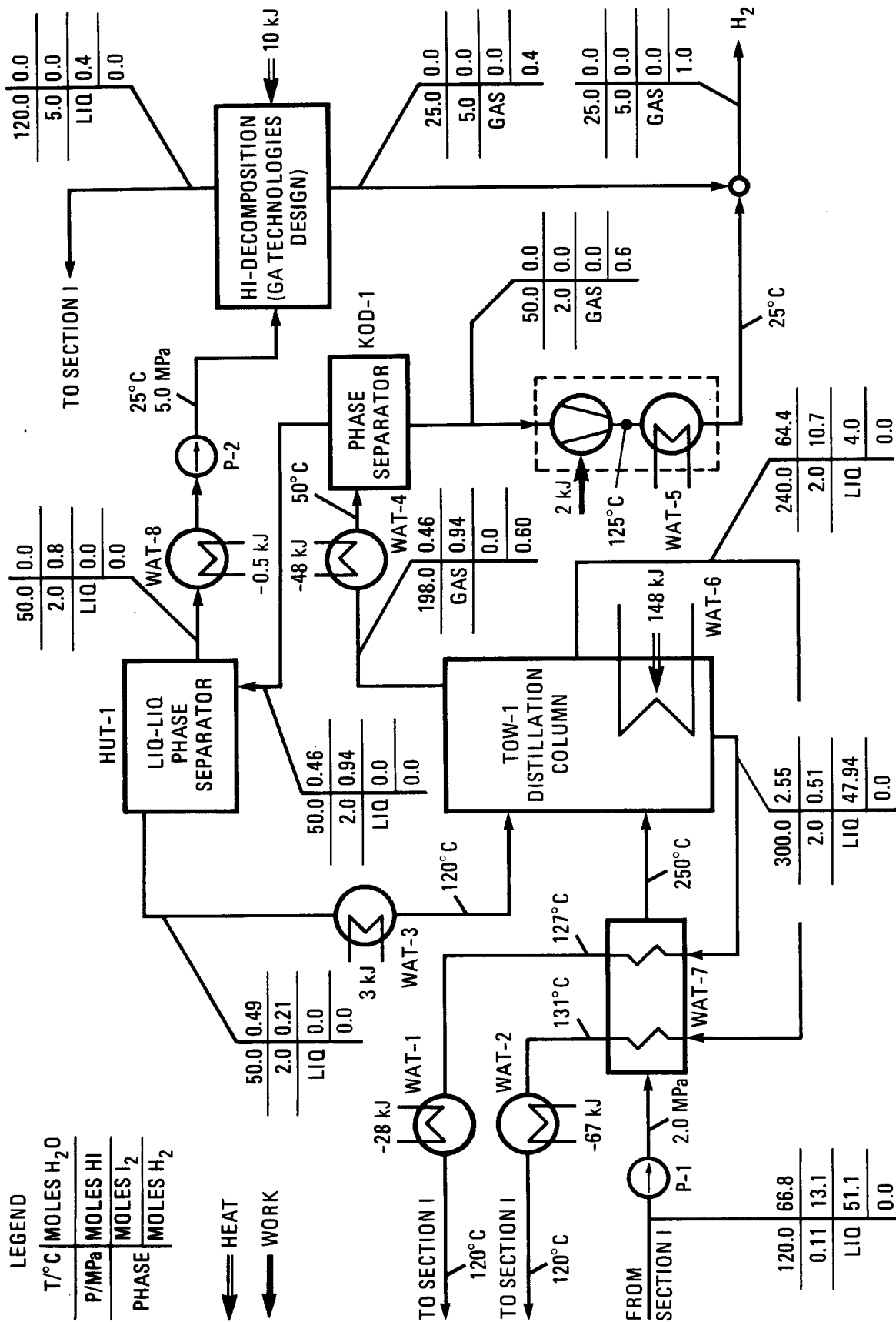


Figure 2-8 University of Aachen Flowsheet Replacement for Sections III and IV. Molar quantities are for one mole of hydrogen product.

E. Component Design and Materials Issues

This thermochemical cycle contains several severely corrosive process streams. In Section II the concentration of the sulfuric acid is increased from 57% to 98%, passing through a composition range where metals are severely corroded. Boiling and decomposition of the sulfuric acid constitute other corrosive environments; these will be discussed in the solar interface portion of this report. In Section I, the I_2 - HI - H_2O solutions create a complex of HI^x species which are severely corrosive. In Section IV pure HI, HI and I_2 ; and HI and H_2 mixtures exist. All are corrosive but not as aggressive as the streams in the other sections.

In Section II the concentration of sulfuric acid is accomplished in two stages, using a high pressure (7.6 MPa) staged concentrator to increase the acid concentration to 79% and a low pressure distillation column (0.02 MPa) to increase the concentration to 98%. The vessels for both components are made of fluorocarbon-lined mild steel with acid brick internal insulation for thermal protection of the fluorocarbon. Heat transfer tubes in the concentrator and in the reboilers of the distillation column are made of silicon-impregnated silicon carbide (SiSiC) U-tubes and headers. The internal trays of the distillation column are also made of SiSiC.

Fluorocarbon-lined mild steel is also the construction used for the iodine - separation column of Section III, the HI decomposer of Section IV, the O_2 scrubbers, boost reactor and SO_2 stripper of Section I and the feed stream pipes, vessel tube sheets and heads of the main reactor. A hydrocarbon lining is used in the H_2 scrubber of Section IV where the corrosive environment is less severe. For the HI distillation column in Section III, where water, HI, iodine, and phosphoric acid are all present, the trays are Hastelloy C-276 with the column being mild steel clad with Hastelloy C-276. In Section IV where the distillation column is exposed to only HI and iodine, Hastelloy B-2 is used for the trays and column cladding.

Most of this construction is typical for chemical plant components, although metallic cladding requires special attention to design and fabrication. The use of ceramics for heat exchangers, components, and distillation trays is unique. For the trays the mechanical loads are not severe and conditions that would thermally shock the trays are not expected to occur in the column, so the application of ceramics is not expected to be difficult. Ceramic heat exchanger components similar to the design used here have been constructed for development purposes but are not yet common in the marketplace. In addition, the proposed design of the heat exchanger for the high pressure staged concentrator uses U-tubes 2 m high from head to apex. Large ceramic components such as this are expected to need significant development effort.

The main reactor of Section I has some of the most severe corrosion problems. To date only refractory metals have shown adequate corrosion resistance. The reactor tubes and tube sheet liner are made of niobium and must be welded together. Because refractory metal welding requires vacuum equipment, special fabrication techniques will be required for the reactor tube bundle. One of the liquid phases of the product stream of the main reactor contains 50% sulfuric acid. Niobium has exhibited a moderate corrosion rate (0.27 mm/yr) at slightly more concentrated acid levels, 60%. This may require a different refractory metal to be used.

For the alternative HI decomposition method, the product stream is taken directly from Section I and the HI is decomposed at 300°C and 2.0 MPa. The reaction takes place from the water-HI-iodine solution. Corrosion testing (Ref. 14) for containment materials of this solution has previously been conducted for the main reaction at ambient pressures and temperatures from 23 to 125°C. At 125°C, some metals which did not corrode at 97°C were now incompatible with this solution. No corrosion testing has been performed at higher temperatures, but the corrosion environment is expected to be severe. Quartz tubes have been successfully used in laboratory experiments, but quartz lined vessels are not typically used at elevated pressures. The heat exchanger prior to the distillation column uses the iodine stream to heat the water-HI-iodine stream, so corrosion protection will be needed for both fluid streams. Significant corrosion testing and component development will be needed to implement this new part of the process.

For the more established parts of the process, fluorocarbon-lined mild steel is used. Depending on the final component design, less expensive construction, such as hydrocarbon or glass lining may be suitable. Where metallic construction is needed, careful materials selection will be particularly important because of large differences in cost for both materials and fabrication. Flowsheet development for Section I has been performed with an attempt to minimize component size where niobium is required. Further flowsheet modifications are expected as increased knowledge of the corrosive effects of these solutions is acquired.

F. Internal Heat Recovery

In any thermochemical process there always will be a number of endothermic steps and a number of exothermic steps. For example, in sulfuric acid decomposition, the acid must be concentrated, decomposed to SO₃ and H₂O and the SO₃ decomposed. These are endothermic steps. Cooling the product gases for further processing is an exothermic step. Energy from the exothermic steps must be recovered to supply the energy requirements of other parts of the process. If electricity is required, it may be necessary to operate power cycles which utilize heat from exothermic process steps.

In general, it is desirable to minimize internal heat recovery since the required heat exchangers are expensive and they cause irreversibilities. On the other hand, it is necessary to recoup heat internally in order to keep the efficiency up. Finally, the amount of internal heat recovery should be decided on the basis of economics. Designing a flowsheet for very high efficiency may result in very expensive process equipment, which will cause the capital recovery portion of the production cost to be high. However, when the efficiency is high, the energy component of the production cost is low. There is a trade-off between capital cost and efficiency, and the minimum production cost comes from flowsheet variations along with cost estimates for the associated process equipment.

Table 2-1 shows the energy balance of the sections for the 1979 process version. A total of 1720 kJ/g mole H_2 of heat are recovered from and used in various sections of the process. This is six times the heating value of the hydrogen produced.

Potentially high process thermal efficiency is one of the attractive features of thermochemical processes. By the very nature of thermochemical processes, various streams must be heated and cooled. If none of the heat were recovered, and the 1720 kJ were added to the rejected heat, the process efficiency would fall to 13%. The internal heat recovery situation is also affected by the amount of material recirculation required by the process.

Tables 2-2 through 2-4 are summaries of the heat matching tables for flowsheets of the different sections. They show the internal heat recovery within the sections along with the temperature range and the energy recovered. The heat recovery in each section is specialized for a particular purpose. In Section III, the heat from the vapor recompression evaporator is used to preheat the water-HI-iodine stream for distillation. The many small temperature ranges used in the heat recovery increase the process efficiency. Whether this is a reasonable design depends on the overall size of the plant and the nature of the heat recovery streams. The smallest heat load of any heat exchanger is 0.3 kJ/mole of H_2 . For a plant sized to the MARS reactor, however, this corresponds to a thermal duty of 15 MW. While using many small temperature ranges will increase the number of heat exchangers, for a large plant size parallel units of heat exchangers will be required to accommodate the total thermal load. The process efficiency may be improved by using smaller temperature differences and heat exchanger units in series instead. A review of the individual heat exchangers in the flowsheets showed the minimum temperature difference (hot side in to cold side out) used in the process is $10^{\circ}C$. While small, this temperature difference is within the normal heat exchanger practice. However, this will result in greater surface area requirements for the heat exchanger. For corrosive process streams, this will further increase the capital costs. In Section II about half the energy recovered is from water removed from the sulfuric acid. However, most other heat recovery is from HI, I_2 , $SO_2-SO_3-H_2O$ and phosphoric

TABLE 2-1
ENERGY BALANCE

kJ/ mole H ₂						Process	Section V	Overall Total
	Section I	Section II	Section III	Section IV	Process Sections Subtotal			
Gross Power Load	0.50	31.32	126.53	0.01	158.79	239.27	398.06	
Power Recovery	23.53	0	22.90	0	46.43	351.97	398.40	
Net External Power Demand	-23.03	31.32	104.06	0.01	112.36	-112.70	0	
Gross Heat Load	191.24	792.47	1087.18	98.26	2169.15	558.29	2727.44	
Heat Recovery	186.19	512.74	944.20	77.39	1720.52	33.70	1754.22	
Heat from Other Sections	5.05	0	151.43	8.45	164.93	0	164.93	
Net External Heat Demand	0	421.29	0	27.34	448.63	159.84	608.47	
Net External Energy Demand	-23.03	452.61	104.06	27.35	560.99	47.14	608.13	
Heat to Other Sections	0	141.56	8.45	14.92	164.93	461.05	625.98	
Reject Heat	116.18	0	140.86	18.18	275.22	44.76	322.98	
Enthalpy Δ	-134.16	311.05	106.18	2.70	285.77	0	285.77	

TABLE 2-2
INTERNAL HEAT RECOVERY IN SECTION II

Temperature	Energy
°C	kJ/mole H ₂
871 - 537	73.00
537 - 434	22.55
434 - 372	13.53
372 - 355	3.72
355 - 340	36.83
340 - 300	45.32
300 - 263	31.83
263 - 222	16.83
222 - 207	11.06
207 - 177	95.82
177 - 152	75.07
152 - 132	4.06
132 - 120	5.05 to Bottoming Power Cycle

TABLE 2-3
INTERNAL HEAT RECOVERY IN SECTION III

Temperature	Energy
°C	kJ/mole H ₂
250 - 247	12.01
247 - 237	41.76
237 - 218	81.23
218 - 205	58.71
205 - 187	143.91
187 - 172	222.00
172 - 163	79.02
163 - 143	85.47
143 - 95	58.37 to Bottoming Power Cycle

TABLE 2-4
INTERNAL HEAT RECOVERY IN SECTION IV

Temperature	Energy
°C	kJ/mole H ₂
440 - 352	6.78
352 - 258	7.30
258 - 224	2.60
224 - 120	23.33
120 - 75	9.89
75 - 35	8.70 to Bottoming Power Cycle

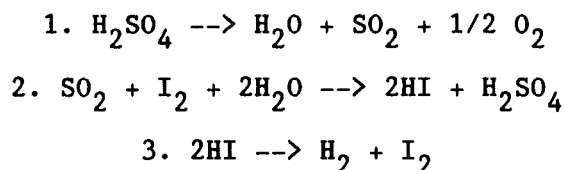
acid streams. Where it is necessary to recover large amounts of heat from corrosive streams, such as in Section III, the use of an intermediate heat transfer fluid may be advisable. The flowsheets do not indicate such features.

An important consideration in future flowsheet development will be the variation of the amount of internal heat recovery. In the selection of intermediate heat transfer media, the minimum temperature differences for heat exchangers and the resulting component size, materials of construction and thermal efficiency will be a major factor in the economics of hydrogen production.

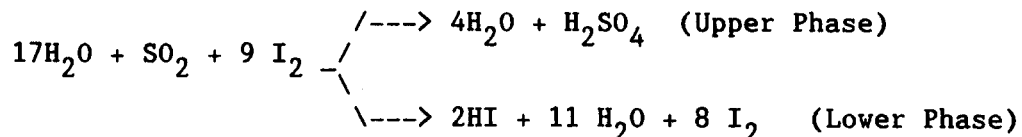
G. Recirculation of Process Streams

The stoichiometry of a thermochemical process determines the minimum recirculation of process streams. It is always desirable to minimize the actual recirculation since it affects both heat transfer and separation requirements. Both worsen as the amount of material recirculation increases. The chemistry of the process and the design of the flowsheet determine the amount of material recirculation.

The three reactions of the GA process show that the use of sulfuric acid as a reagent requires only one mole of water to recirculate:



This, however, is not the cause of the large recirculation quantities. The requirement of the second reaction - the so-called Bunsen reaction - in the flowsheet devised by GA is that two phases must be formed. The upper phase contains the H_2SO_4 and the lower phase contains the HI. The reactions written with approximate real mole quantities are:



As can be seen, 15 excess moles of water must be handled along with 8 excess moles of I_2 . The large amounts of both water and iodine are introduced because they create the two immiscible liquid phases. Much experimentation in devising phase separation techniques led to the selection of these phase compositions. However, this results in the need to concentrate the H_2SO_4 from the upper phase by boiling off some of the water.

This water vapor must be condensed and, if possible, the heat of condensation recovered for use elsewhere. From the lower phase the I_2 must be recovered for recycle and the HI must be recovered for

decomposition to the hydrogen product and I_2 for recycle. As the recirculation of process streams increases, the capital cost of the plant also increases. Additional equipment and/or larger equipment is required for the separation and transport of the process streams.

In Section III, 18 moles of phosphoric acid form a recirculation loop with 15 moles of water from the HI stream. Here a minimum of 4 moles of water remains within the phosphoric acid loop. Earlier flowsheets removed more of the water, but a flowsheet improvement showed that the required concentration of the acid could be lowered. In this case, it was found that more recirculation was better than increased costs of higher acid concentration in other portions of the cycle. The phosphoric acid cycle is not intrinsic to the thermochemical cycle (Reactions 1-3) and, therefore, its elimination has been sought in process improvement studies.

Because of previous recirculation prior to Section IV, the pure HI stream is decomposed to the greatest extent possible. The decomposer converts only 48% of the HI stream. Reaction schemes that would allow a greater conversion of the HI would be desirable.

The chemistry of the process is known well enough to design a flowsheet. In this process there are five components and two phases. The effect of temperature, composition and pressure on the behavior of the system was determined in a GA laboratory program conducted during the 1970s. Another laboratory program in Aachen is aimed at obtaining the physical and chemical data required to improve the HI separation and decomposition step.

H. Process Thermal Efficiency

The process thermal efficiency is defined to be the higher heating value of the hydrogen produced, ΔH , divided by the total thermal energy, ΔQ_t , (heat) required to produce the hydrogen. The higher heating value is used because liquid water is assumed to be the feedstock. It has nothing to do with burning the product.

Chemical processes are subject to a Carnot-type limitation on their efficiency.

$$\text{where } \eta = \frac{\Delta H}{\Delta Q_t} \leq \frac{T_m - T_o}{T_m} \frac{\Delta H}{\Delta G}$$

T_m = thermodynamic mean temperature

T_o = sink or atmospheric temperature

ΔG = Gibbs function change for water decomposition = 237.2 kJ/gmole

ΔH = 285.8 kJ/gmole

The ΔH and ΔG are standard values at 25°C for liquid water decomposition to gaseous hydrogen and oxygen.

For example, if the thermochemical process is supplied by a stream which enters at 1255° K and leaves at 773° K the thermodynamic mean temperature, T_m , is 1014° K. If the sink temperature is 300° K, the maximum value is 0.85. For the current process this efficiency

may be further refined by adding the 28.6 kJ/mole for work of separation for water-HI-iodine phase and a maximum temperature of 870°C. This results in an efficiency maximum of 0.74. Unavoidable irreversibilities reduce the thermal efficiency and cause heat rejection to occur. The flowsheet for the process determines both the thermal efficiency and the cost of the process equipment and each of these affects the hydrogen production cost. The process requirement for large recirculation volumes necessitates heat recovery and introduces additional irreversibilities as the process becomes more complex.

The original GA flowsheets resulted in a 47% overall process thermal efficiency. This number has not been independently verified. Based on the reduced heat demand of Section III, the alternate Aachen approach would increase this efficiency to 50% with approximately the same capital costs.

Another study (Ref. 4) proposed the use of a 1250°C helium stream and a silicon carbide reactor to heat the sulfuric acid to 1086°C for decomposition. While details of the flowsheets were not given, it was estimated that the cycle would have an efficiency of 53%.

The process efficiency is strongly coupled to the capital costs of the plant. Decisions to reduce capital cost by limiting the equipment used for heat recovery will reduce efficiency. For the MARS fusion reactor (Ref. 5), the proposed freon bottoming power cycle was replaced with a low temperature steam cycle. Electricity as well as heat was input to the process. Calculating the thermal equivalent of the electricity results in lowering the efficiency to 40%. However, a low temperature steam cycle operates between 130 and 380 °C at an efficiency of .13. It provides 25% of the electrical energy of the system, and eliminating it would drop the cycle efficiency to 35%. Compared to the plant capital costs, the bottoming cycle does not significantly raise the total plant investment. However, because many of the process streams are corrosive, rejecting the heat instead of using bottoming cycles has the added advantage of allowing greater temperature drops within the components. The smaller size that would result may lead to significant cost savings especially where expensive materials must be used. In these cases, only detailed flowsheet analysis will be able to determine whether greater efficiency in the design is desirable.

GA has estimated that interfacing the process to a solar heat source causes the efficiency to drop (Ref. 13). With the use of the 24-day sulfur storage concept, it was estimated that the efficiency would drop from 47% to 40%. For a nitrate salt - SO₂ storage, the efficiency was estimated to be 41%, with the storage of SO₂ accounting for 4 percentage points of the efficiency decrease.

3. STATUS OF THE SOLAR INTERFACE

For every heat source considered, new flowsheets are needed for the process. For solar this is especially important. While the diurnal nature of the solar source is a major difference, the receiver design and heat recovery systems within the solar power system need close consideration. Sections I, III, and IV of the process do not require close coupling to the energy source. In most designs, however, they are closely coupled to the other process sections by the transfer of power and heat through heat recovery systems (Refs. 3, 4, 6). The large plant sizes used in previous flowsheets cause additional uncertainty in adaptability for solar. A large, single solar system would have a design point capacity of 640 MWt (Ref. 29). Such a plant would supply a chemical plant with an approximate continuous capacity of .25 k-mole H_2 /sec. By comparison flowsheet efforts to date have been for plant capacity sizes of 1 and 5 k-mole/sec. The smallest heat exchanger in the chemical plant must transfer .3 kJ per mole of H_2 produced. For a solar plant this heat exchanger is 750 kWt, which is still an appreciable size. While the question of capital cost and corrosion protection remains unanswered, it appears from a thermal duty standpoint that all heat exchangers listed in the flowsheets are large enough to be built for commercial sizes of solar systems. For heat exchangers larger than about 20 MWt, parallel units will be needed.

Numerous parallel units and components exist in the designs for the large nuclear reactor powered plants. Because these plants are of a size where nearly all process components are taking on modular form, there may be less economy of scale realized. The chemical plants that were sized for the expected capacity of nuclear reactors and not optimized based on the chemical plant design. A smaller chemical plant size with a solar central receiver heat source cannot be considered a less desirable configuration based on economies of scale.

It would be expected, then, that the general use of heat exchangers for heat recovery would be the same for a solar plant as in earlier flowsheets for large nuclear plants. Differences would mostly arise from physical constraints of receiver design imposing limits on the placement of heat recovery units, incorporating energy storage design features, and using the thermal transport media that is shown to be appropriate for solar thermal systems.

A. Temperature and Heat Requirements

Table 3-1 lists the gross and net thermal energy demands for the process. Because of the incorporation of features from updated flowsheets (Ref. 5), some of the values in this table differ slightly from the 1979 energy balance. The process must also be supplied with 141 kJ/mole of work, mostly to Section III. While shaft power can be used in some of these applications, it is expected that most power recovery would have to be in the form of electrical generation. For the .25 k-mole H_2 /sec capacity hydrogen plant, this corresponds to a total heat demand of 115 MWt

TABLE 3-1
HEAT DEMAND OF THE CHEMICAL PROCESS

	Net Heat Demand kJ/mole	Gross Heat Demand kJ/mole	Temperature °C
Section II			
Decomposer	158	254	527 - 900
Boiler	132	145	360 - 540
Concentrator	50	391	120 - 370
Section III			
HI distillation column	72	571	150 - 282
Vapor recompression evaporator	21	*	282
Section IV			
HI - I ₂ distillation column	16	32	260 - 440
HI reactor preheater	2.2	35	130 - 225

and 35 MW_e, with 40 MWt of the heat demand required at the decomposer temperatures while the rest is needed for processes below 870°C.

The heat demand for the process exists over a wide temperature range. This restricts the use of a single heat transfer medium as is commonly used for solar thermal applications. Several solar interface designs and design features have been examined. Similar to other fuels and chemicals applications for solar, the use of chemical energy storage has also been examined. For nuclear interfaces, a helium secondary heat transfer loop is used. However, such an interface presents several disadvantages and is not necessary for solar. Most concepts use an in-receiver reactor to decompose the sulfuric acid to SO₂. Because of the wide temperature range for other heat demands, additional receivers are usually included. With the large heat recovery requirement, thermochemical hydrogen plants are expected to be capital intensive. The hydrogen portion of the plant is usually configured for continuous operation.

Capital costs have been estimated only for the interfaces, using the nitrate salt-SO₂ and the SO₂-O₂ storage concepts and the sulfuric acid decomposition interfaces (Ref. 15) that do not include storage. In Ref. 15 some of the component designs and costs are not included.

B. Interface Descriptions

i. Nitrate Salt - SO₂

This solar configuration uses two types of storage. Figures 3-1 and 3-2 show the energy balance for day and night operation of the system (Ref. 9). A nitrate salt receiver is used to store heat during the day and supplies heat for the distillation and phosphoric acid concentration in Sections III and IV as well as 19 MW of power. The nitrate salt is discharged only at night. During the day enough SO₂ is made to run the plant continuously. The SO₂ is stored as an aqueous solution of 2 moles of SO₂ and 12.2 moles of water at 0.2 MPa. An "SO₂ Solution System" is used to cool a portion of the SO₂ - O₂ output of the decomposer, reject the oxygen, introduce water, and form the solution for storage. During the night the aqueous solution is discharged by supplying Section I. The additional water is not a problem because a large amount of water is required in the main reaction. This is normally supplied by the water returning from the Section III phosphoric acid reconcentration step. Here, that water is stored during the night and used to make the aqueous SO₂ solution during the day. The dilute sulfuric acid produced by Section I is stored during night operation and, like the decomposition, is concentrated only during the day. Section I operates in a somewhat different manner during the day and the night because no oxygen evolves during the night and the SO₂ process stream is cooler.

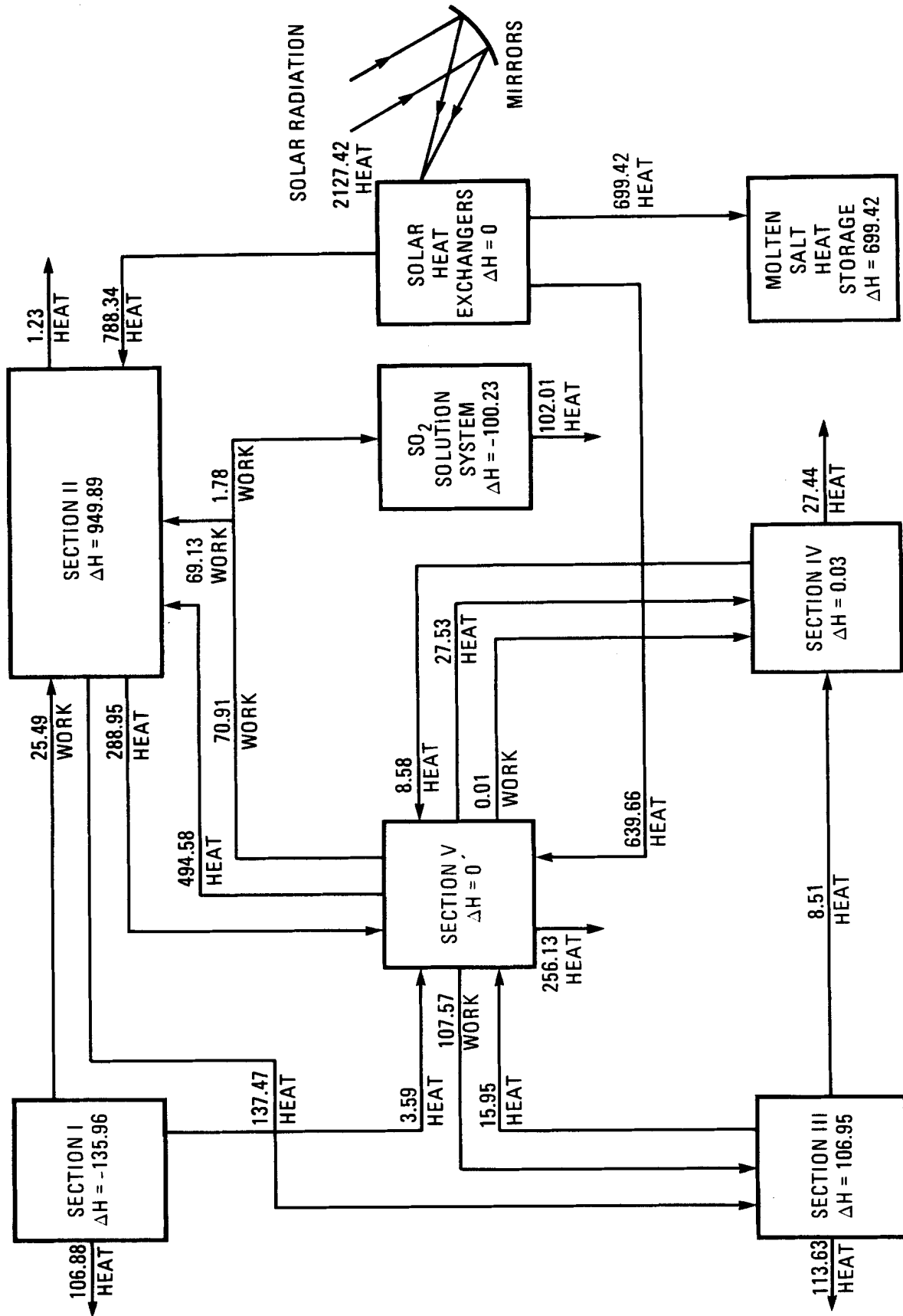


Figure 3-1 Daytime Energy Flows and Enthalpy Changes for Molten Salt Heat Storage - SO_2 Solution Storage (Ref. 9). Quantities are kilojoules for one mole of hydrogen product. Reject heat is represented by unconnected arrows.

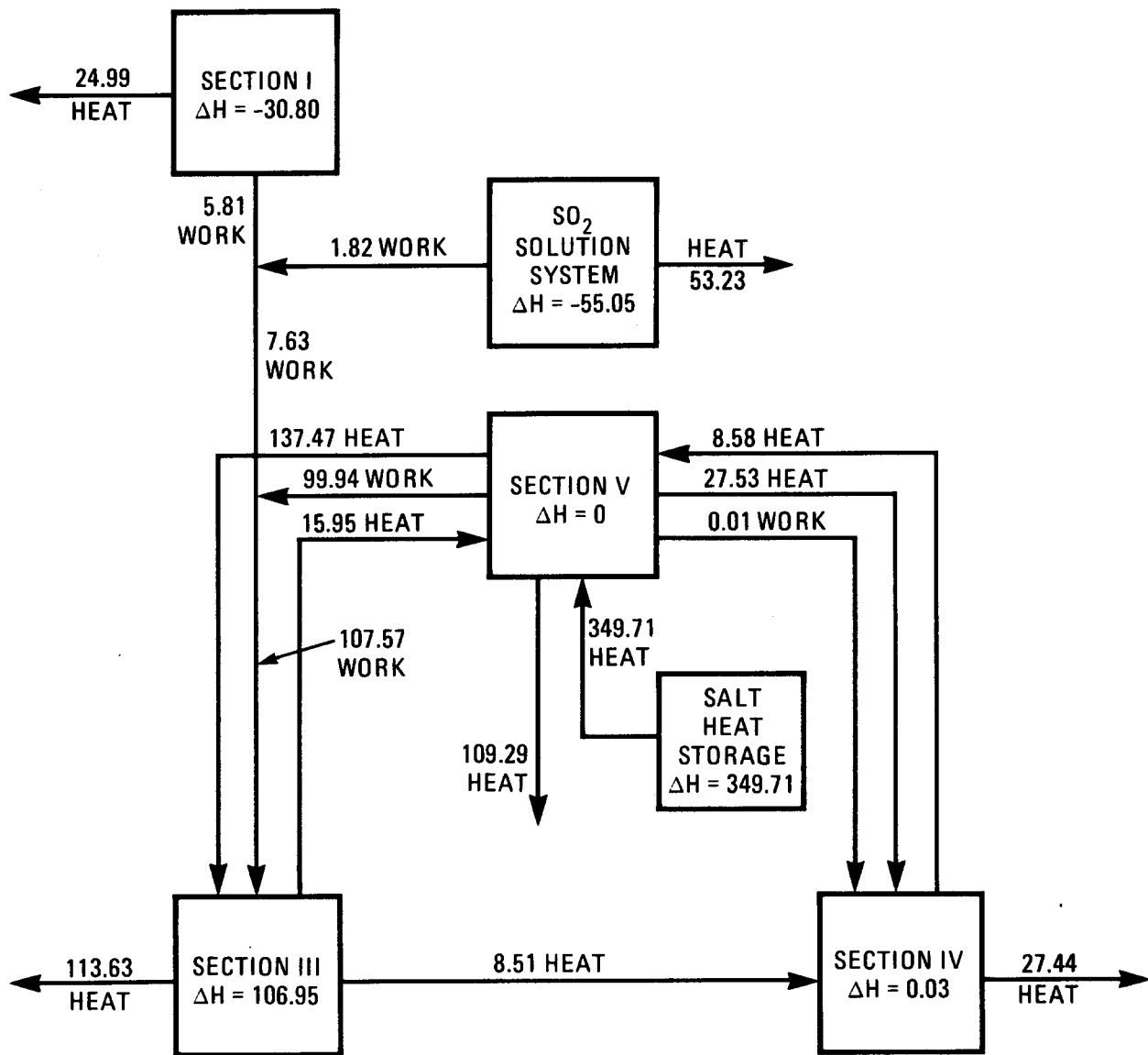


Figure 3-2 Nighttime Energy Flows and Enthalpy Changes for Molten Salt Heat Storage - SO₂ Solution Storage. Quantities are kilojoules for one mole of hydrogen product. Reject heat is represented by unconnected arrows.

Additional receiver systems and heat transport cycles are included in the interface. Because there is a large, nearly isothermal heat demand above the critical temperature of water, mercury was chosen as a more efficient heat transfer medium, operating at 465°C , where the latent heat of condensation is used. There is a mercury receiver, which provides some power as well as the heat to vaporize the sulfuric acid. The nitrate salt circuit uses three mercury cycles, two which supply only power and a third which supplies both power and heat for Sections III and IV. In addition to these three mercury cycles, the nitrate salt circuit has three steam-water cycles analogous to the mercury cycles, but at slightly lower temperatures.

The value of using mercury in rankine cycles has been recognized for a long time. In fact, several mercury power generation plants have been built. These have now been closed. The toxic and materials problems that mercury presents makes it unlikely that these cycles would be included in commercial designs.

A fourth, helium, receiver is included in the design. This helium stream provides the heat for the distillation column in Section IV.

The decomposer receiver contains three recuperation cycles where the outlet gas is used to preheat the incoming gas stream. A second helium cycle is used to provide a portion of the heat to the distillation column in Section IV. A freon bottoming cycle generates considerable power.

The material balance indicates that heat transfer from the nighttime streams is performed directly with the process stream of the distillation column. It is difficult to envision either molten salt or HI-I_2 solutions traveling between the molten salt tank and the distillation column. This is particularly true because of the range of temperatures which is specified for the salt, $227\text{--}600^{\circ}\text{C}$, compared to the recommended range of $288\text{--}566^{\circ}\text{C}$ and its melting point, 221°C . In addition the pumps for the molten salt, sulfuric acid, and helium appear to be omitted (Ref. 6).

It is expected that this interface design would undergo considerable revision in more detailed designs. The mercury and helium receivers as well as the helium recuperation cycle would be eliminated. An additional thermal transport media would be used to avoid freezing problems where the present design uses nitrate salt below 288°C .

The solar plant for this interface design is sized at 400 MWt peak capacity and assumes that solar energy will be gathered at full power for 8 hours a day. The plant is assumed to run continuously, using storage for 16 hours a day. A 64 hour storage capacity is used. Section V would be considered to contain all the heat transfer circuits with the exception of the sulfuric acid decomposer circuit. The heat out of the molten salt during the night is half the daytime heat input. Charging storage above 16 hours is not included in the energy balance and is assumed to occur when excess solar energy is available. The only effect of the storage capacity

selection on the design is the increased capital cost of the tanks. The level of detail of this interface design uses only the above assumptions and does not incorporate energy availability on a daily balance to determine receiver, storage size and dispatch strategies. From the energy balance in Figures 3-1 and 3-fff2, the thermal efficiency of the process is calculated to be 41% for continuous day and night operation.

ii. SO₂ - O₂

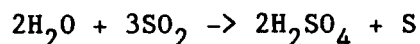
This interface replaces the nitrate salt receiver with an expanded SO₂ loop (Ref. 6). The water is condensed from the decomposer outlet stream. A portion of the gaseous outlet stream is sent to the SO₂ solution system used in the previous interface design. The oxygen is separated and discarded. An aqueous solution of SO₂ is produced to provide the reagent needs of the chemical plant. The remaining outlet stream is a mixture of SO₂ and O₂ that is stored in the gaseous phase at 0.2 MPa pressure. The SO₂ - O₂ storage is used solely as a nighttime energy source through the combustion formation of SO₃. Water is added to the SO₃ gas to form sulfuric acid in another exothermic reaction from which heat is recovered. Only a small amount of water is needed for this, so the product is concentrated sulfuric acid instead of the more dilute acid produced by the Section I reaction. This storage concept only slightly increases the sulfuric acid concentration requirements of the plant.

The remainder of the interface includes the helium and mercury receivers and the same power cycles as described for the nitrate salt - SO₂ solution system. The same assumptions regarding the acquisition of solar energy and the nighttime operation off of storage are also used. This system is slightly more efficient, 43%. However, the need to store the oxygen as a gas results in a large and expensive storage tank that dominates the system cost. This results in a cost 4 times the nitrate salt system.

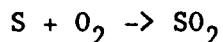
By compressing the gas, expelling the oxygen, and liquifying the SO₂, the storage size could be reduced. Air is used for combustion but the entrainment of nitrogen in the system results in increased sizes for some components and a slight efficiency loss. The end result is that the system is less expensive but is still estimated at twice the cost of the nitrate salt system.

iii. Elemental Sulfur

When water reacts with SO₂, a disproportionation reaction will produce elemental sulfur (Ref.13):



The sulfur would be used as a storage medium and combusted to release energy:



The disproportionation reaction would be performed around 0.25 MPa and 149°C where liquid sulfur would be produced. While this reaction does not require a catalyst, it is slow, and the SO₂ must be dissolved in the water. About 95% of the SO₂ will react in one hour. Because the solubility of the SO₂ gas in water is only 0.6 molar %, large quantities of water will be needed. It is believed that the additional gas will easily dissolve in the water as the formation of H₂SO₄ removes it from the water and that the reactor design could be relatively simple, using existing reactor technology and a sparging system to dissolve the SO₂ into the water. It is expected that the sulfuric acid exit stream would have approximately the same concentration (57.6%) as the acid from Section I. The disproportionation reaction is exothermic, 262 kJ/mole of S, and this low grade heat would be used in the acid concentration step of Section II. It is possible that a catalyst could speed the reaction, but no development efforts have been performed in this area.

Because the storage of oxygen is not economically practical, the sulfur combustion (301 kJ/mole of S) would be performed with compressed air and a ceramic turbine at 1225°C. This will provide the power, 94.16 kJ/ mole of H₂, and heat, 171.33 kJ/ mole of H₂, to operate the hydrogen plant at night. This will provide both adequate energy and SO₂ reactant to operate Sections I, III, and IV. Part of the Section II concentration of the acid, to 72%, can be performed at night, but the final concentration will require daytime solar energy.

Flowsheets exist only for the partial acid concentration step (Ref. 13). Detailed flowsheets for the sulfur production or combustion are not documented. Considering the long reaction time for the disproportionation reaction, the concept needs to be developed further before reaction vessels and intermediate storage capacities can be defined. Similarly, component costs cannot be estimated. Preliminary designs suggest that phosphoric acid reconcentration would be performed in direct contact heat exchangers within the sulfur combustion system. Because, in the current design, the vapor recompression components of Section III represent a significant portion of the capital cost and energy consumption of the entire plant, the purpose of redundant components for nighttime use is unclear. Comparison with Table 3-1 suggests that the heat and work derived from sulfur combustion is most efficient with the liberation

of more heat but with less power than the vapor recompression system requires. Direct contact heat exchangers used at night would be a better match to the sulfur burning heat source.

The combustion of sulfur using air poses the problem of carryover of nitrogen as an inert gas. The preliminary design suggests that a gaseous mixture of SO_2 , O_2 , and N_2 would enter Section I in the boost reactor, pass through the main reactor and expel the nitrogen with the oxygen from the scrubber. This would require nearly the entire Section I system to handle five times the gas volume. The biggest impact involves the main reactor whose physical size should be minimized because of the need for niobium in its construction. It represents 40% of the cost of all of Section I. A more plausible approach would be similar to the "SO₂ Solution System" described for the SO₂ aqueous storage concept. After heat recovery from the combusted gases, the SO₂ would be dissolved in water, rejecting the O₂ and N₂ before entering Section I. In this case the system could be continuous during the nighttime and no significant storage capacity would be required.

This system might also be used during the daytime to prepare the portion of the process stream from Section II that will enter the sulfur production system.

The attraction of the elemental sulfur storage concept is that it can provide indefinite chemical energy storage in a cheap, easily contained material. The sulfur will probably be stored as a liquid in carbon steel tanks at 120-150°C, although it is also possible to store it as a solid. The indefinite nature of the storage has suggested the term "seasonal storage" to indicate its use for extended periods of low insolation on a yearly basis. A 24 day storage capacity is proposed. While it is assumed to be cheap enough to store large amounts for long periods of time, there is no basis given, such as annual energy availability, for the selection of 24 days.

In addition, several other factors must be considered. For every mole of sulfur that is stored (which when combusted produces one mole of hydrogen), three moles of SO₂ must be produced. Assuming 16 hours of nighttime operation, for daily nighttime use Section II must be enlarged seven times. In addition, accompanying storage must be supplied for the 72% sulfuric acid that nighttime or storage-driven operation produces. Because four times the storage volume as well as stainless steel construction will be required, the sulfuric acid will dominate the storage costs. It is estimated that the process efficiency with the sulfur storage is 40%. It is not known whether this includes the annual build-up of 24 days of storage or is for daily operation. The lack of process details does not permit independent determination of this efficiency.

Comparisons of storage size requirements does not lead to the conclusion that this storage method would be vastly cheaper than others. Energy storage density is higher than other media, but when the H₂SO₄ storage requirement is added, the elemental sulfur

storage density is 3384 MJ/m^3 . Nitrate salt, assuming a 380°C temperature difference and requiring equal volumes for storage of the hot and cold salt, has a density of 532 MJ/m^3 . Still, a nitrate salt storage concept requires the storing of SO_2 aqueous solution and dilute H_2SO_4 adding 60% to the total storage volume required for a system using nitrate salt. However, the sulfur storage concept requires the production of three times the SO_2 to supply the disproportionation reaction. For the 24 days storage, the total volume of storage capacity would be 12 times greater than for the molten salt system. Also, the entire solar system and most of the Section II capacity would have to be increased by a factor of 2.4 for the sulfur system. If a large storage capacity is required to limit the frequency of chemical plant shut downs, then elemental sulfur storage costs are approximately one fourth those for nitrate salt. However, if considerably less than 24 days of storage is required, reduced capital costs for a system using nitrate salt storage make it slightly cheaper than elemental sulfur.

iv. Decomposer Interface

Four different sulfuric acid decomposer interface configurations have been examined (Ref. 15) for the generic application of solar decomposition of sulfuric acid. These different configurations were compared to each other but did not include storage or an interface to a chemical process plant. The configurations include the concentration, vaporization, decomposition and heat recovery functions analogous to Section II operations. In three cases, the decomposition was performed within a solar heated cavity with 1) solar heat supplying energy to both the vaporizer and the decomposer but storage (presumably nitrate salt) supplying heat for concentration; 2) solar supplying heat to the decomposer with a recuperative vaporizer so that only 20% of the heat for vaporization is supplied by solar, 3) only the decomposition being supplied by solar heat with all the vaporization performed using energy from storage. Case 4 completely decouples solar from the chemical stream and uses helium at 0.86 MPa pressure as a heat transport medium. While the maximum temperature for solar heat decomposers was 900°C , the helium peak temperature was 976°C .

Conceptual designs and capital cost estimates were made for all components. The decomposer reactor used Incoloy 800H (I800H) tubes filled with catalyst pellets. The reactor also consisted of a preheater where I800H tubes were used to heat the process stream to 700°C before entering the catalyst bed. These tubes were filled with inert ceramic pellets to improve heat transfer. The preheater and reactor tubes were both U-shaped tubes on the inside wall of a circular cavity with a downward facing horizontal aperture. For the acid vaporizer, recuperated vaporizer, and concentrator, U-shaped silicon carbide tubes are used where liquid acid may be present. Because of the higher temperatures involved, the helium loop of Case 4 uses similar silicon carbide tubes in the receiver.

One dimensional calculations were made to determine the design of the reactor and other components. Maximum solar fluxes were determined based on temperature limitations of the material and limiting the maximum pressure drop to 0.1 MPa. However, detailed incident flux and thermal analyses within the receiver cavities were not performed. For the catalyst-packed reactor tubes, the average heat flux was 40 kW/m^2 for the conservative design and 65 kW/m^2 for a more optimistic design. This design employed 648 tubes, with 73.0 mm O. D., 4.76 mm wall thickness, and 1.8 m in length. The flux for the preheat tubes is 92 kW/m^2 . For the acid vaporizer, the silicon carbide tubes see 200 or 400 kW/m^2 for the conservative and optimistic designs, respectively. However, even with the use of silicon carbide, the fluxes are lower for other components using different heat transfer media. The salt heated vaporizer in Case 3 has an average heat flux of 23 kW/m^2 and the recuperated vaporizer, heated by the hot product gases exiting the decomposer, has a heat flux of 27 kW/m^2 . With helium, the silicon carbide receiver flux is 100 kW/m^2 . For the helium heated vaporizer, the heat flux is 80 kW/m^2 . The decomposer, including both the reactor and preheat sections, has an average heat flux of only 22 kW/m^2 .

While capital cost estimates were made, it was difficult to directly compare costs or efficiencies for the first three cases. Each varies in complexity - and therefore costs - that directly relate to the amount of heat recovery performed within the decomposer section. For all cases the "rejected" heat would be recovered somewhere within the hydrogen plant installation. However, some component comparisons can be made. For the decomposer and vaporizer units, the difference in cost between the optimistic and conservative designs is substantial. For the decomposers, the difference is 40%, while for the vaporizer, it is over 50%.

The helium heated system of Case 4 performs the same functions as does Case 2. Its capital cost is 45% higher. This increased cost is due primarily to additional equipment such as the receiver being separate from the decomposer and needing a high temperature compressor to pump the helium. The lower heat flux of other components also contributes significantly to the increased cost. The power requirement of the compressor dictates that approximately 10% of the thermal energy input to the system be supplied as electrical energy from compression work. Because this is converted to heat, there is little difference in the thermal efficiency between the two systems; however, because (presumably cheaper) heat can be used in Case 2, we expect that the energy costs for the helium system will be greater. Very large improvements in operational performance and flexibility would be needed to justify selection of such a helium system for a complete thermochemical system. Because there is no thermal storage between the helium loop and the decomposer, and current gas storage designs do not operate at the high temperatures needed (Ref.26), it is unlikely that storage buffered operation can provide the operational flexibility desired.

C. Component Designs

i. Decomposer Experiments

Two experiments have been performed to determine the structural, materials and chemical performance of catalytic reactors (Refs. 16, 17). The first of these experiments was an atmospheric pressure reactor in a cavity receiver with a bottom aperture tested at the Advanced Components Test Facility (ACTF) at Georgia Technical Research Institute (Figure 3-3). The second experiment was a high pressure reactor designed to operate at 0.5 - 1.0 MPa, the pressure range where a commercial hydrogen plant is expected to operate. In the second experiment, two parallel reactors were centered in a cavity surrounded by resistive heating elements (Figure 3-4). More controlled energy inputs could be achieved and transient tests could be performed. The reactors performed only the SO_3 to SO_2 decomposition step. Both experiments were open loop, using separately heated boiler and superheater units to supply acid vapor to the reactor. A water-cooled condenser was used to condense the unreacted products which were not recycled but sampled to determine chemical performance of the reactor.

Initial design studies (Ref. 18) attempted to design a flat plate tubular reactor where the solar flux would directly impinge on the reactor tubes. However, it was discovered that in order to stay below the allowable stress levels, it was necessary to maintain a uniform temperature distribution on the outer circumference of the tubes. To achieve this requirement, the reactors were designed to receive only indirect, reradiated and reflected flux from the insulated interior surfaces of the cavity.

For both experiments, the reactor tubes were 1/2 in. diameter schedule 40 Incoloy 800H (12.7 mm OD, 2.77 mm wall thickness), 0.51 m long. The tubes were filled with catalyst-coated pellets held in place by a perforated sheet of I800H welded to the bottom of the tubes. Within the reactor, the stream was heated to 870°C to limit the maximum metal temperature to 940°C. In the ACTF experiment, the reactor tubes were given an aluminide protective coating and used an iron oxide catalyst. The acid vapor inlet temperature was 600°C. For the second experiment the reactor tubes were uncoated and the two separate circuits used two different catalysts, the iron oxide catalyst of the first experiment and a platinum catalyst coated on a zirconia ceramic pellet.

The reactors were constructed with a design life of 200 hours for the first experiment and 400 hours for the second. Special consideration was given to the area where the reactor tube joins to the manifolds. In both experiments the manifolds were in the heated cavity and insulated to minimize heat loss. For the high pressure reactor, the insulation was specially shaped, as shown in Figure 3-5, to minimize stresses caused by steep thermal gradients. The experimental components contained metal samples of alloys shown to be promising candidate materials of construction during laboratory corrosion tests. At the conclusion of the reactor test program,

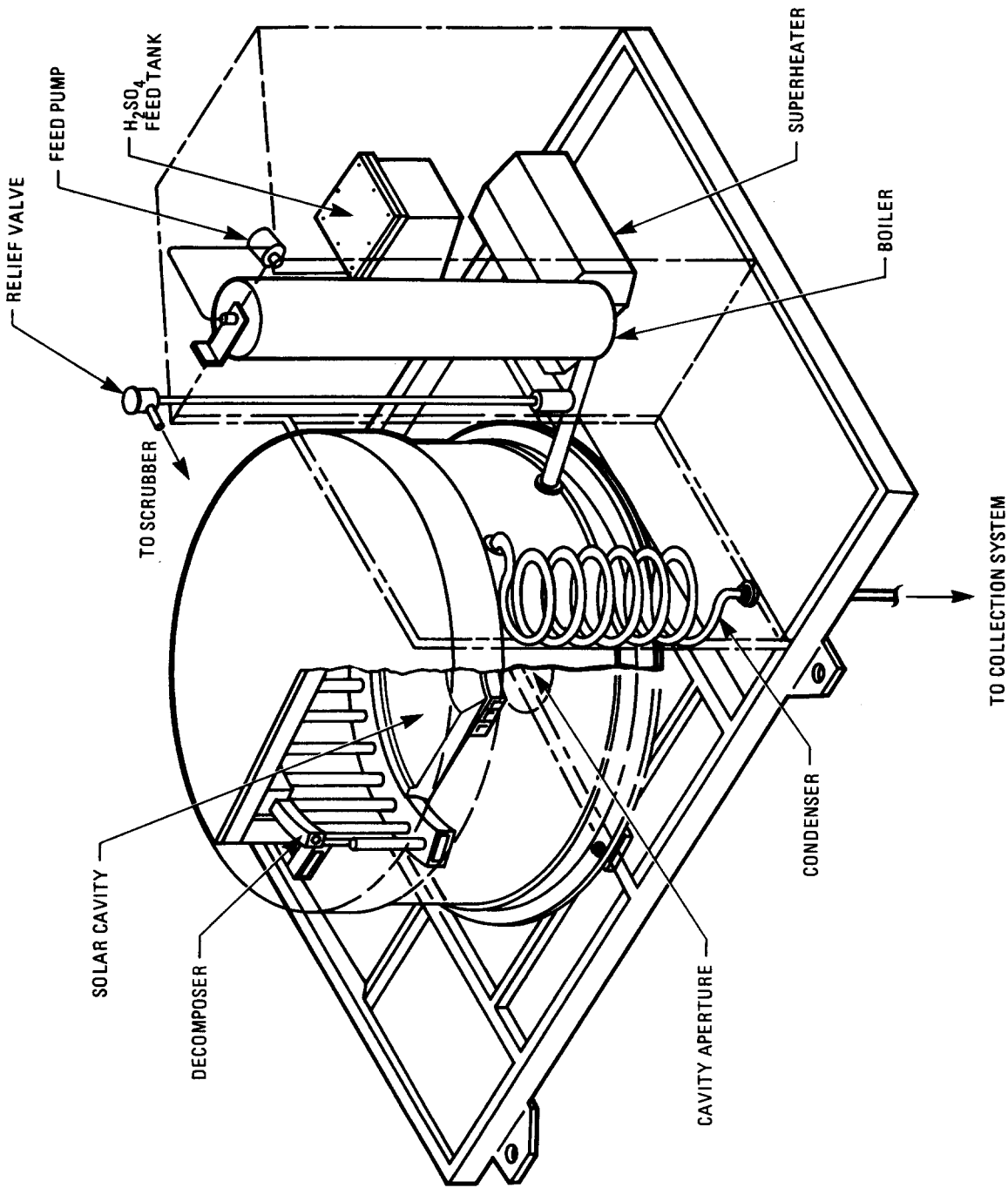


Figure 3-3 Atmospheric Pressure Sulfuric Acid Decomposer Solar Experiment
(Ref. 16)

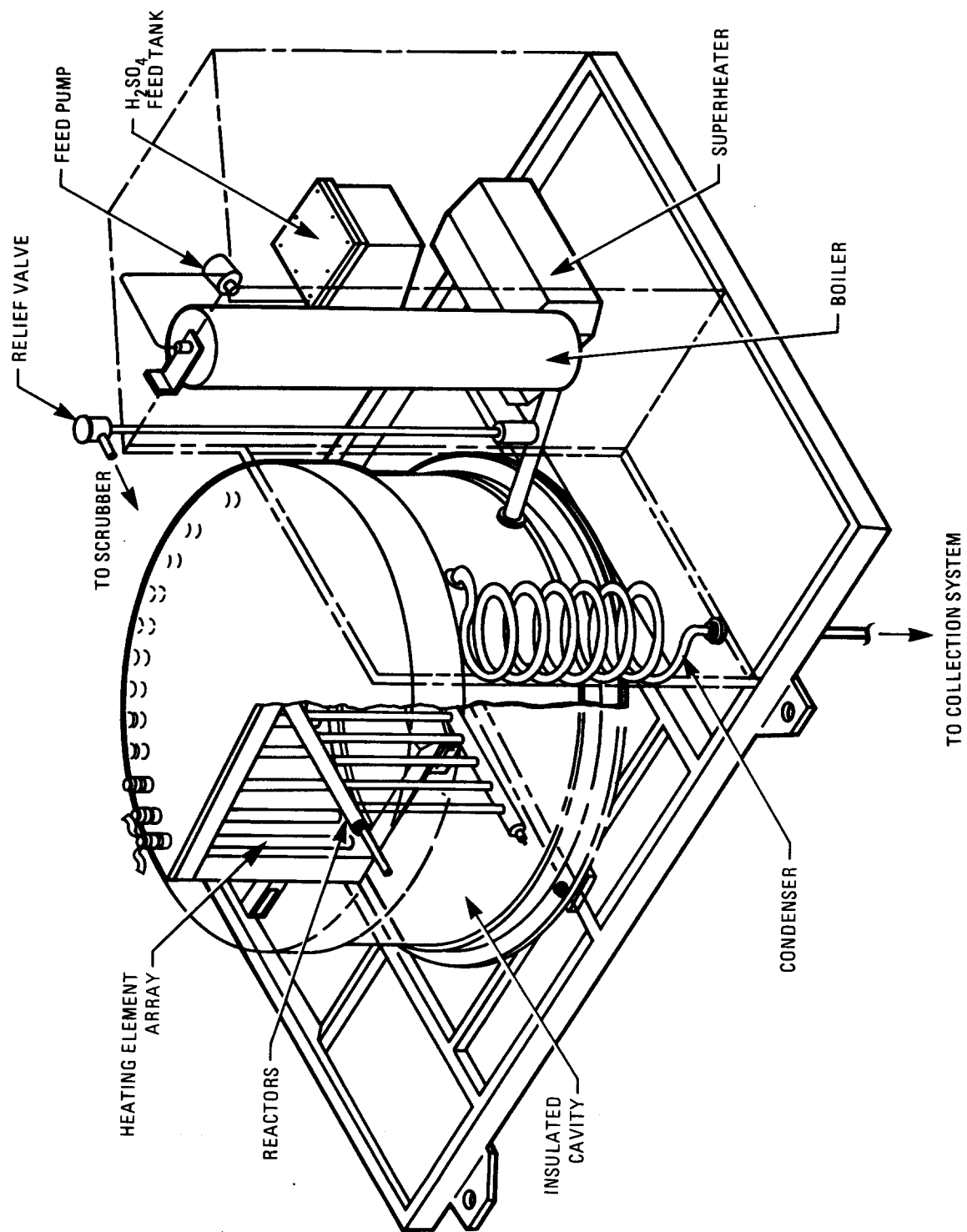


Figure 3-4 High Pressure Sulfuric Acid Decomposer Experiment
(Ref. 17)

these specimens, along with samples of the catalysts, were examined to determine materials compatibility within a more realistic chemical production environment.

The chemical performance during these experiments was good. The catalyst was always active, and conversion to SO_2 was always achieved. Experimental conditions at the start and end of the test program showed little difference in the performance of either catalyst, but the total operation time was too short to certify the catalysts for commercial plant lifetimes. The performance data was analyzed by several methods to determine the kinetic behavior. Both thermal and chemical data showed that the iron oxide catalyst had a greater temperature dependence than did the platinum catalyst. A chemical kinetic model gave a reasonable fit to the experimental data. The model assumed the decomposition rate constant was based on the standard Arrhenius form, $k = A \exp(-T_a/T)$, with the forward and reverse reactions being first order in sulfur dioxide and the reverse reaction being half order in oxygen. The greater temperature dependence of the iron oxide catalyst correlates well with a reversible sulfate reaction that occurs with the iron oxide at lower temperatures. The result is that less conversion takes place in the lower, cooler portions of the reactor, but in the hotter regions the iron oxide catalyst becomes very active, achieving equilibrium conversion ratios in some cases. Platinum is relatively insensitive to temperature and performs better than the iron oxide at lower temperatures. Analysis of the thermal data for a particular experimental case (Figure 3-6) displays the catalyst behavior in terms of effective heat capacity as a function of temperature (and position along the reactor length). The effective heat capacity includes the thermal energy absorbed by the process stream as chemical energy according to the actual amount of the endothermic reaction that has occurred. With the equilibrium calculation as a comparison, the completion of the H_2SO_4 to SO_3 reaction can be seen at lower temperatures. For the platinum catalyst the reaction becomes slightly more active with increasing temperature but does not exhibit the large temperature dependence of the iron oxide. At higher temperatures, both catalysts tend to "catch up" to equilibrium with greater effective heat capacities.

These results show that while the reactors exhibit kinetic behavior that is measurably different from equilibrium, the differences are not so great that serious degradation in chemical performance occurs. In a receiver design, if an iron oxide catalyst selection were made, the maintenance of high temperatures would be important. The use of the more expensive platinum catalyst in the lower cooler regions of the reactor may be considered, but materials compatibility may be an issue. Transient tests were performed as step changes to initially steady state conditions of the operating reactors. The major parameters used as forcing functions for the transient tests were power, flow rate, and pressure. By comparison of the transient thermal response of the reactors to a simple model, the behavior of the power and flow rate transients appears to be first order reactions while the pressure transient is not. The

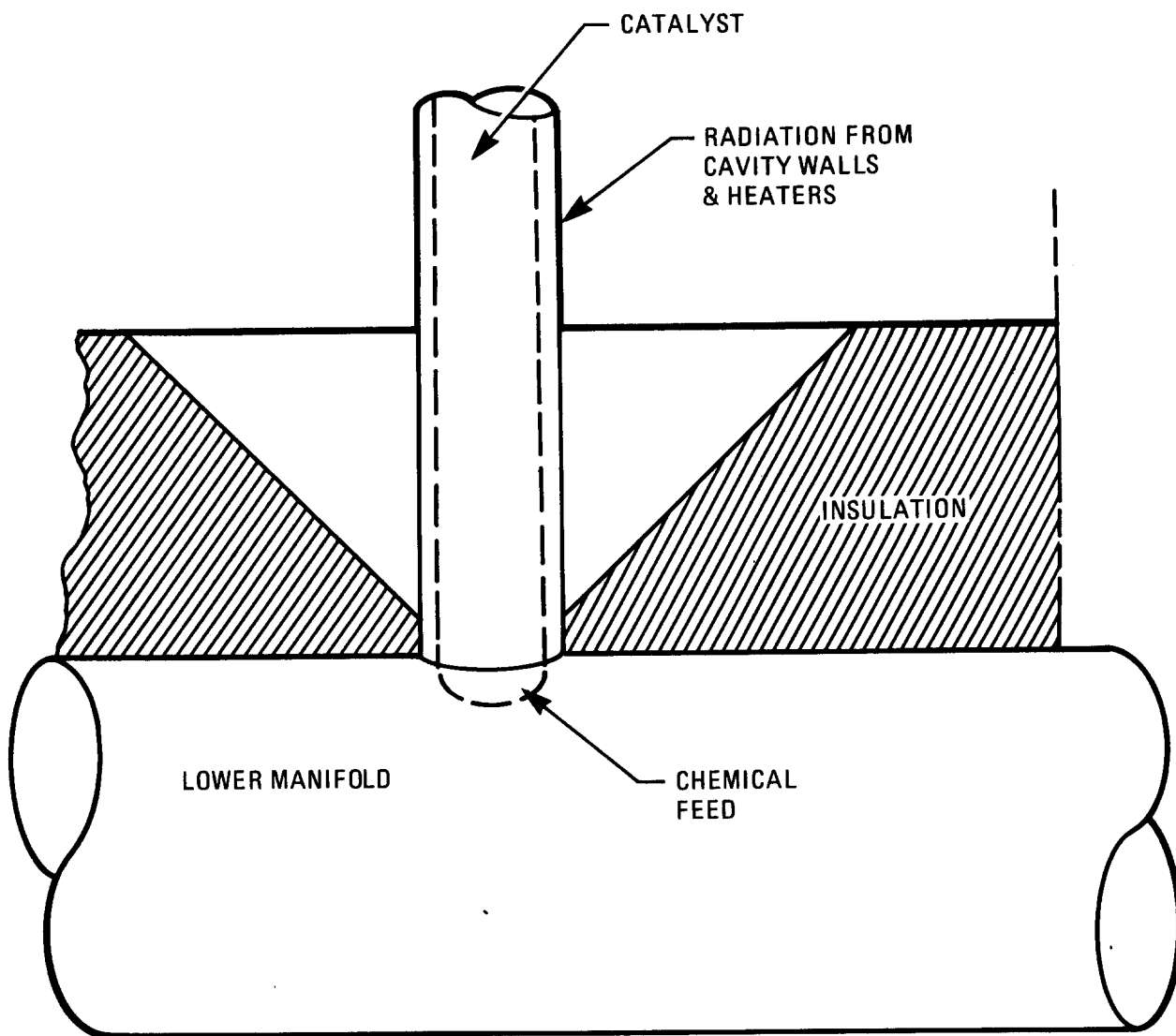


Figure 3-5 Insulation Design Detail for Inlet Manifold

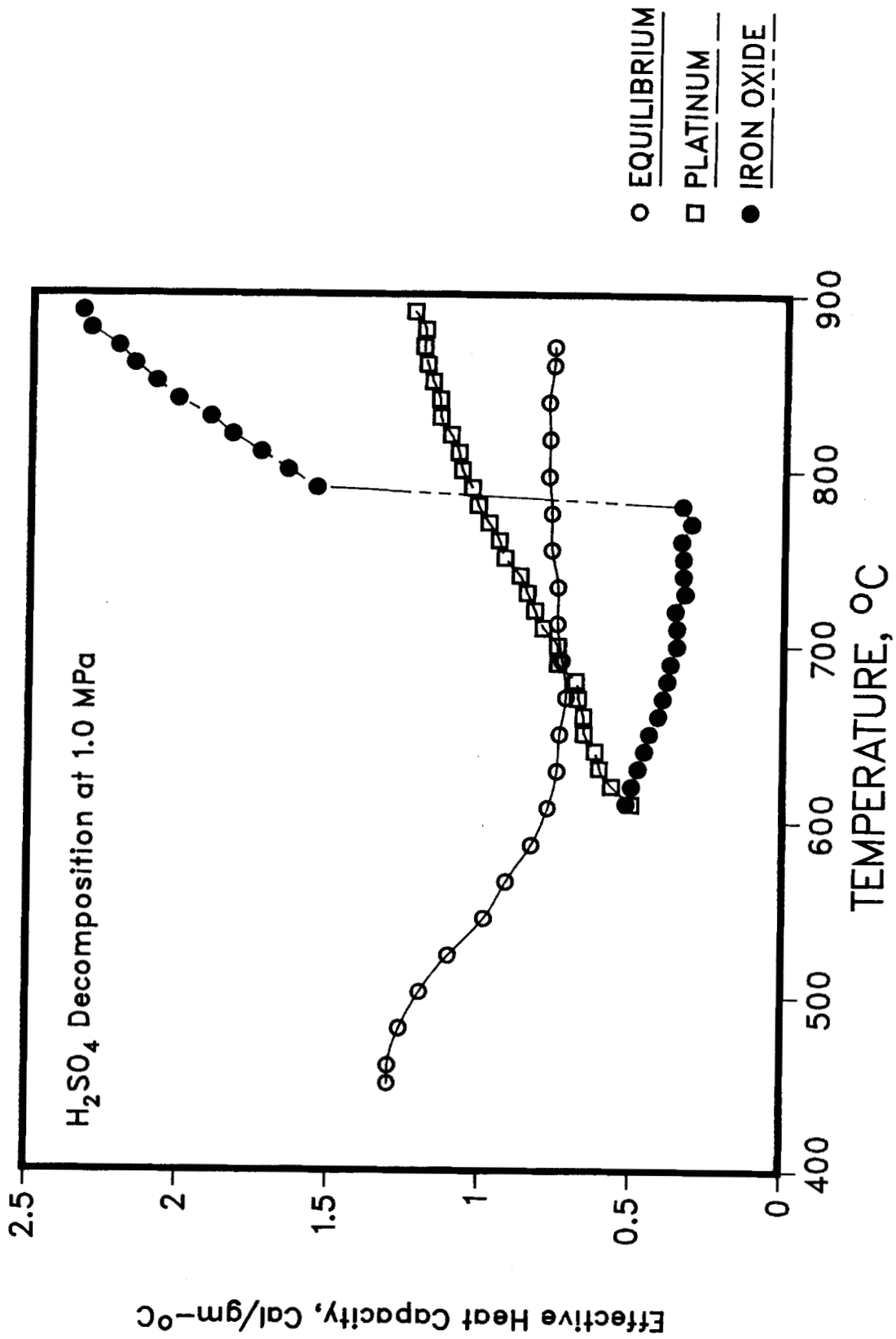


Figure 3-6 Catalyst Performance in High Pressure Acid Decomposer Experiment

model shows that the power transient of the reactor is dominated by the thermal transient response of the insulated wall of the cavity. More importantly, as the time constants in Table 3-2 show, the flow rate can successfully be used as a controlling parameter during power (cloud) transients because its time constant is significantly shorter than for the power transient. Furthermore, because the power transient is dominated by the insulation, reactor design can be used to tailor the power transient by varying the amount of insulation built into the cavity walls.

The atmospheric pressure reactor experiment revealed a corrosion problem where aluminide coated I800H reactor tubes contacted the iron oxide catalyst. For the high pressure experiment, bare I800H was used. For the iron oxide catalyst, this was moderately successful. The corrosion rates were higher than for bare I800H in air, by an approximate factor of three; or .76 mm/yr. For the platinum system the corrosion was much worse, approximately 7.6 mm/yr with similar or greater corrosion rates for coupons of alternate candidate materials such as Inconel 617 and Hastelloy X. Aluminide coated coupons of I800H showed much better corrosion resistance in the platinum system, being approximately equal to the corrosion resistance of bare I800H in the iron oxide system. However, there are indications that if not completely sound and adherent, point defects in the aluminide coating would result in localized areas of severe corrosion. Where optimal performance for a solar reactor design would suggest the combined use of platinum and iron oxide catalysts, these materials issues will require attention.

ii. Decomposer Design

Significant design issues remain for optimal reactor component design. The principal concerns have been reactor geometry and heat flux distribution. The experiments described above showed that metallic catalytic reactors can perform successfully. However, the design for packed bed catalytic reactors requires short small diameter tubes to prevent excessive pressure drops within the reactor. This necessitates large numbers of small reactor elements to scale up to commercial decomposer sizes. For alloys such as I800H, the need for indirect and uniform heat flux presents additional design problems. With a large number of short reactor tubes, either many penetrations through the insulated cavity wall or vertically layered manifold structures will be necessary.

The use of adiabatic reactors has been proposed as an alternative, where empty I800H tubes are used to preheat and reheat the process gas between successive reaction steps. This approach uses short reactor beds in which little heat transfer occurs (Ref. 19). Even though this design will reduce fabrication costs by reducing the number of metallic tubes and increasing their length, flux levels are still expected to be relatively low, 75 - 120 kW/m², with no decrease in the large receiver size. In addition, the performance of the adiabatic reactors themselves has not been established. With superheated SO₃ vapor reacting within a thin layer of the

TABLE 3-2
TRANSIENT BEHAVIOR OF THE DECOMPOSER REACTOR

Parameter	Average Time Constant, Min	Calculated Time Constant, Min
Power	23.8	18.4
Flow Rate	2.80	2.76
Pressure	0.48*	---

* Analogous time constant, not a first order reaction

catalyst bed, large thermal gradients are likely. The ceramic substrates used for the catalysts may rapidly degrade in such an environment.

Several other metallic reactor design concepts have been proposed. These include empty, catalyst-lined reactor tubes and tubes with catalyst sleeves designed to promote radial flow of the process stream through the catalyst material. These designs would reduce the pressure drop and allow the use of longer reactor tubes. Along with adiabatic reactors, these concepts require further analysis before meaningful comparisons can be made.

While reactors of metallic construction are limited by temperature and heat flux distribution, ceramic materials such as alpha phase sintered silicon carbide are not. Several ceramic receivers have been proposed for high temperature operation with outlet temperatures up to 1360°C with direct incident solar flux. (Ref. 20) At temperatures of above 980°C , the decomposition reaction will proceed to over 95% completion without the use of catalysts. Because nuclear reactors are not generally considered capable of heating a process stream to these temperatures, little detailed work has been performed to flowsheet such a thermochemical hydrogen cycle. Ceramic reactor tubes using a helium heat source would be 15.5 m in length, 3 cm in diameter with a 1mm thick tube wall (Ref. 4) with an average heat flux of 400 kW/m^2 . With the reaction occurring by thermal decomposition without the use of a catalyst, backreaction while the exiting process stream cools must now be considered. Rapid cooling with the use of an eductor, where a portion of the dilute sulfuric acid liquid stream cools the vapor to 880°C , will limit the back reaction to approximately 2%. Because the liquid addition will compose only 16% of the process stream, exergy losses caused by the rapid cooling are limited to less than 2% of the overall plant efficiency.

Fabrication of such a ceramic receiver will require significant development, but progress in ceramic technology puts such a design nearly within the state-of-the-art. The ceramic tubes are likely to be extruded sections joined into U-tube configurations. For ceramic assemblies, U-tubes have the advantages of minimizing tube stresses and joint loading due to thermal expansion and providing simple means to compressively load the ceramic joints. In addition the inlet and outlet manifolds can both be located at the bottom of the receiver and the receiver height can be reduced by one half of the needed tube length, both advantages in receiver design. Joint design is the greatest developmental concern. The joint to connect the two straight sections to form the U-tube must be a ceramic to ceramic joint. Because sintered alpha silicon carbide will be required instead of the more common siliconized silicon carbide, demonstrated joints using a metallic silicon braze technique will not be applicable here. Green state bonding has been proposed for sintered alpha material but has not been demonstrated on components such as this. Manifold seals for ceramics have been demonstrated for heat exchangers where slight leakage rates 0.1 - 1.0% are permissible. Here, however, the corrosive nature of the process

stream will require high performance from the sealing technique. The high temperature seal developed for the ceramic acid vaporizer would be suitable for the inlet manifold for a ceramic reactor but a higher temperature sealing material will be needed for the outlet manifold. An alternative high temperature seal would be "Helicoflex" seals proposed by Lin and Flaherty (Ref. 21). Here, the sealing gasket is a metal spring with initial tension that is wound into a toroidal shape and wrapped in a sheet of corrosion resistant metal.

iii. Vaporizer

A vaporizer experiment using a single ceramic tube was successfully completed. The experiment was performed by Garrett Airesearch Manufacturing Company. The apparatus used four resistance heated elements to simulate the solar flux (Figure 3-7). Thermal analysis showed that the vaporizer could be operated in direct solar flux. To perform a laboratory test, having the vaporizer tube surrounded by the heating elements was more practical than using a single wall of elements with little difference in the circumferential temperature distribution owing to the high thermal conductivity of silicon carbide. The tube 25.4 mm OD. with a 3.2 mm thick wall contained a central 15.9 mm diameter annular rod to increase heat transfer to the sulfuric acid. Average heat flux for the four foot long heated tube surface exceeded 100 kW/m^2 during the experiment. The hot and cold end seals are shown in (Figures 3-8 and 3-9). Prior to the experiment, laboratory tests were conducted to determine the performance of these seals and the corrosion resistance of the silicon carbide.

The seal tests included displacing the mating surfaces of the sealing assembly by as much as a 3° angle. The cold end seal successfully sealed up to 3° , but only with the use of gold gaskets was the hot end seal successful. The hot end seal, a variant of commercial "Voishan" seals could withstand angles of up to 0.5° , although the goal was at least 2° . Other materials - such as platinum - that are suitable for higher temperature service did not seal successfully.

Corrosion tests were performed for periods greater than 6 months. Ceramic ring samples of silicon carbide produced by three different manufacturers were tested in hot and boiling sulfuric acid and in sulfuric acid vapor. The results of the corrosion testing showed virtually no effect of the environment on the specimens, confirming that sintered alpha phase silicon carbide is an excellent material for boiling sulfuric acid service.

The results of the vaporizer experiment showed no problems with the performance of the ceramic tube and the seals. Because of pressure fluctuations in the acid feed system, however, the experiments were conducted with continuous acid flow even during start up and shut down. This prevented the liquid level in the tube from rising and falling which would thermally shock the inner surface of the tube. It is not known whether these fluctuations would have actually caused a failure of the ceramic tube because the thermal analysis

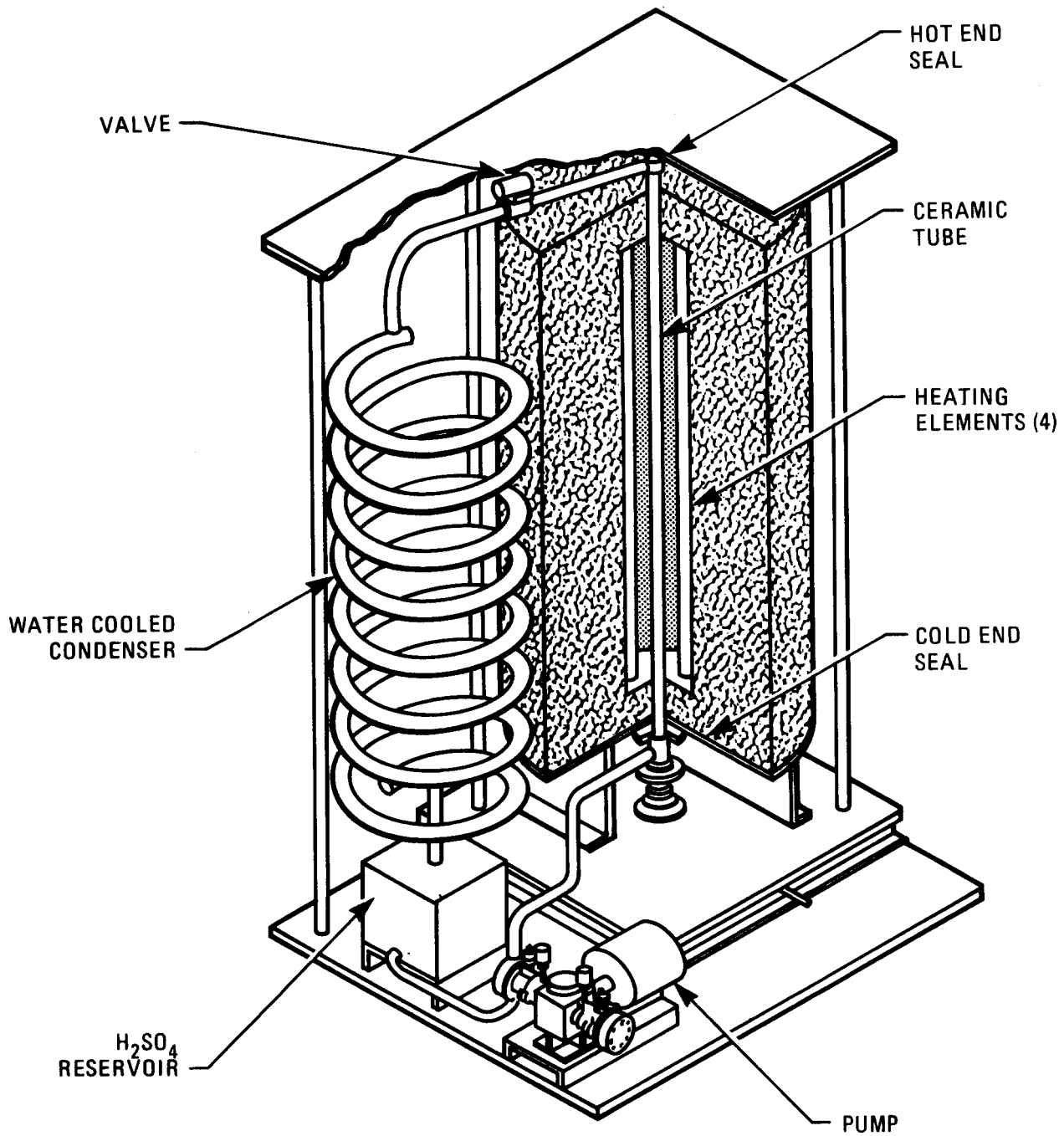


Figure 3-7 Single Tube Ceramic Acid Vaporizer Experiment

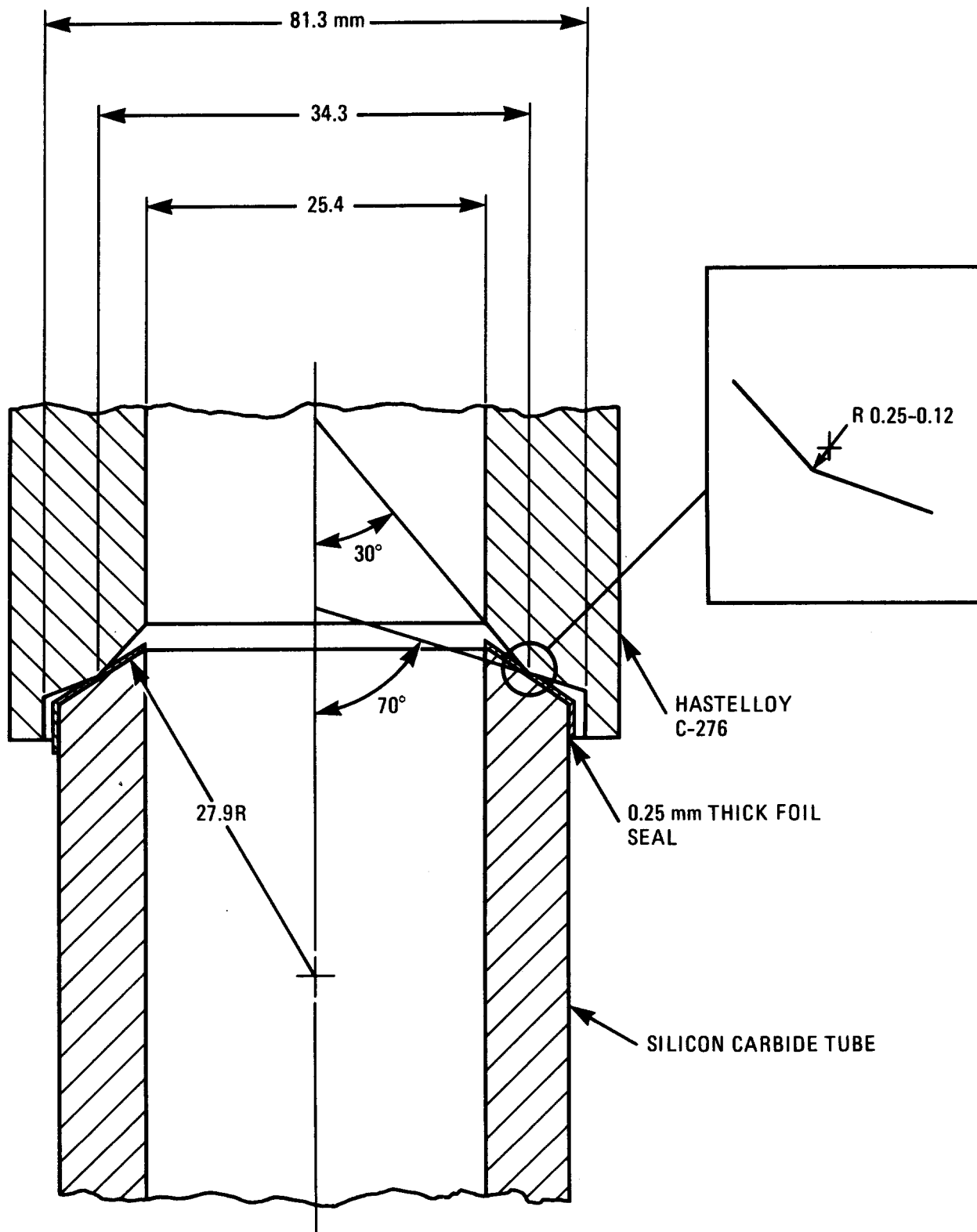


Figure 3-8 Hot End Seal Design

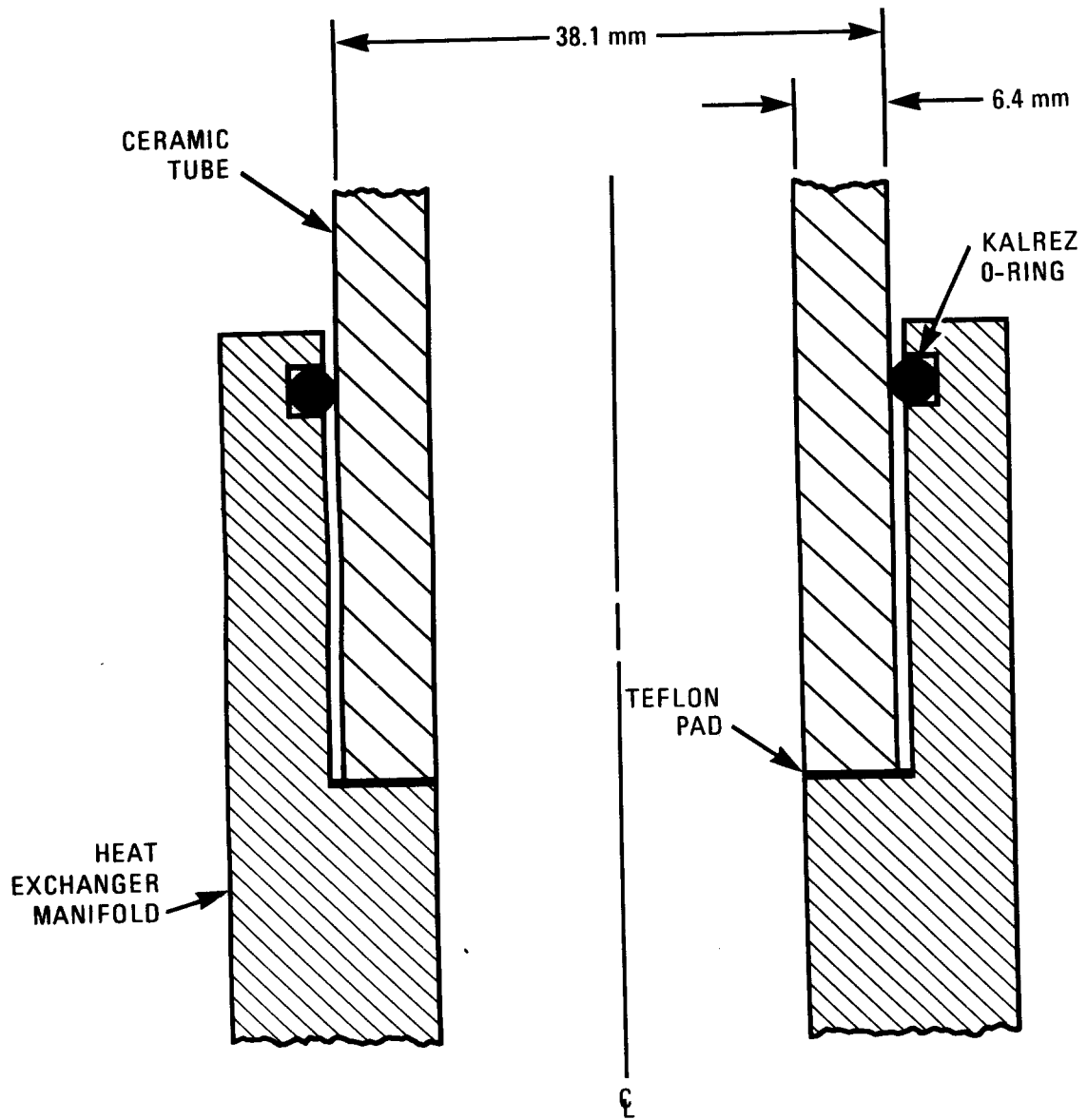


Figure 3-9 Cold End Seal Design

performed did not have sufficient level of detail. Such a practice is not suitable for commercial use because condensation of sulfuric acid vapor would occur in the metal outlet manifold of the vaporizer during the daily start up and shut down operations. This would lead to unacceptably high corrosion rates for any applicable metal alloy.

Transient tests were performed with the greatest transient being where the power to the heating elements was reduced from 12.6 kW to zero. While the data show that pressure fluctuations occur during these transients, they dampen out within ten minutes after the start of the transient with no apparent harmful effects (silicon carbide material is not susceptible to slow crack growth failure mechanisms; if the thermal shock does not fail the tube, it is not considered to have suffered any incremental damage). Because the vaporizer is not sensitive to such transients, more practical start-up procedures, where the acid is introduced into a heated tube and the flow rate is slowly increased, should be feasible.

iv. Condenser and Recuperators

For both the vaporizer and the decomposer experiments, the same design was used for the condenser unit. Because neither of these experiments was closed loop cycles, and because decomposer chemical samples were needed, the condenser was designed to cool and condense the outlet stream as rapidly as possible with no attempts to recover the thermal energy. The design consisted of a double heat pipe coiled heat exchanger, 8.2 m in length with the inside tube 27 mm O. D. Incoloy 825 having a wall thickness of 3 mm and the outside tube made of 42 mm OD 304 stainless steel. Cooling water between the tubes cooled the process stream from 700°C at the inlet to approximately 20°C at the outlet. No provisions were made to maintain concentricity within the double pipe coil to obtain uniform cooling in the condenser. Coupon samples of Incoloy 825 were placed at the both the inlet and outlet of the condenser. Also a 0.9 m long, 1.5 mm dia wire of Inco 65 (the weld wire alloy counterpart to Incoloy 825) was inserted along the inlet region of the condenser to determine where the maximum corrosion would occur as the sulfuric acid vapor condensed.

Both coupon samples showed significant amounts of uniform corrosion. Corrosion of the Inco 65 rod was so severe that only a .2 m length was recovered. Based on the total exposure time, the corrosion rates varied from 1 to 13 mm/yr. Since the actual operating time was a fraction of the total time, the true corrosion rates are likely to be substantially higher. Samples of Hastelloy C-276 placed in the boiler at the liquid vapor region exhibited a maximum corrosion rate of 2 mm/yr. If Hastelloy C-276 were used, the corrosion rate is still great enough that frequent periodic replacement of subcomponents for a production condenser unit would be required.

As noted in the description of the thermochemical cycle, heat recovery of the Section II outlet stream is very important. Where recuperation is done completely in the vapor phase, it may be possible to use I800H. During transients and low flow rates, this would be one of the units most likely to experience condensation of the process stream. From a practical sense, one may expect a metallic recuperator to experience high rates of corrosion because of this condensation.

The condenser of a commercial plant has even more demanding corrosion conditions. The best way to use the large amounts of energy released during the condensation of the process stream would be to recover that energy by heat transfer to the boiler. This will require a boiler/condenser unit to have tubes where both sides are exposed to the boiling environment. Silicon carbide construction may be a solution to this problem; however such a unit has never been designed. While the vaporizer experiment was successful, it still uses design concepts that were only recently developed. It is tempting to propose designs for the Section II components that ever increasingly depend upon ceramic materials with more complicated sealing requirements not yet developed. In order to obtain practical designs that can be built in the near term, it will be necessary to

make compromises in efficiency to avoid unreasonable expectations of the capabilities of ceramic technology.

D. Receiver Designs

There are three types of receivers that may be considered for the high temperature decomposition of SO_3 : indirect flux heated cavities, direct flux heated cavities, and cavity receivers using a high temperature heat transfer medium. The first two are integrated receivers with the reactor contained and operated within the receiver. The last provides heat through a receiver heated media to a separated chemical reactor.

Experiments to date have assumed the use of indirect flux heated reactors. Because the flux is relatively low, it is sometimes thought that the size of such receivers would make them undesirable. However, the entire tube surface area of the reactor is active, compared to conventional receivers where the projected area of one side of the tube assembly is active. The receiver /reactor cavity structure would be larger to obtain the proper internal reflections and re-radiation for the required uniformity of flux. However, where the maximum flux level for the reactor tubes may be only one sixth of that for a conventional cavity receiver, the volume is only twice as great (Refs. 22, 23). As the design of such receivers is refined, and the allowable flux distribution on reactor tubes becomes better known, the volumetric and size differences are expected to decrease. In addition, a comparison of various solar interface combinations for the steam reforming of methane showed an integrated receiver to be the most economical (Ref. 24).

Alternate reactor designs, such as the adiabatic reactor, would use empty tubes to heat the SO_3 gas and then perform the reaction in close proximity to the receiver. These varying designs would all closely approximate the catalytic reactor in the use of the indirect flux receiver design.

Direct flux receivers could be used for a ceramic acid vaporizer as presently configured. As ceramic materials progress to become suitable for other components, the allowable flux levels of these components will also increase. Ultimately, direct flux ceramic decomposers will be possible. There should be advantages to the use of direct flux reactors in integrated receivers, as determined by the maximum operating temperature, the limitations of heat transfer into the process stream, and size reduction of the cavity structure.

The use of an intermediate thermal transport medium has the advantages of allowing the design of the receiver to be optimized without the constraints of the corrosive nature of process stream or chemical reaction kinetics. It has the advantage of allowing the Section II components to be sized and operated as part of a continuous hydrogen plant. Several media have been identified for high temperature use: carbonate salt, helium, air at atmospheric pressure and solid particles. Recent fuels and chemical applications

studies (Refs. 23, 25) selected carbonate salt because it was felt that it could be developed for commercial use most readily. However, because most engineering materials experience high corrosion rates with carbonate salt, it was found to require expensive components everywhere within the heat transfer loop. Gaseous media have two problems, high pumping costs and storage difficulties. Storage is typically accomplished with the use of heat transfer to rock or a ceramic matrix (Ref. 26). These designs typically have large temperature drops between the solar heated media and media of end use. So while the receivers have been designed to operate at sufficiently high temperatures, 1000°C , the system cannot supply heat from storage above 500°C . Solid particle receivers appear feasible (Ref. 27); and would provide a high temperature storage media. With the use of silicon carbide's high abrasion resistance, heat transfer from the solid particles to the reactor tubes may be feasible. At this time designs for solid particle heat exchangers and storage are either highly conceptual or non-existent. Considerable development is needed before it will be possible to determine the suitability for the application of solid particles. However, at this time solid particles remain the only identifiable medium for further consideration.

4. ECONOMIC CONSIDERATIONS

A. Capital Costs, Efficiency, and Production Costs

We decided to present the economics of the process in terms of product cost of hydrogen. We used the levelized cost approach developed by Battelle for solar thermal energy systems (Ref. 28). The costs are life cycle costs that include expected values of return on investment for commercial chemical plant operations. The production costs, PC, are estimated from:

equation 4-1:

$$PC = \frac{(CAP + O\&M + C_E)}{(AOUT)}$$

where CAP is the annualized capital related costs; O&M is the annualized operating and maintenance costs; C_E is the annualized cost of primary energy supplied to the process and AOUT is the total annual energy produced. In terms of the nomenclature of the Battelle approach,

equation 4-2:

$$PC = \frac{(TPI)(PVF_1)(FC_1) + (O\&M)(PVF_2)(FC_2) + (Q_t)(H)(C_E)}{(Q_t)(H)(\eta)}$$

or,

equation 4-3:

$$PC = 1/\eta [(PVF_1)(FC_1) \frac{TPI}{Q_t H} + (PVF_2)(FC_2) \frac{O\&M}{Q_t H} + C_E]$$

where,

PC = production cost, \$/GJ

η = thermal efficiency of the process

PVF_1 = factor to obtain the present value of TPI

TPI = total plant investment for the chemical portion of the plant

FC_1 = fixed charge rate for the capital recovery factor of the chemical plant

Q_t = rating of the primary energy source, GJ/hr

H = hours per year of operation

PVF_2 = factor to obtain present value of O&M

FC_2 = fixed charge rate for the capital recovery factor for O&M

O&M = 1st year O&M cost, \$

C_E = cost of the primary energy (ie, heat), \$/GJ

For solar thermal industrial process heat (Ref. 28):

$PVF_1 = 1.1934$

$PVF_2 = 9.2083$

$FC_2 = .1175$

Five parameters remain for which values are required in order to determine the production cost.

1. Overall process efficiency (annual basis), η
2. Capital recovery factor for the chemical plant, FC_1
3. Total plant investment for the chemical plant per unit of primary energy input, $\frac{TPI}{[Q_t^H]}$
4. O&M cost per unit of primary energy input, $\frac{O\&M}{[Q_t^H]}$
5. Cost of primary energy supplied to the process, C_E

Parameters 1, 3, and 4 depend on the configuration of the flowsheets which specify how the chemical plant is to be built and operated. Parameter 2 depends on financing methods. Parameters 3 and 4 also depend on the annual operating hours. Parameter 5 depends on the nature and characteristics of the heat source utilized.

For a solar heat source, cost and efficiency estimates exist (Refs. 6, 29) which may be used to estimate the value of the five parameters mentioned above. GA Technologies has presented estimates for capital and operating costs for their process adapted to a solar source. A sulfur storage system is included which allows part of the plant to be operated continuously. The high temperature processes along with their heat transfer systems are operated on a diurnal basis. The annual hydrogen output for this plant is 5.68×10^6 GJ. The diurnal operations are assumed to occur for 8 hours a day and are sized to operate at 1.9 kmol/sec of hydrogen production. The continuously operating equipment is one third this size, 0.63 kmol/sec. The thermal efficiency of this plant with the sulfur storage - solar interface is taken to be 40%.

Capital costs are shown in Table 4-1. These costs were updated using the Marshall & Swift cost index for capital equipment of chemical plants (Ref. 30). Included is the increase in equipment size because of the entrainment of nitrogen from the sulfur combustion. However, the flowsheets and equipment lists for the sulfur production, storage and combustion from which these values are derived (Ref. 6) have never been documented. This limits the economic evaluation of the system and the determination of the effect of variations in the configuration to generalized comparisons. Section II includes the sulfur disproportionation and storage equipment. For Section V, the solar/process interface which includes the sulfur storage system, true cost estimates are not available because a design of the interface in this configuration has never been performed. Section Va includes the equipment that operates only during the daytime. Based on the expectation of its relative simplicity compared to Section V designs for nuclear heat, it was estimated to cost only 40% of the process coupled to fusion power sources (Refs. 3, 5). Section Vb includes the continuous

TABLE 4-1
 GA PROCESS - SOLAR ADAPTATION
 5.68 x 10⁶ GJ/yr of Hydrogen
 1986 Dollars

Section	Total Capital Cost, M\$
I HI and H ₂ SO ₄ Synthesis	19
II SO ₂ Synthesis	162
III HI Separation	118
IV H ₂ Production	16
Va Energy Transport	144
Vb Energy Transport	65
TOTAL	524
O & M	48

Notes:

- Section Va includes sulfur production and storage
- Section Vb includes sulfur combustion
- Section II and Va operation diurnally
- Other sections operate continuously

Section V operations where the sulfur combustion and power conversion equipment are also located.

For solar energy, recent estimates have been made for the capital cost of a molten salt receiver system operating at 1050^oF (566^oC) and delivering 320 MWt (Ref. 29). These results are shown in Table 4-2. Here it is important to recognize the delineations between the solar system and the chemical plant sections. The catalytic reactor is costed as part of Section II while storage and storage energy conversion subsystems are part of Section V. The solar cost portion of the receiver includes only the cavity structure without the heat exchanger. By comparison with cost breakdowns for integrated receivers for methane reforming (Ref. 31), an estimate for this "empty" receiver was taken to be one fourth the capital cost for the nitrate salt receiver. The annual O&M cost is also scaled to this portion of the capital cost.

Because the average temperature of a receiver used for sulfuric acid decomposition would be 900^oC, its efficiency will be lower than the nitrate salt receiver due to increased thermal losses. Its efficiency is estimated at 80% (Refs. 22, 32) and results in a 12% cost penalty when compared to the 550^oC, 320 MWt system. Recent studies showed that receivers operating at this temperature will have an annual operating time equivalent of 2370 hours of full power operation (Ref. 25) based on annual solar energy calculations using DELSOL (Ref. 33). The fixed charge rate for the capital recovery factor for the solar plant supplying industrial process heat, FC₃, is taken to be .134, also from Battelle (Ref. 28).

The resulting levelized cost of solar heat is \$5.69/GJ. If the cost for mass produced, stressed membrane heliostats is used (\$40/m² from Ref. 34), the cost of solar heat becomes \$2.69/GJ. These are much lower costs than what is currently accepted as the present capabilities for solar industrial process heat. It is more appropriate to consider these results as the cost for the concentration of solar thermal energy because the heat exchanger, piping and storage are not included in this cost but are accounted for as part of the chemical plant.

The total hydrogen production costs are presented in Table 4-3. With an efficiency of 40%, the input energy for the hydrogen plant listed in Table 4-1 is 14.2x10⁶ GJ. For 2370 hours of solar operation a year, the required solar power consumption is 1,670 MW. This is much greater than the 320-640 MWt size range of solar plants usually considered. No economies of scale are claimed by this plant size. The cost method implies the use of modular central receiver installations by using the cost of solar heat determined with a solar plant capacity of 320 MWt. (No cost penalty is attached to the division of Section II into smaller units for each of the required solar systems; however, the accuracy of the hydrogen plant capital costs is insufficient to provide a meaningful correction factor). The capital recovery factor for the hydrogen plant, FC₁, is taken to be 0.2, which is an accepted value for chemical plants. As Table 4-3 shows, the capital costs of the plant account for

TABLE 4-2
SOLAR HEAT COSTS

	Capital Costs
Land	2.3 M\$
Collector System	61.3 M\$ (based on \$120/m ²)
Tower	7.7 M\$
Receiver (1/4)	6.1 M\$

TOTAL	77.4 M\$
O & M	1.43 M\$

$$\begin{aligned}
 \text{TPI}/Q_t &= \frac{77.4 \times 10^6 * 1.12}{320,000 \text{ kW}} \\
 &= \$270/\text{kW}_t \\
 \text{O\&M}/Q_t &= \$5/\text{kW}_t \\
 \text{CE} &= \frac{\text{PVF}_1 * \text{FC}_3 * [\text{TPI}/Q_t] + \text{PVF}_2 * \text{FC}_2 * [\text{O\&M}/Q_t]}{\text{H} * 3600 \text{ sec/hr}} \\
 &= \frac{(1.1934)(.134)(270) + (9.2083)(.1175)(5)}{(2370)(3600)} \times 10^6 \text{ GW/KW} \\
 &= \$5.69/\text{GJ}
 \end{aligned}$$

TABLE 4-3
COST OF SOLAR THERMOCHEMICAL HYDROGEN

$$\begin{aligned} \text{TPI}/[(Q_t)(H)] &= \frac{524 \times 10^6}{14.2 \times 10^6} \\ &= \$36.9/\text{GJ} \end{aligned}$$

$$\begin{aligned} \text{O\&M}/[(Q_t)(H)] &= \frac{48 \times 10^6}{14.2 \times 10^6} \\ &= \$3.4/\text{GJ} \end{aligned}$$

$$\begin{aligned} Q_t &= \frac{14.2 \times 10^6}{2370 \times 3600} \\ &= 1,670 \text{ MW} \end{aligned}$$

From equation 4-3

$$\begin{aligned} \text{PC} &= 1/\eta[(1.1934)(.2)(36.9) + (9.2083)(.1175)(3.4) + 5.69] \\ &= \frac{1}{0.4} * [8.8 + 3.7 + 5.69] \\ &= \$45.5/\text{GJ} \end{aligned}$$

approximately half the hydrogen cost while 30% of the cost is attributable to solar energy. If the solar energy cost was \$2.69/GJ, then the cost of the hydrogen would be reduced from \$45.5/GJ to \$38.0/GJ. It should be emphasized that these costs include the expected rates of return for the chemical industry. Once the value of hydrogen on the open market equals or exceeds this product cost, these plants become commercially attractive.

B. Irreversibilities, Efficiency and Production Cost Sensitivities

Production costs include the capital cost of the plant as well as the thermal efficiency of the process. No equipment operates reversibly. The irreversibilities, or entropy production, lower the efficiency and thereby increase the production cost. Equipment can be made more efficient with an increase in capital cost. Heat exchangers, for instance, can be designed to increase process efficiency by lowering the temperature difference between the two process streams. This lowers heat transfer and requires larger surface areas, hence bigger and more expensive heat exchanger components. Therefore, there is a relationship among capital costs, irreversibilities, process efficiency, and production cost. For thermochemical hydrogen production plants, this relationship was first discussed by Funk and Knoche (Refs. 35, 36, 37). The importance of the process flowsheet is underscored by this kind of analysis. The flowsheet specifies operating conditions such as temperature, pressure, conversion, etc. as well as flow rates and composition. These parameters fix the design of the equipment, the thermodynamic conditions of the inlet and outlet process streams, the irreversibility associated with the equipment, and the cost of the equipment. This relationship is shown in Figure 4-1. The overall sum of the cost and irreversibilities determines the efficiency and production cost.

A useful measure of the irreversibilities in these plants is the exergy loss, Ex , which is defined to be $T_0 \dot{S}$ where T_0 is a reference

temperature (eg. 300 K) and \dot{S} is the entropy production.

It has been

shown (Refs. 35, 36, 37) that for the overall process efficiency, η :

(4-B-2)

$$\frac{1}{\eta} = \frac{T_m}{T_m - T_0} \frac{\Delta G}{\Delta H} \left[1 + \frac{\Sigma Ex}{\Delta G} \right]$$

or $\frac{1}{\eta} = \frac{1}{\eta_{ideal}} \left[1 + \frac{\Sigma Ex}{\Delta G} \right]$

(4-B-3)

where η_{ideal} = ideal, or reversible, overall process thermal efficiency

T_m = thermodynamic maximum process temperature

ΔG & ΔH = change in Gibbs function and enthalpy for water decomposition

ΣEx = sum of all the exergy losses in the plant.

Using equations 4-B-2 or 4-B-3, one can determine the effect that any section of the process has on the overall thermal efficiency by determining the exergy losses in that section. Engels, Knoche and Roth (Ref. 10) determined the exergy losses in the GA process for the original GA flowsheet (Ref. 6).

The ideal efficiency for the process is about 82% while the efficiency for this flowsheet is 47% for continuous operation and 40% with the solar sulfur adaptation. With these exergy losses and the costs calculated using equation 4-B-3, a production cost-efficiency diagram for the solar driven plant was prepared. The exergy loss, section thermal efficiencies and product cost components are presented in Table 4-4. Figure 4-2 shows the same data in graphical form.

The constant capital cost lines in the figure represent the effect of the relationship of capital cost and thermal efficiency on the cost of the hydrogen. It can be seen that the efficiency and costs of Sections II and V dominate the process. With the sulfur synthesis and storage included in Section II, these two sections represent the least developed portion of the entire process. Therefore, there is significant uncertainty in the product cost data based on the lack of knowledge of these two sections. The greatest progress and improvements in the process can be accomplished by concentrating development efforts on these two sections. It is expected that work on the flowsheets and designs of Sections II and V, which contain the solar interface, will result in improved efficiency and lower production costs. These effects are affected by the diurnal operation of some of the process operations. Sections II and V are tripled compared to a continuous plant operation. Conversely, from the perspective of chemical process engineering for the development of a continuously powered hydrogen plant only, development in Sections III and I are most warranted.

C. Effect of Solar Availability

The cost estimates performed above were based upon the following assumptions regarding the input of energy into the process:

1. The solar plant runs 8 hours a day. The capacity of the diurnally operated sections of the hydrogen plant needs to be triple the capacity of the continuous operating sections.
2. The capital cost of the hydrogen plant includes 24 day capacity of sulfur storage.

TABLE 4-4

Energy Losses, Thermal Efficiencies and Product Cost Components

	MJ			η	M\$		\$/GJ Product Cost *
	E_x	ΣE_x	$\frac{\Sigma E_x}{\Delta G}$		Capital Cost	Σ Capital Cost	
O&M	0	0	0	.82	0	0	9.2
I,III,IV	43	43	.174	.70	153	153	15.6
II	93	136	.551	.53	162	315	22.4
V	45	181	.733	.47			
					209	524	31.3
V (Solar)	79	260	1.053	.40			

*less the cost of heat

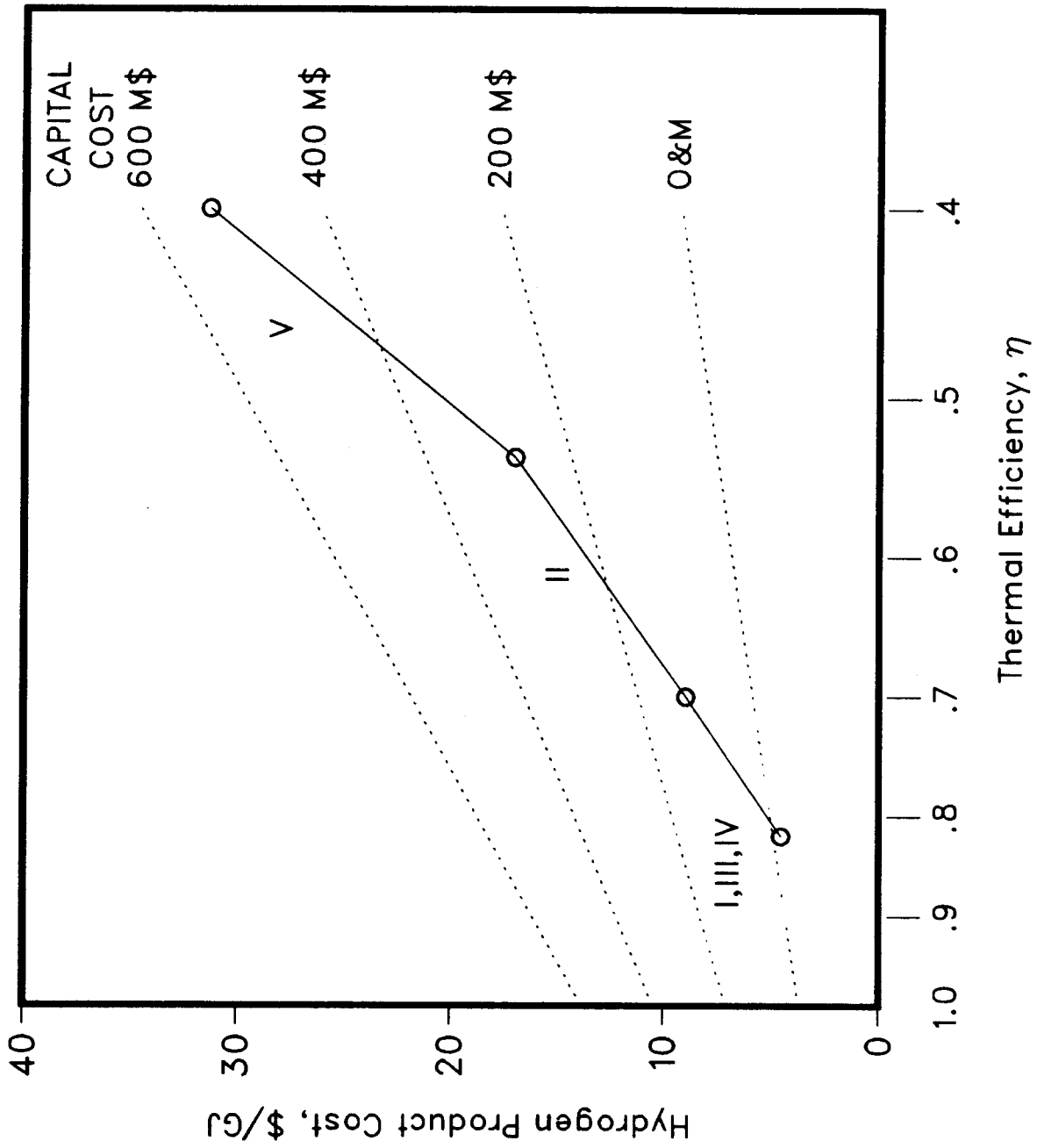


Figure 4-2 Process Related Costs for Solar Thermochemical Hydrogen

3. The operation of the sulfur-coupled hydrogen plant allows for the usage of direct solar energy during most of the daytime to make pure SO_2 . Sulfur provides a nitrogen-diluted SO_2 supply during the nighttime. The overall efficiency drop from all solar related chemical activities is 7% compared to a continuous plant.
4. Total annual operation time, 2370 hours, is based on a cloudiness factor which is uniformly applied to the seasonal variations in daily solar energy.

A more realistic determination of annual plant operation was calculated using the SOLERGY code (Ref. 38) which uses actual weather data. The data, measured every 15 minutes for the whole year of 1984 at the Solar One pilot plant at Barstow, California, totaled an annual direct normal insolation of 2342 kW-hr/m^2 - compared to the 25 year average of 2592. While this value is slightly low it is typical of variations that will be encountered in solar plants and adds a slight amount of conservatism to the comparison.

The code uses an electrical power plant configuration for a nitrate salt receiver very similar to the one used in determining the solar capital costs in report Section 3 a. Here, the power plant is replaced by the hydrogen plant. The energy is calculated as power flows from the collector field to receiver to storage and finally to the hydrogen plant. All energy is assumed to go to storage and from there to the hydrogen plant. This neglects any need for complex dispatch strategies for running the hydrogen plant with directly solar produced SO_2 or nitrogen diluted SO_2 from sulfur combustion. The transient response of the receiver was assumed to be the same as that for a receiver using nitrate salt as the thermal transport medium. Because the catalytic reactor experiment showed that the transient response of the receiver can be tailored by insulation, this assumption is probably valid. Parasitic and thermal losses within the receiver, and storage system were left unchanged. Start up energies and transient response for the electric turbine which the plant replaces were left unchanged. While it is unlikely that they have identical transient behavior, this has no effect on the results because the configurations selected have the hydrogen plant running almost continuously.

The major objective was to determine the configuration of the plant that would provide the minimum number of plant shutdowns while maintaining a high capacity factor for the hydrogen plant. Continuous operation would be important for the hydrogen plant to maintain steady state conditions for the many chemical reactions, to minimize the thermal cycling of components exposed to highly corrosive environments, and to maximize the utilization of the large capital investment. Dispatch strategies to maximize the value of the energy produced do not exist for a energy carrier product like hydrogen as it does for the production of electricity. Similarly, considering the end use of an energy carrier product, it does not make sense to hybridize the plant with another energy source such as

natural gas or coal. Turndown of the chemical plant was not performed in the simulation although turndown ratios of approximately 50% would probably be possible. The effect on efficiency of using turndown ratios is unknown; the maturity of the plant design is insufficient to supply such information.

Three parameters were found to have major impact on the continuous plant operation: (1) solar multiple, the relative capacity of the hydrogen plant compared to the solar system, (2) the storage capacity, and (3) the set point, the minimum energy level in storage before plant start up. There are interrelationships between all these parameters. Small solar multiples require large storage capacities to keep running, but large solar multiples may also require large storage capacities to keep from stowing heliostats because storage is full during long periods of high insolation. The minimization of wasted solar energy was a secondary objective in determining plant configuration. It is possible that dispatch strategies where turndown ratios are used based on current incoming energy and weather predictions could lead to a more economical plant configuration. Such strategy determinations should be part of an optimization effort that is beyond the scope of the effort here.

The plant configurations that require less than 20 start up and shut down cycles per year are listed in Tables 4-5 through 4-7, according to varying solar multiples. In these simulations, the solar plant size was fixed while the chemical plant size was varied for some of the different configurations. To maintain a constant basis of comparison, the storage capacity and set point are presented in terms of hours of operation of the solar plant. The production fraction is the percentage of annual solar energy that is used to produce hydrogen. The capacity factor is the percentage of the hydrogen plant capacity that is actually used to produce hydrogen on an annual basis. Typically the hydrogen plant would run at 100% capacity for a given length of time until the energy in storage was exhausted. The hydrogen plant would then remain shut down despite favorable weather conditions until the stored energy reached the set point when full capacity production resumed. For a plant configured to have a low number of start up cycles, the chemical plant would typically run at full capacity for about three weeks, then be shut down for approximately one week. With the large set points used, the few weather forced outages of the chemical plant would be sufficiently long to allow ample time to perform scheduled maintenance. It is possible to obtain higher capacity factors for the larger solar multiple configurations but only at the expense of greatly increasing the number of start-up cycles. With the lengthy outages, the plant is assumed to cool to ambient.

If more detailed designs were to show that even the relatively few annual thermal cycles were unacceptable, warm stand-by features could be included into the plant design. The power consumption of such features is normally 0.5% of the thermal rating of the equipment in the chemical plant and 1% of the annual receiver output for the Section II components (Ref. 22). If needed, the warm stand-by capability would make the small number of annual start up

TABLE 4-5
ANNUAL PRODUCTION RESULTS
SOLAR MULTIPLE OF 2.7

Plant Starts, #	Storage Capacity Hours*	Storage Set Point, Hours*	Capacity Factor %	Production Fraction, %
17	42	38	57.2	98.5
17	216	38	57.5	98.9
17	84	38	57.5	98.9
10	84	63	58.4	99.2
8	216	75	53.0	99.8
4	216	150	56.5	97.3
3	216	188	54.0	93.4

* Hours based on solar plant size, independent of solar multiple

TABLE 4-6
ANNUAL PRODUCTION RESULTS
SOLAR MULTIPLE OF 3.2

Plant Starts, #	Storage Capacity Hours*	Storage Set Point, Hours*	Capacity Factor %	Production Fraction, %
15	27	25.0	66.8	95.2
14	42	25.0	68.1	97.0
14	84	25.0	69.6	99.0
10	42	37.5	67.8	96.6
10	84	37.5	69.1	98.6

* Hours based on solar plant size, independent of solar multiple

TABLE 4-7
ANNUAL PRODUCTION RESULTS
SOLAR MULTIPLE OF 4.0

Plant Starts, #	Storage Capacity Hours*	Storage Set Point, Hours*	Capacity Factor %	Production Fraction, %
17	42	6.3	81.0	91.7
13	84	6.3	83.2	94.0
12	27	12.5	79.6	90.3
12	18	15.6	76.8	88.4
11	42	12.5	80.5	91.2
10	126	6.3	84.9	96.0
8	84	12.5	83.0	93.8
8	168	6.3	86.3	97.5
7	42	25.0	81.0	89.3
7	126	12.5	84.8	95.8
6	42	37.5	78.1	88.6
5	168	12.5	86.4	97.5
5	216	12.5	86.4	97.5
3	216	37.5	85.1	96.1

* Hours based on solar plant size, independent of solar multiple

cycles less advantageous. Storage capacity would then be reduced to minimize plant capital costs.

The relationships for minimizing annual plant starts are shown in Figures 4-3 and 4-4. There is a finite storage capacity above which there is little gain in reducing the number of plant starts. The dispatch strategy in terms of set point has a strong influence, with some plant configurations being insensitive to storage capacity over a large range.

Figures 4-5 and 4-6 show the production fraction and capacity factor of the various plant configurations. Different data points for the same combination of solar multiple and storage size have different set points. The vertical spread between these points shows how dispatch strategy can affect the productivity of the plant with no change to the plant configuration or capital investment. For example, for a storage capacity of 42 hours and a solar multiple of 4.0, the production fraction varies from 88.6 to 91.7% by changing the set point from 37.5 to 6.25 hours. Also, the annual number of plant starts increases from 6 to 17. The set point has less an effect on production fraction and capacity factor that it does on the number of plant starts.

For small chemical plants (i.e., a solar multiple of 4), greater storage sizes are needed to achieve high production fractions. It appears, however, that there is little advantage in increasing the storage greater than 100 hours. This, for a 3.0 solar multiple, as is used by the GA Technologies sulfur interface design, corresponds to 12.5 days of storage. By comparison, the 24 day storage capacity as proposed by GA Technologies for sulfur interface design seems unnecessary. Still, these storage capacities are quite large, and for the other systems, where nitrate salt is used for thermal storage, the capital cost of the salt system would begin to dominate the cost of the entire chemical plant, even though 50% of the energy is actually stored in the form of SO_2 as a reagent.

The cost of hydrogen with these effects can be determined using the same relationships shown in report Section 4-A. The capital cost of storage associated with Section II is 87 M\$. For the different storage sizes it was assumed to scale linearly. The remainder of Section II and Section Va are scaled and costed as part of the solar system. They operate as part of the solar system and are independent of the solar multiple. A correction factor was added to the results shown in Tables 4-5 through 4-7 because an efficiency of 47% was used in the simulation while a more appropriate efficiency for sulfur storage systems is 40%. Equation 4-2 in report Section 4-A becomes:

$$PC (\$/GJ) = \frac{(59.7/\text{solar multiple}) + (0.042 * \text{storage hours}) + 32.9}{\text{production fraction}}$$

These hydrogen costs are shown in Figure 4-7. These costs are only slightly higher than those presented in report Section 4-A. With the relatively low storage costs, a small chemical plant with lots of

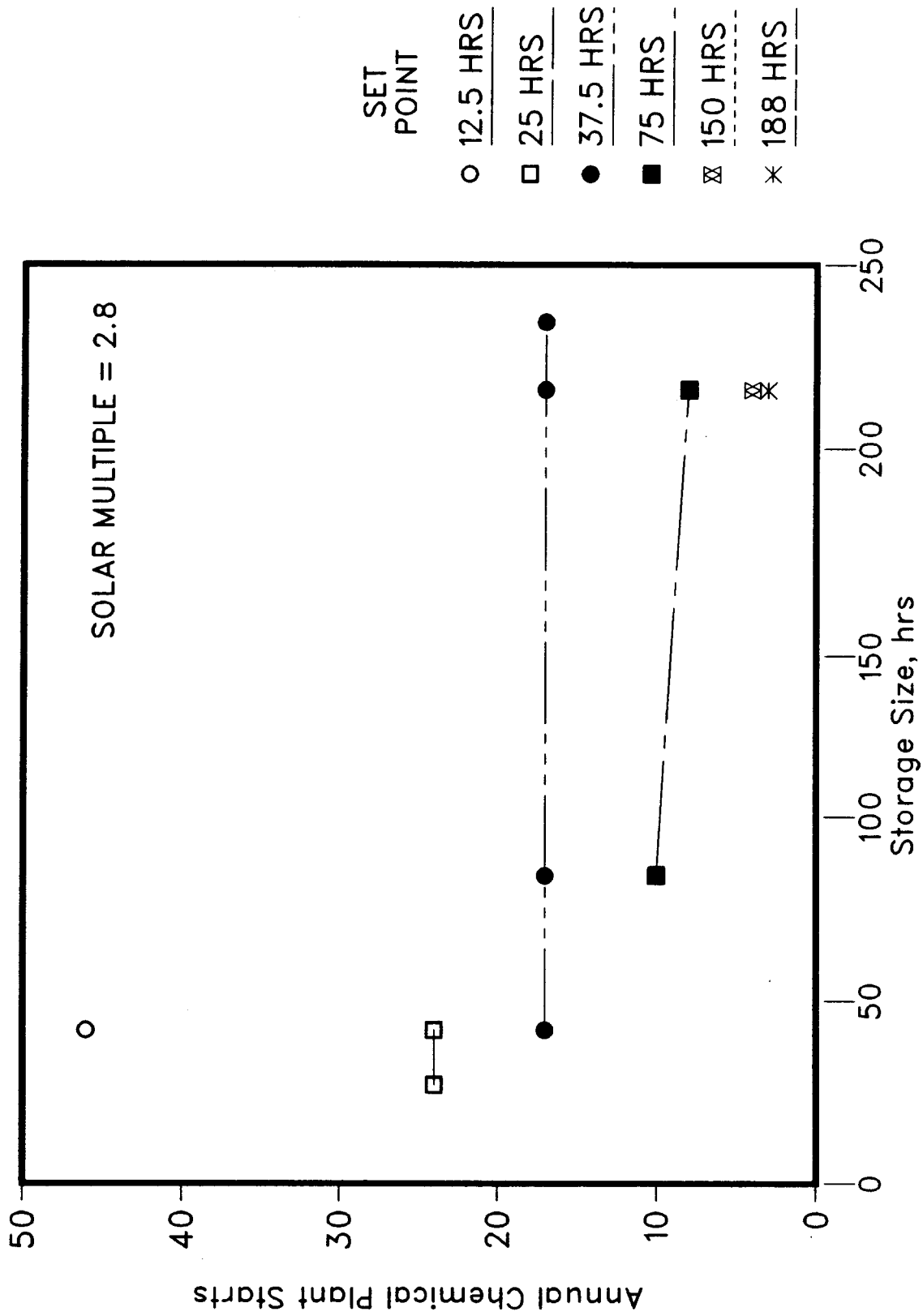


Figure 4-3 Chemical Plant Starts, Solar Multiple = 2.8
Based on Solar Availability Data

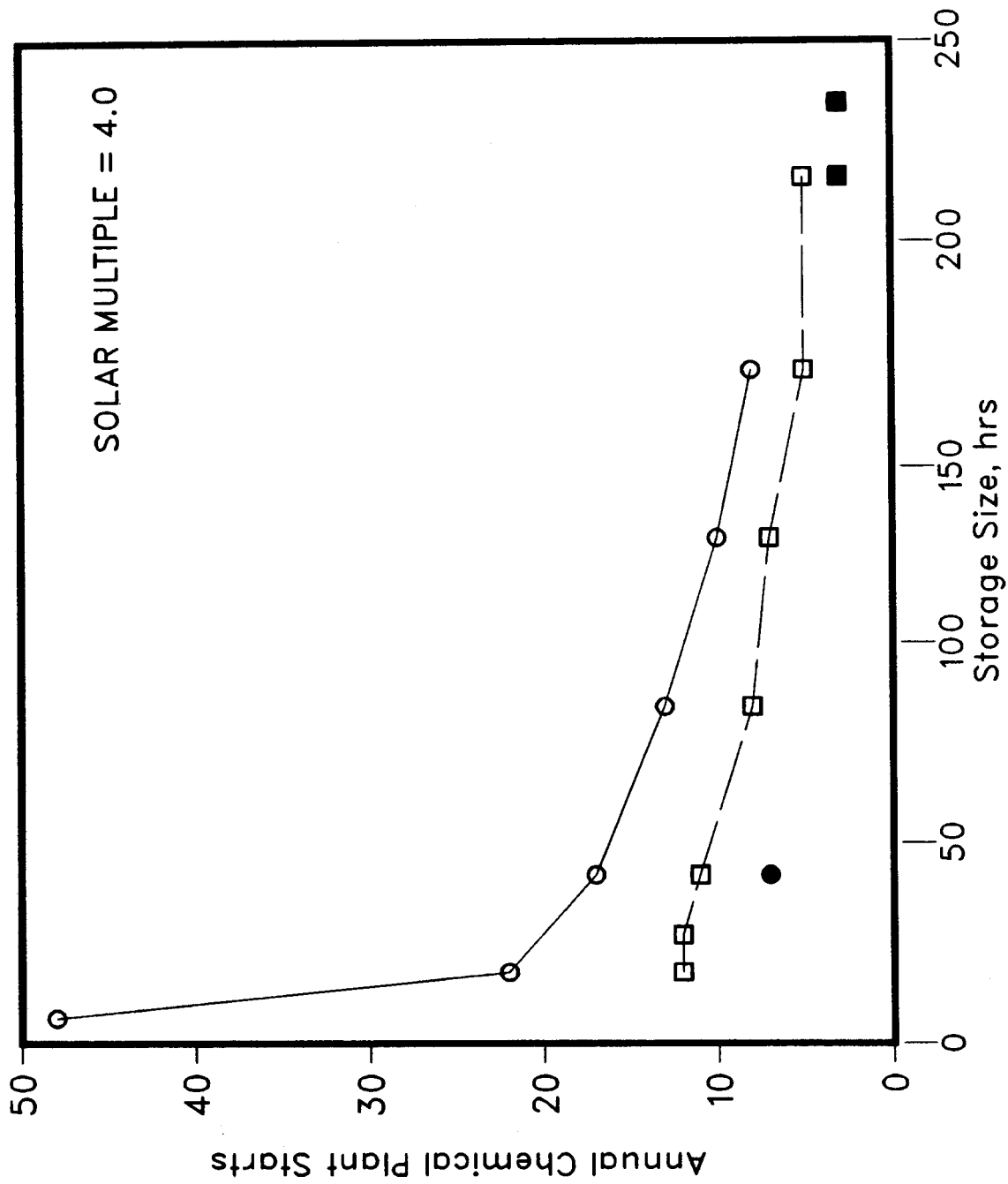


Figure 4-4 Chemical Plant Starts, Solar Multiple = 4.0
Based on Solar Availability Data

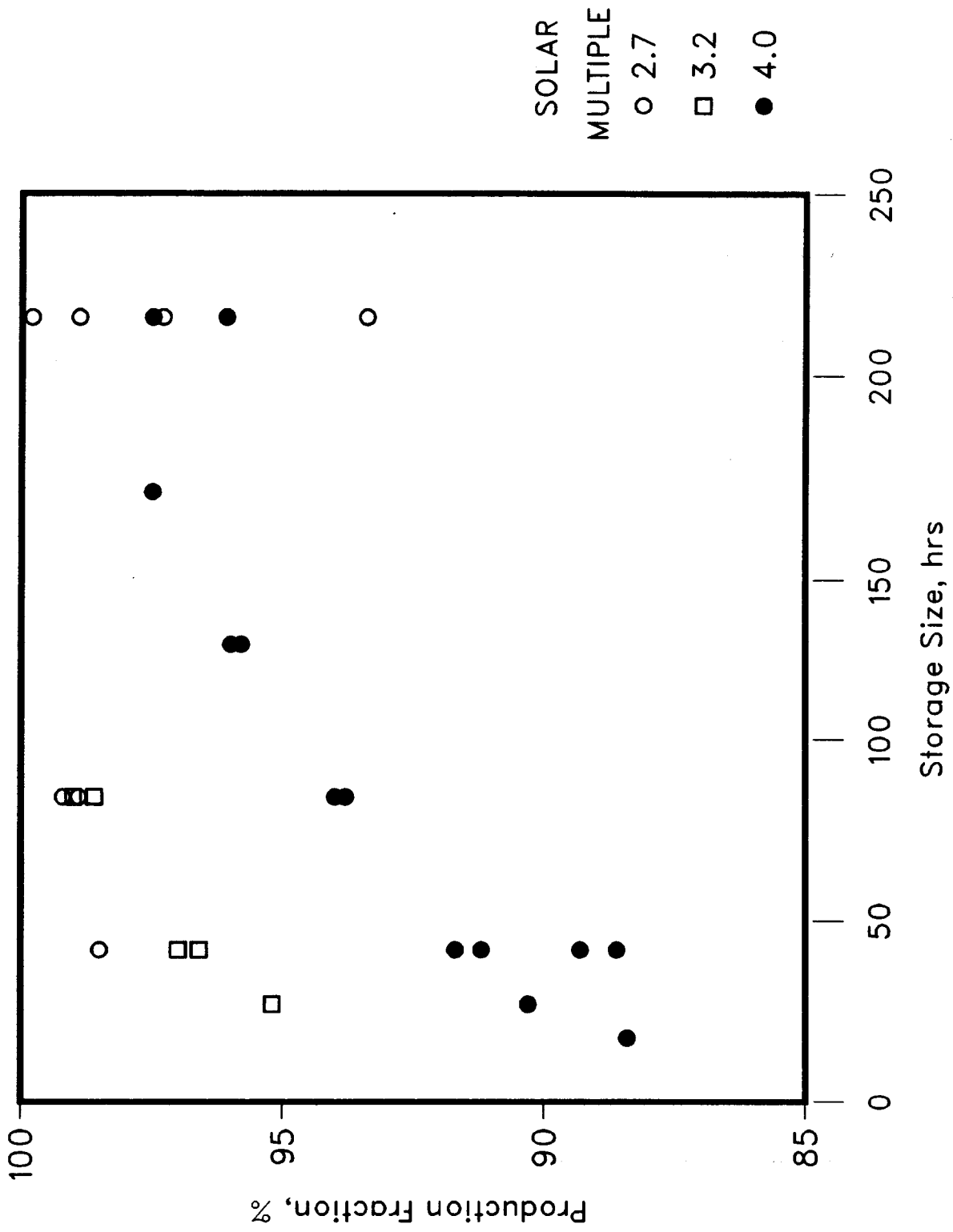


Figure 4-5 Production Fraction for Different System Configurations Based on Solar Availability Data

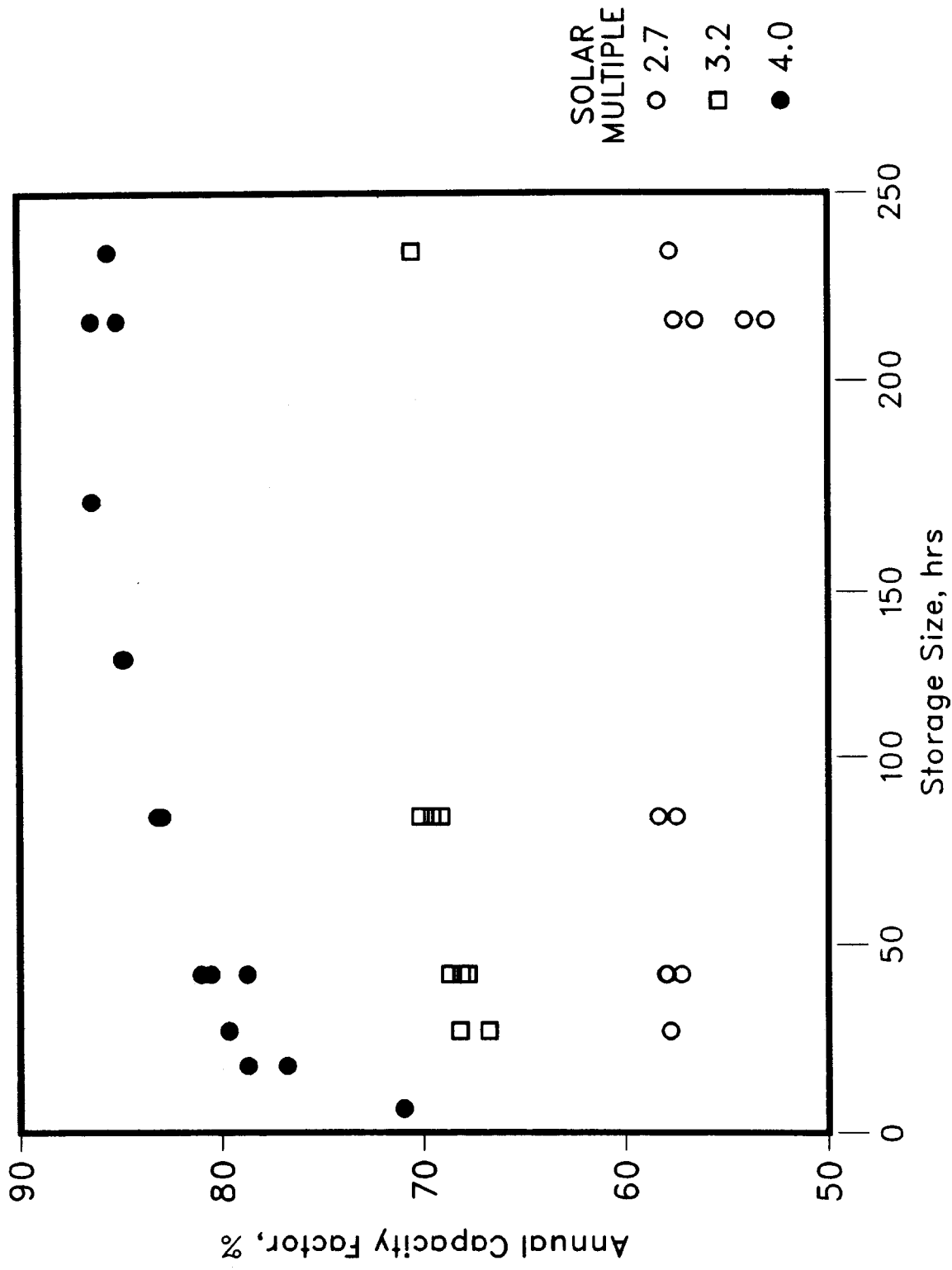


Figure 4-6 Annual Capacity Factor for Different System Configurations Based on Solar Availability Data

storage is most favored. While this is not an optimized parameter set, the lowest costs are around eight annual plant starts (with a solar multiple of 4.0 and 27 hours storage). While there is a generalized trend to lower costs with increasing plant starts, there comes a point where the under utilization of the plant increases production costs. With small storage, 6.25 hrs, the production costs range from 60 to 65 \$/GJ for a wide range of solar multiples, 5.3 to 2.6. The cost of heliostats has a slightly greater effect here. With \$40/m², the reduction in cost is 18% versus 14% for the results in report Section 4-A.

D. Liquid SO₂ Storage

A more valid assumption in determining the hydrogen product costs using solar energy availability data would be to examine a plant configuration where the process chemistry did not change from diurnal to continuous operation. If the Section II process stream exiting the receiver is compressed, the SO₂ can be liquified and separated from the O₂ and stored at 1.0 MPa. Nitrate salt is used for thermal energy storage while the SO₂ is used solely for reagent needs. For liquid SO₂ storage, flowsheets and cost estimates for an existing chemical heat storage concept design (Ref. 39) can be modified for this use. Table 4-8 lists the capital costs for such a plant. The energy required to liquify the SO₂ will reduce the thermal efficiency by approximately 0.25 percentage points. The Section V capital costs were scaled from Reference 3 to account for the reduction in plant equipment because without sulfur combustion there is no nitrogen dilution. The nitrate salt costs are consistent with the other solar costs used in report Section 4-A. Because the storage costs are considerably higher, the lowest hydrogen costs occur with less storage and more plant start-up cycles, from 40 to 50 per year. With this amount of plant cycling, warm stand-by design features would be employed. The cost relationship for such a plant design is:

$$PC (\$/GJ) = \frac{(36.9/\text{solar multiple}) + (0.72 * \text{storage hours}) + 24.82}{\text{production fraction} - [0.02 + 0.1 * (1 - \text{capacity factor})]}$$

The effect of the plant configuration on hydrogen costs is shown in Figure 4-8. The warm stand-by operations increase the cost by approximately 5% with no major effect based on the varying plant configurations. These costs are somewhat lower than are the costs for the elemental sulfur plant which uses significantly more storage. The feasibility of configurations used here depends on the ability to cycle the chemical plant with warm stand-by. If steady state operation of the chemical plant is too difficult to achieve, the economics will depend on the efficiency of running the plant at various turndown ratios. Still, the capacity factors obtained with these plant configurations indicate that with the development of a dispatch strategy using turn-down ratios for the plant during periods of low insolation, the plant could be run with very few shut down cycles using only a moderate amount of storage.

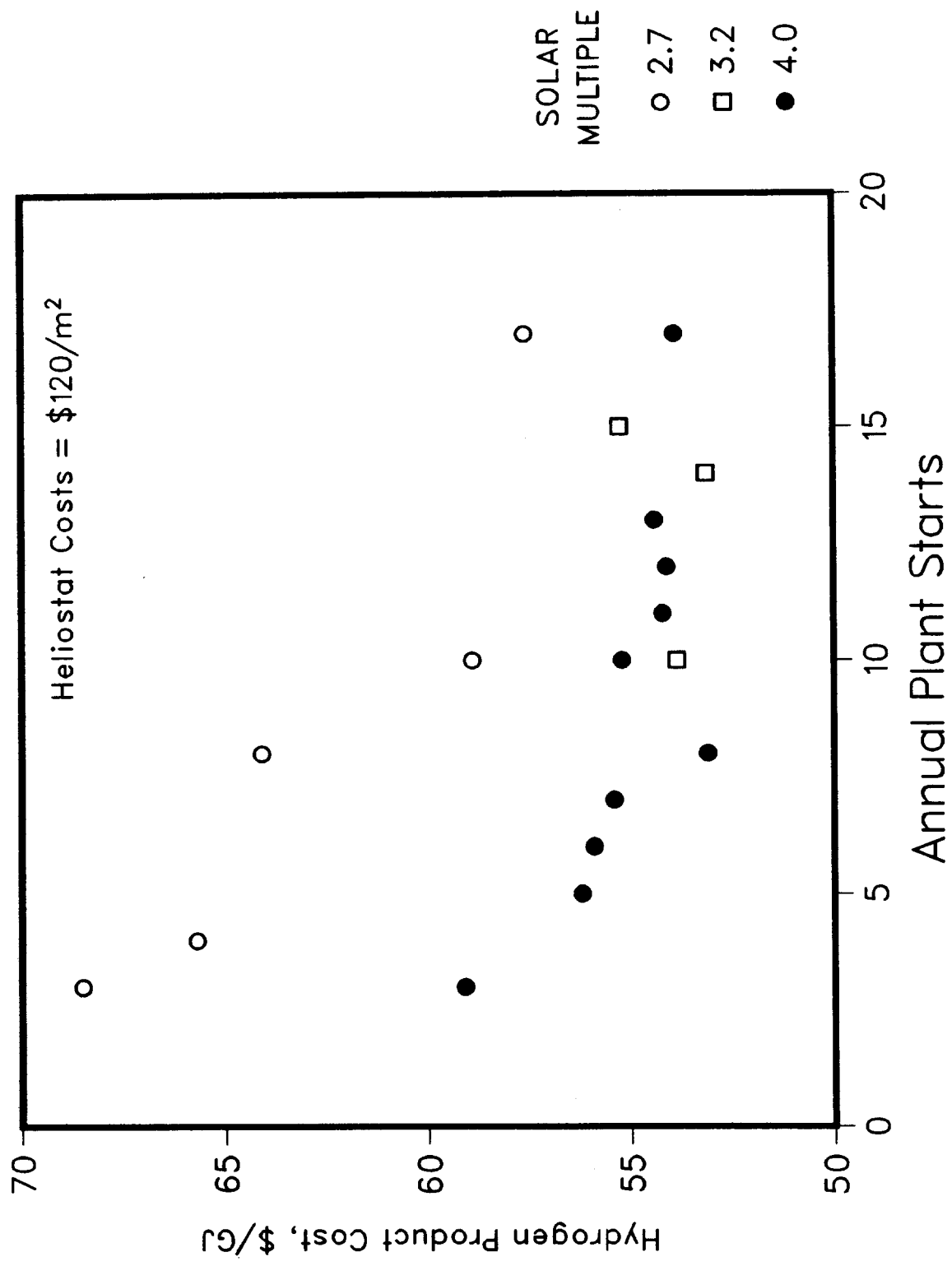


Figure 4-7 Hydrogen Costs for System Configurations Using Elemental Sulfur Storage. Based on Solar Availability Data

TABLE 4-8
 PLANT DESIGN WITH LIQUID SO₂
 AND NITRATE SALT STORAGE

Capital Costs		
	<u>1986 M\$</u>	
SECTION I	19	
SECTION II	98*	
SECTION III	118	
SECTION IV	16	
SECTION Va	53	
SECTION Vb	29	
<u>Storage</u>		
	Costs	Volume
	K\$/MW _t -HR	m ³ /MW _t -HR
Salt	15.07 ⁺	—
Liquid SO ₂	0.27	.22
Sulfuric Acid	0.31	.75

Required Compressor Power: 2.3kJ/mole H₂

* Includes 23 M\$ for compressors

⁺0.48 MW_t-HR of salt storage required per MW_t-HR of plant operation

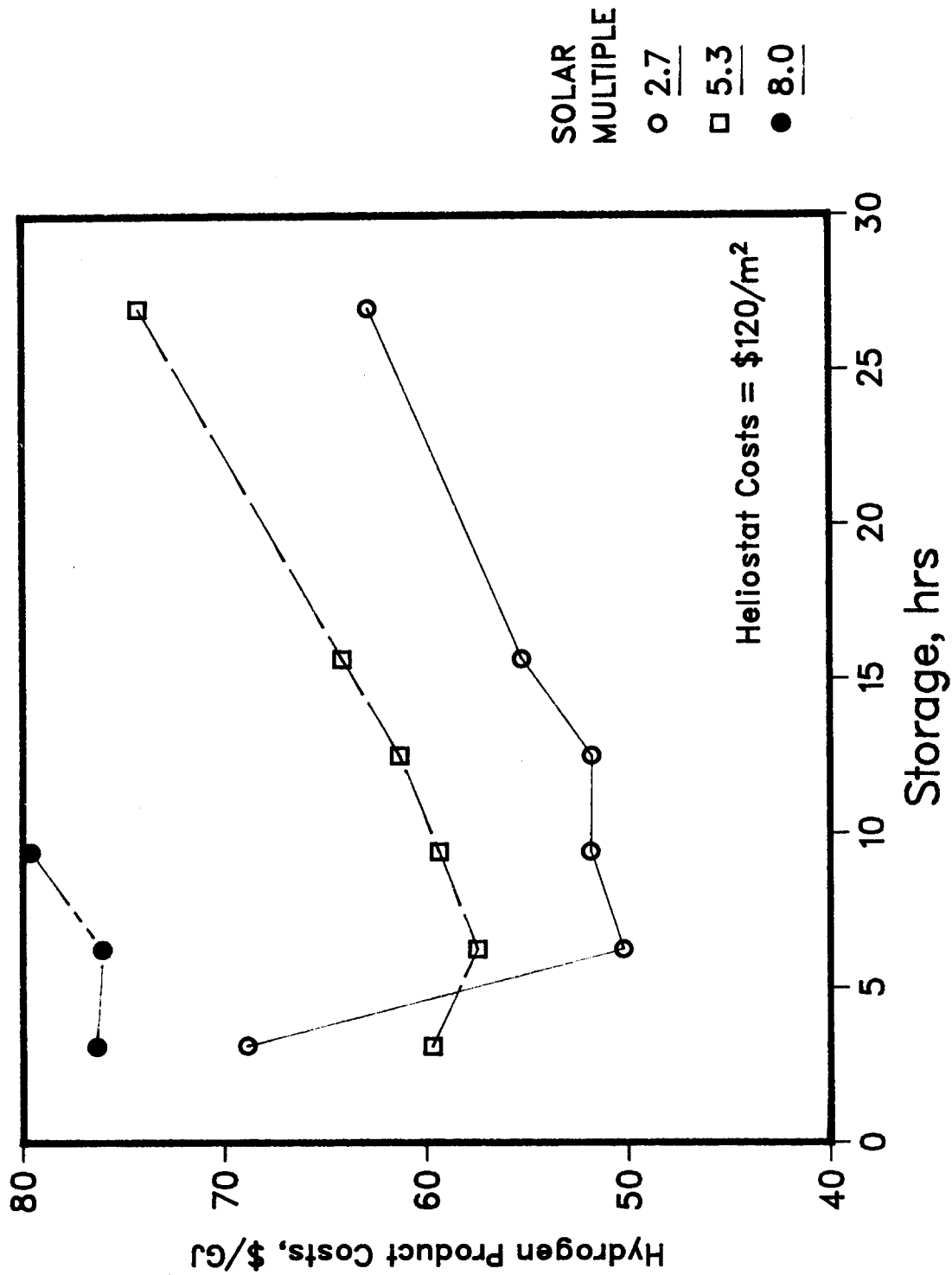


Figure 4-8 Hydrogen Costs for System Configurations Using Nitrate Salt and Liquid SO₂ Storage with Warm Standby. Based on Solar Availability Data

5. OTHER CYCLES

The GA process is a three reaction, "pure" thermochemical process. That is, most of the energy required by the process is supplied as heat rather than useful work (electricity). This cycle emerged from a world wide search during the 1970's for attractive processes. Several thermochemical cycles have been shown to be technically feasible and three H_2SO_4 based cycles (one of which is the GA process) are under development in Europe. These H_2SO_4 cycles are shown in Figure 5-1.

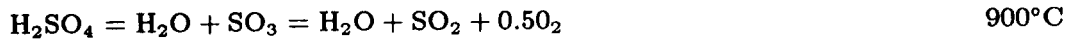
In so-called "hybrid" thermochemical processes one of the reactions is accomplished electrochemically. The closures marked 1) and 3) in Figure 5-1 are hybrid cycles which have been developed to the point of a closed loop bench scale laboratory model. It may turn out that hybrid cycles yield sufficient process simplification to justify selection. In general, however, the hybrid is a retreat from the advantages of a pure thermochemical cycle and must include capital costs for both a thermochemical plant and an electrolysis plant. The potential efficiency advantages become limited by the necessity to produce electricity as well as increased capital costs due to the modular nature of electrode cell equipment.

A number of thermochemical hydrogen cycles are being evaluated and developed in Japan. Six of these cycles are shown in Figure 5-2. Progress on the UT-3 cycle was reported at the 6th World Hydrogen Energy Conference held in Vienna, Austria in July 1986. Table 5-1 lists the research activities reported by the Japanese at this meeting. Thermochemical activities are conducted at many universities and research institutes and are funded by a number of government ministries and agencies. The nature of the work varies from basic research on reactions and materials to applications studies with process design and cost estimates. The UT-3 (University of Tokyo, Number 3) process has emerged as one cycle for further development (Refs. 40,41)

The process uses solid compounds of Br, Ca, and Fe in the four chemical reactions shown in Figure 5-2. The first reaction, the hydrolysis of $CaBr_2$, is performed at 700 - 750°C. The reaction of Fe_3O_4 with HBr is the low temperature reaction. It is performed at 200-300°C. All the solid-gas reactions in the UT-3 cycle are performed by switching the gaseous reactant streams (HBr, H_2O , and Br_2) from one reactor to another while keeping the solid reactants in place. A bench scale model of the process called MASCOT has been constructed and successfully operated for 200 hours.

Preliminary designs and cost estimates for a commercial size plant based on the UT-3 process has been conducted. The plant was designed to produce 2.1×10^6 GJ/yr of hydrogen with a helium cooled HTGR as the primary energy source. The helium loop leaves the HTGR at 850°C and returns from the hydrogen plant at 700°C. For a heat recovery system where power generation has an efficiency of 30%, the process thermal efficiency of the hydrogen

High Temperature Step



Closures

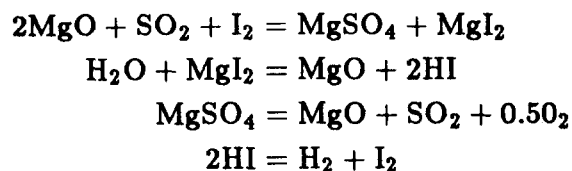
- | | | |
|----|---|---------------|
| 1) | $\text{SO}_2 + 2\text{H}_2\text{O} = \text{H}_2\text{SO}_4 + \text{H}_2$ (Electrochemical)
A "Hybrid" Process - Los Alamos
Westinghouse
ISPRA Mark II | 27°C |
| 2) | $2\text{H}_2\text{O} + \text{I}_2 + \text{SO}_2 = \text{H}_2\text{SO}_4 + 2\text{HI}$
$2\text{HI} = \text{H}_2 + \text{I}_2$
A "Pure" Thermochemical Process - GA Technologies | 27°C
300°C |
| 3) | $2\text{H}_2\text{O} + \text{Br}_2 + \text{SO}_2 = \text{H}_2\text{SO}_4 + 2\text{HBr}$
$2\text{HBr} = \text{H}_2 + \text{Br}_2$ (Electrochemical)
A "Hybrid" Process - ISPRA Mark 13 | 77°C
77°C |

Figure 5-1. Sulfuric Acid Based Thermochemical Cycles

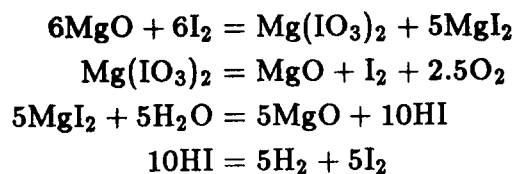
TABLE 5-1
JAPANESE THERMOCHEMICAL THERMOCHEMICAL RESEARCH ACTIVITIES,
6TH WORLD HYDROGEN ENERGY CONFERENCE

- S. Mizuta & T. Kumagai, Ibaraki, Japan.
Progress report on the MG-S-I Water Splitting Cycle: Continuous Flow Demonstration
- H. Kameyama, Y. Tomino & K. Yoshida, Tokyo, Japan.
Process simulation of Mascot Plant using UT-3 Thermochemical Cycle for Hydrogen production
- K. Yoshida & H. Kameyama, Tokyo, Japan.
Economical and Technical Evaluation of UT-3 Thermochemical Hydrogen Production Process on an Industrial Scale.
- S. Sato, et. al., Gunma, Japan
Studies on the Methanol-Iodine-Sulfur Process.
- H. Tagawa, Yokohama, Japan.
Thermal Decomposition of Metal Sulfates as an Oxygen Generating Reaction in Thermochemical Process for Hydrogen Production.

MAGNESIUM-SULFUR-IODINE CYCLE
National Chemical Laboratory for Industry (NCLI)



IODINE-MAGNESIUM CYCLE
National Chemical Laboratory for Industry (NCLI)



IRON-BROMINE CYCLE
Government Industrial Research Institute

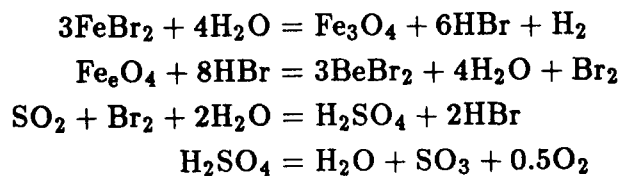
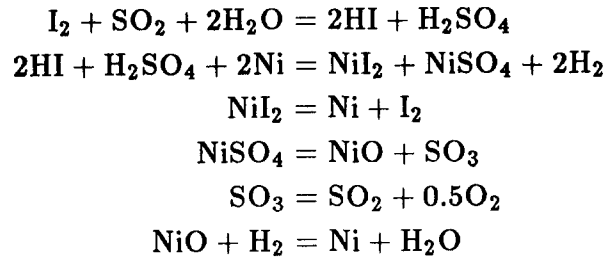
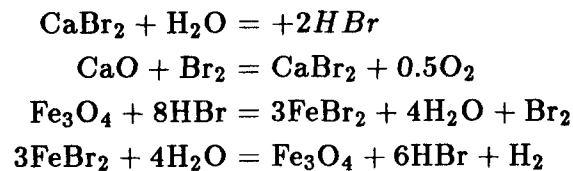


Figure 5-2. Thermochemical hydrogen cycles under development in Japan

NIS PROCESS
Japan Atomic Energy Research Institute



UT3 CYCLE
University of Tokyo



PHOTO/THERMO/ELECTRO CHEMICAL HYBRID CYCLE
Yokohama National University

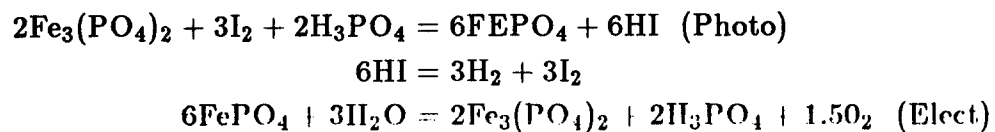
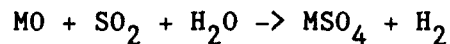
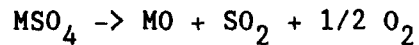


Figure 5-2. (Cont.) Thermochemical Hydrogen Cycles under development in Japan

plant is 45%. The hydrogen product cost is estimated to be 42% greater than hydrogen produced at present by steam reforming of natural gas. It is projected the escalating prices of fossil fuels will make the UT-3 process economically competitive by the year 2000.

The high temperatures at which solar central receivers can supply process heat have extended the range of thermochemical cycles which may prove to be economically viable. Cycles based on the decomposition of metal oxides or metal sulfates could be used with a solar source. The idealized cycle is two (or more) steps:



Bowman (Ref. 42) has discussed these cycles and suggested a number of possibilities for future work. One of the advantages of decomposing a metal sulfate or oxide is that the concentration and decomposition of relatively dilute H_2SO_4 can be avoided. Laboratory experiments have indicated some promise for the use of solid particle receivers and sulfate powders. The decomposition of sulfates occurs almost isothermally. While this does not interface well with gaseous heat transfer media typically used for high temperature nuclear reactors, it is ideally suited for direct flux solar receivers. However, low temperature solid reactions analogous to the HI synthesis step for the GA process need to be identified. At present this step can only be performed by the formation of sulfuric acid as in the GA process. The result is the formation of dilute aqueous solutions that must be reconcentrated and dried. The energy expended in these operations negates the advantages of the solid sulfate decomposition. Work is continuing to identify appropriate solid reactions.

While serious development is continuing on these cycles, the GA sulfur iodine cycle is the most developed and has the greatest demonstrated efficiency.

6. CONCLUSIONS

Compared to other solar thermal applications, thermochemical hydrogen is unique for three reasons:

- 1) The process is not mature. Other applications, such as the Rankine and Brayton cycles for electric power generation and, for chemical production, the steam reforming of methane, have been fully developed for decades. The GA process has been demonstrated in closed loop cycles in laboratory bench scale experiments, but nothing approaching the pilot plant scale has been built. There are additional process improvements that have been identified, such as the elimination of Section III and improved HI decomposition catalysts. These improvements require much additional development to determine their effect on the process design and performance.
- 2) Heat recovery is more important with the GA process than most typical chemical processes. Without heat recovery, the thermal efficiency would be reduced to 13%. There is no reason why heat recovery cannot be accomplished, technically or economically, but it requires a different chemical engineering philosophy towards plant design than most typical chemical plants.
- 3) The process has potential for improved performance at the higher temperatures obtainable only with solar thermal central receivers. Few processes show a similar "solar unique" capability. Because other energy sources are not capable of the higher operating temperatures, flowsheets which document the process performance are based on non-optimum conditions. There is no information available to describe the advantages of an optimized solar thermal interface for the process.

The experiments performed to date have been successful as a first step in developing components for the sulfuric acid decomposition of Section II. There have been no great technical obstacles confronting this development. The catalytic reactor performs well. Kinetic effects are not far from the performance predictions based on equilibrium chemical behavior. The one dimensional chemical models are adequate for determining reactor performance. Radial gradient effects were once predicted to adversely affect reactor performance. They were not observed to have any effect.

The transient performance of the reactor is well behaved. Feasible control schemes have been demonstrated experimentally. Various receiver designs appear practical for the sulfuric decomposition reaction. As ceramics technology improves, Section II and receiver components performance will improve.

The Garrett experiment was a demonstration of a significant advancement in ceramic seals applicable to the condenser and recuperator as well as the acid boiler. Additional development of the hot end seal is required for it to be more tolerant of misalignment.

Alternate reactor designs may be more desirable, but this would be due to lowered construction costs, not chemical performance. Some of the suggested alternate designs, such as adiabatic and radial flow reactors, have had little process analysis performed. Still, various reactor designs need to be seriously considered and analyzed to arrive at the most economical reactor design. Figure 6-1 shows the evolution path for thermochemical hydrogen receivers. The present capabilities are limited by metallic corrosion resistance to the boiling/condensation of sulfuric acid and the ceramic seals. With the completion of the development of ceramics for the receiver design, the higher temperatures where more complete chemical conversion occurs can be performed without the use of catalysts.

A second possibility for receiver designs is the use of solid particles. Solid particle receivers can operate at the higher temperatures where the same favorable chemical performance exists. The reaction would then take place in a ceramic heat exchanger where the wear resistance of the silicon carbide would provide compatibility with the solid particles as well as corrosion compatibility with the chemical process stream.

The interface of solar energy to the chemical process and process design for solar application needs considerable development. The existing interface designs are based on the heat-temperature profiles from nuclear reactors. The chemical plant design and interface are not completely interchangeable with different energy sources. Flowsheets have also been designed with a maximum of heat recovery and efficiency which results in large capital costs. The most cost effective combination of heat recovery and capital investment has not been determined. For solar interfaces, the power cycles in Section V must be simplified. An interface should be designed with nitrate salt for thermal storage, an SO_2 reagent storage subsystem, and a steam power cycle. The tradeoffs for a low temperature steam or freon power cycle need to be determined. An additional heat transfer loop using oil or steam is also needed. The current configurations require the use of nitrate salt too close to its freezing temperature. Also, in some heat recovery loops, it is not practical to transport either salt or HI bearing process streams long distances. For Section III, this is especially true. In fact, some of the biggest advantages of the Aachen process improvement may be in the elimination of the heat recovery needs of Section III, as well as in process efficiency and possible capital costs.

The sulfur storage concept needs considerably more development before its performance can be determined. Little is known about the process stream and components for the disproportionation reaction and combustion of sulfur. The existing flowsheets contain ambiguities in terms of the heat and work supplied by the sulfur interface and the equipment requirements for Section III. The large 24 day storage capacity does not appear to be needed. While sulfur storage itself appears to be cheaper, the additional capital costs and the complicated dispatch strategy required may make more traditional storage concepts more attractive. Ultimately, the ability to achieve acceptable behavior of the chemical reactions

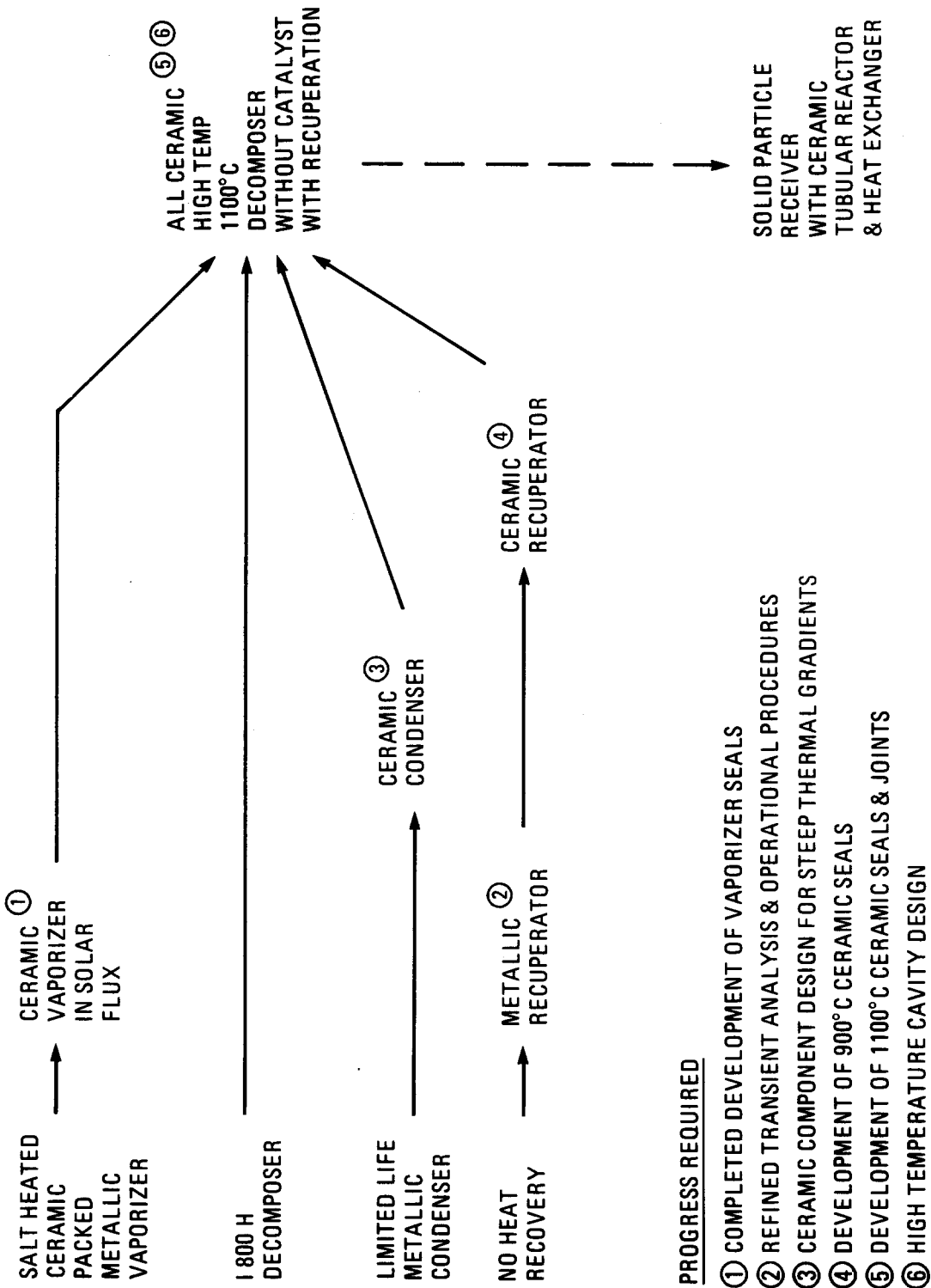


Figure 6-1 Evolutionary Path for Solar Thermochemical Hydrogen Receiver

with a moderate number of plant starts using warm stand-by procedures will determine the storage system design.

There is technical concern in one area - corrosion. The corrosive environments caused by the condensation of sulfuric acid and HI process streams are the biggest concern. The condenser in the GA experiment showed that such metallic components would require frequent replacement. Where the possibility of condensation of sulfuric acid exists there is a need for careful process control. In Section I the main reactor appears to require niobium or tantalum liners. Because refractory metal costs are five times that of stainless steel, the concern about this requirement is largely economic. In Section IV a similar concern exists. Also, the use of the Aachen process improvements will require compatibility with HI at higher temperatures and pressures than previously used. Laboratory compatibility testing of materials for the sulfuric acid decomposer showed much better results than the reactor experiments themselves where the occurrence of corrosion of the aluminide coating with iron oxide catalyst and of bare I800H with the platinum catalyst were unexpected. While the behavior of bare I800H with the iron oxide catalyst was good, more corrosion testing in realistic reactor conditions is needed because of this lack of predictability. Reactor experiments need to operate for much longer periods of time than the experiments performed to date.

The economics for solar thermochemical hydrogen show a price range of from 38.0\$/GJ for low cost heliostats and simplified assumptions regarding solar energy availability, to 55\$/GJ using sulfur storage to limit the number of annual plant starts with actual Solar One weather data. If moderate plant cycling is feasible, the hydrogen costs range from 45 to 48\$/GJ, depending on whether warm stand-by procedures are needed. Compared to present bulk hydrogen costs from the steam reforming of methane (16\$/GJ), the price disparity is similar to that for current capabilities for solar electricity and the long term program goals. For the use of hydrogen as a primary energy carrier, however, the disparity is somewhat greater. In the past, conceptual studies have coupled very large hydrogen plants to nuclear power. The economies of scale do not greatly favor large plant sizes. The limiting size of heat exchangers and similar equipment dictate that those plants use 6 or more parallel streams in some areas. Solar thermochemical plants may be nearly as economical at about 600MWt. These economic comparisons should be viewed with uncertainty consistent with the assumptions required at this stage of development of the process. As Figure 4-1 shows, the greatest areas of uncertainty are for Sections II and V. The development of these areas is important for solar thermochemical hydrogen, while from a chemical process perspective Sections I, III and IV are most important.

For solar thermochemical hydrogen production, the major areas for continuing work are:

- 1) Complete development of the process, defining the performance of Sections I and IV using the identified process improvements.

- 2) Define a solar interface and flowsheet. Determine the most feasible power cycles for Section V and optimize the capital equipment costs optimizing thermal efficiency and heat recovery.
- 3) Analyze the sulfur storage concept to determine the most economical storage system and plant configuration based on detailed equipment designs and flowsheets.
- 4) Perform a comparative analysis of the various sulfuric acid decomposer concepts including adiabatic reactors to identify necessary receiver development.
- 5) Qualify candidate component construction materials and designs with long term corrosion experiments.

REFERENCES

1. National Energy Policy Plan (NEPP IV) - DOE 1983; I. Borg, March 1983.
2. T. Ohta, Solar-Hydrogen Energy Systems, Pergamon Press, 1979.
3. UDID-19311, "Synfuels from Fusion - Using the Tandem Mirror Reactor and a Thermochemical Cycle to Produce Hydrogen," O. H. Kirkorian, ed., Lawrence Livermore Laboratory, February 9, 1982.
4. GA-A16813, "Utility Fusion Synfuel Study, Phase III of A study of Chemical Production Utilizing Fusion Energy," I Maya, et al., GA Technologies, Northeast Utilities Service, and Public Service Electric & Gas Company, July 1983.
5. UCRL-54380, "Mirror Advanced Reactor Study - Volume 2, Commercial Fusion Synfuels Plant," Lawrence Livermore National Laboratory, July 1984.
6. GA-A16713, "Thermochemical Water-Splitting Cycle, Bench-Scale Investigations, and Process Engineering," J. H. Norman, et al., GA Technologies, May 1982.
7. GRI-80/0105, "Thermochemical Water-Splitting for Hydrogen Production" Final Report (January 1975 - December 1980), Gas Research Institute, March 1981.
8. GA-A12889, "Production of Hydrogen from Water, Final Report for the Period October 1, 1972, through December 31, 1973," J. L. Russell, GA Technologies, February 15, 1974.
9. GA-A16022, "Thermochemical Water Splitting with Solar Thermal Energy: Final Report," G. E. Besenbruch and K. H. McCorkle, GA Technologies, February 1981.
10. H. Engels, K. F. Knoche, M. Roth, "Direct Dissociation of Hydrogen Iodide - An alternative to the General Atomic Proposal," Proceedings of the Sixth World Hydrogen Energy Conference, Vienna, Austria, July 1986.
11. K. F. Knoche, et al., "Direct Dissociation of Hydrogeniodide into Hydrogen and Iodine from HI/H₂O/I₂ Solutions," Proceedings of the Fifth World Hydrogen Energy Conference, Toronto, Canada, 1984
12. H. Engels, et al., "Vapor Pressure, Pseudo Azeotrope and Miscibility Gap of the System HI/H₂O/I₂," Proceedings of the IEA Annex I Workshop, Honolulu, HI, 1985.
13. GA-C16493, "Solar Production of Hydrogen Using the Sulfur-Iodine Thermochemical Water Splitting Cycle," J. H. Norman, et al., GA Technologies, September 1981.

14. GRI-80/0081, "Assessment and Investigation of Containment Materials for the Sulfur-Iodine Thermochemical Water-Splitting Process for Hydrogen Production," Gas Research Institute, January 1980.
15. WAESD TR-83-1011, "Solar Thermochemical Process Interface Study," Westinghouse Electric Corporation, February 1984.
16. GA-A17573, "Decomposition of Sulfuric Acid Using Solar Thermal Energy," GA Technologies, February 1985.
17. GA-A18285, "High-Pressure Catalytic Metal Reactor in a Simulated Solar Central Receiver," GA Technologies, February 1986.
18. GA-A16833, "Solar Thermal Sulfuric Acid Heat Exchanger and System Test," GA Technologies, March 1983.
19. FWC/FWDC/TR-84/30, "Solar Hydrogen Thermochemical Process Design Study," Foster Wheeler Solar Development Corporation, April 1985.
20. Report # 85-21779, "Solar Components for a Steam Injected Gas Turbine Solar-Electric Power Plant," Garrett Airesearch Manufacturing Company, January 1986.
21. S. S. Lin and R. Flaherty, "Design Studies of the Sulfur Trioxide Decomposition Reactor for the Sulfur Cycle Hydrogen Production Process," International Journal of Hydrogen Energy, Vol.8, No.8, 1983.
22. DOE/SF/10735-1, "Solar Central Receiver Reformer System for Ammonia Plants PFR Engineering Systems, Inc., July 1980.
23. "Production and Regeneration of Activated Carbon: Solar Fuels and Chemicals Design Study," Babcock and Wilcox Company, April 25, 1986
24. "Design and Assessment of Different Solar Methane Reforming Systems Followed by a Chemical Production Plant," Draft Summary, Lurgi Corp. and M.A.N Technologie, May 1986.
25. SAND86-8178, Contractor Report, "Solar Fuels and Chemicals System Design Study (Ammonia/Nitric Acid Production Process), Foster Wheeler Solar Development Corporation, June 1986.
26. M. Geyer, "Sensible Heat Storage for High Temperature Applications," Proceedings of the IEA-SSPS Meeting on High Temperature Technology and Applications, June 1985.
27. SAND86-8211 "A Technical Feasibility Study of a Solid Particle Solar Central Receiver for High Temperature Applications," J. M. Hruby, March 1986.
28. T. A. Williams and J. A. Dirks, Battelle Pacific Northwest Laboratory, "Economic Evaluation of Solar Thermal Energy Systems Using a Levelized Energy Cost Approach," 7th Miami International Conference on Alternative Energy Systems, December 9, 1985.

29. P. K. Falcone, et al., "An Assessment of Central Receiver Systems", 21st Intersociety Conference Energy Conversion Engineering Conference, San Diego, Ca., August, 1986.
30. "Economic Indicators", Chemical Engineering Magazine, April 28, 1986.
31. "Integrated Reformer-Receiver Design Study", Resource Analysis International Inc., Sandia Contract 86-2963, work in progress.
32. SAND84-8233, "The Performance of High-Temperature Central Receiver Systems," P. De Laquil and J. V. Anderson, July 1984.
33. SAND81-8237, "A User's Manual for DELSOL2: A Computer Code for Calculating the Optimal System Design for Solar Thermal Central Receiver Plants," T. A. Dellin et al., August 1981.
34. "Development of a Stressed Membrane Heliostat," Solar Kinetics Inc., Contractor Report, Sandia Contract #91-8808A, September 1986.
35. "Irreversibilities, Heat Penalties, and Economics for the Methanol/Sulfuric Acid Process," J.E. Funk and K.F. Knoche, Proceedings of the 12th Intersociety Energy Conversion English Conference, Washington DC, August, 1977, pp. 933-938.
36. "Entropy Production, Efficiency, and Economics in the Thermochemical Generation of Synthetic Fuels: I. The Hybrid Sulfuric Acid Process," K.F. Knoche and J.E. Funk, International Journal Hydrogen Energy, Vol. 2, No. 4, December, 1977, pp. 377-385.
37. "Entropy Production, Efficiency, and Economics in the Thermochemical Generation of Synthetic Fuels: II The Methanol Water Splitting Cycle," K.F. Knoche and J.E. Funk, International Journal Hydrogen Energy, Vol. 2, No. 4, December, 1977, pp. 387-393.
38. "SOLERGY - A Computer Code for Calculating the Annual Energy from Solar Central Receiver Power Plants," M. C. Stoddard et al., report in progress.
39. RRC-80-R-678, "Chemical Energy Storage for Solar Thermal Conversion," Rocket Research Company" Contract # 18-2563, April 27, 1979.
40. H. Kameyama et al., "Process Simulation of 'MASCOT' Plant Using the UT-3 Thermochemical Cycle for Hydrogen Production," Proceedings of the Sixth World Hydrogen Energy Conference, Vienna, Austria, July, 1986.
41. T. Aochi et al., "Economical and Technical Evaluation of UT-3 Thermochemical Hydrogen Process for an Industrial Scale Plant," Proceedings of the Sixth World Hydrogen Energy Conference, Vienna, Austria, July, 1986.

42. Bowman, M.G., Future Thermochemical Hydrogen Studies V. Reactions in "Dry" Sulfate Cycles, Proc. 8th Tech. Workshop, Task I, Thermochemical Production, IEA, Honolulu, Hawaii, pp. 163-170, October 28-30, 1985.

UNLIMITED RELEASE
INITIAL DISTRIBUTION

U.S. Department of Energy (5)
Forrestal Building
Code CE-314
1000 Independence Avenue, S.W.
Washington, D.C. 20585
Attn: H. Coleman
S. Gronich
F. Morse
M. Scheve
R. Shivers

U.S. Department of Energy
Forrestal Building, Room 5H021C
Code CE-33
1000 Independence Avenue, S.W.
Washington, D.C. 20585
Attn: C. Carwile

U.S. Department of Energy
Albuquerque Operations Office
P.O. Box 5400
Albuquerque, NM 87115
Attn: D. Graves

U.S. Department of Energy
San Francisco Operations Office
1333 Broadway
Oakland, CA 94612
Attn: R. Hughey

University of California
Environmental Science and Engineering
Los Angeles, CA 90024
Attn: R. G. Lindberg

University of Houston (2)
Solar Energy Laboratory
4800 Calhoun
Houston, TX 77704
Attn: A. F. Hildebrandt
L. Vant-Hull

Analysis Review & Critique
6503 81st Street
Cabin John, MD 20818
Attn: C. LaPorta

Arizona Public Service Company
P.O. Box 21666
Phoenix, AZ 85036
Attn: E. Weber

Babcock and Wilcox
91 Stirling Avenue
Barberton, OH 44203
Attn: D. Young

Bechtel Group, Inc.
P.O. Box 3965
San Francisco, CA 94119
Attn: P. DeLaquil
S. Fleming

Black & Veatch Consulting Engineers (2)
P.O. Box 8405
Kansas City, MO 64114
Attn: J. C. Grosskreutz
J. E. Harder

Boeing Aerospace
Mailstop JA-83
P.O. Box 1470
Huntsville, AL 35807
Attn: W. D. Beverly

California Energy Commission
1516 Ninth St., M/S 40
Sacramento, CA 95814
Attn: A. Jenkins

California Public Utilities Com.
Resource Branch, Room 5198
455 Golden Gate Ave.
San Francisco, CA 94102
Attn: T. Thompson

CIEMAT
Avda. Complutense, 22
28040 Madrid
Spain
Attn: F. Sanchez

DFVLR RF-ET
Linder Hohe
D - 5000 Koln 90
West Germany
Attn: Dr. Manfred Becker

El Paso Electric Company
P.O. Box 982
El Paso, TX 79946
Attn: J. E. Brown

Electric Power Research Institute (2)
P.O. Box 10412
Palo Alto, CA 94303
Attn: J. Bigger
E. DeMeo

Foster Wheeler Solar Development Corp.
12 Peach Tree Hill Road
Livingston, NJ 07039
Attn: S. F. Wu

Mr. James E. Funk (5)
University of Kentucky
Dept. of Chemical Engineering
Lexington, KY 40506

GA Technologies
P. O. Box 85608
San Diego, CA 92138
Attn: G. E. Besenbruch

Garrett AiResearch
2525 West 190th Street
Torrance, CA 90509
Attn: P. Vidano

Georgia Institute of Technology
GTRI/EMSL Solar Site
Atlanta, GA 30332

D. Gorman
5031 W. Red Rock Drive
Larkspur, CO 80118

Jet Propulsion Laboratory
4800 Oak Grove Drive
Pasadena, CA 91103
Attn: M. Alper

P. Kesselring
Swiss Federal Institute
for Reactor Research
CH 5305 Wurenlingen
Switzerland

Prof. Dr.-Ing Karl-Friedrich Knoche
Lehrstuhl für Technische Thermodynamik
RWTH Aachen
Schinkelstrasse 8
5100 Aachen
Federal Republic of West Germany

Los Angeles Department of Water and Power
Alternate Energy Systems
Room 661A
111 North Hope St.
Los Angeles, CA 90012
Attn: Hung Ben Chu

Martin Marietta Aerospace
P.O. Box 179, MS L0450
Denver, CO 80201
Attn: H. Wroton

McDonnell Douglas (2)
MS 49-2
5301 Bolsa Avenue
Huntington Beach, CA 92647
Attn: R. L. Gervais
J. E. Raetz

Meridian Corporation
5113 Leesburg Pike
Falls Church, VA 22041
Attn: D. Kumar

Public Service Company of New Mexico
M/S 0160
Alvarado Square
Albuquerque, NM 87158
Attn: T. Ussery
A. Martinez

Olin Chemicals Group (2)
120 Long Ridge Road
Stamford, CT 06904
Attn: J. Floyd
D. A. Csejka

Pacific Gas and Electric Company
77 Beale Street
San Francisco, CA 94106
Attn: J. Laszlo

Pacific Gas and Electric Company (4)
3400 Crow Canyon Road
San Ramon, CA 94526
Attn: G. Braun
T. Hillesland, Jr.
B. Norris
C. Weinberg

Public Service Company of Colorado
System Planning
5909 E. 38th Avenue
Denver, CO 80207
Attn: D. Smith

Rockwell International
Rocketdyne Division
6633 Canoga Avenue
Canoga Park, CA 91304
Attn: J. Friefeld

Sandia Solar One Office
P.O. Box 366
Daggett, CA 92327
Attn: A. Snedeker

Solar Energy Research Institute (3)
1617 Cole Boulevard
Golden, CO 80401
Attn: B. Gupta
D. Hawkins
L. M. Murphy

Southern California Edison
P.O. Box 325
Daggett, CA 92327
Attn: C. Lopez

Stearns Catalytic Corp.
P.O. Box 5888
Denver, CO 80217
Attn: T. E. Olson

Stone and Webster Engineering Corporation
P.O. Box 1214
Boston, MA 02107
Attn: R. W. Kuhr

6000 D. L. Hartley; Attn: V. L. Dugan, 6200
6220 D. G. Schueler
6222 J. V. Otts
6226 J. T. Holmes (10)
6226 C. E. Tyner
6227 R. B. Diver
6254 J. D. Fish

8000 J. C. Crawford Attn: R. J. Detry, 8200
P. Mattern, 8300
R. C. Wayne, 8400
8100 E. E. Ives; Attn: J. B. Wright, 8150
D. J. Bohrer, 8160
R. A. Baroody, 8180
8130 J. D. Gilson
8133 L. G. Radosevich
8133 A. C. Skinrood (3)
8133 D. N. Tanner
8150 J. B. Wright
8154 D. J. Havlik
8154 C. W. Pretzel (5)
8244 C. Hartwig
8245 R. J. Kee
8265 Publications Division for OSTI (30)
8265 Publications Division/Technical Library Processes Division, 3141
3141 Technical Library Processes Division (3)
8024 Central Technical Files (3)